# POLITECNICO DI TORINO

Mater’s Degree in Civil Engineering

Master’s Thesis

**Healing properties of Asphalt binders modified with recycled waste plastics by means of the Linear Amplitude Sweep (LAS) approach**

Supervisors:

Prof. Orazio Baglieri

Prof. Lucia Tsantilis

Dott. Joseph Nicolas La Macchia

Candidate:

Nahedeh Fatlavi

July 2026

Summary

## Acknowledgement

*It is with great pride and a profound sense of accomplishment that I conclude this important chapter of my academic journey. Pursuing a master's degree in Structural Engineering at Politecnico di Torino, an institution renowned for its academic excellence, distinguished faculty, and strong research tradition, has long been one of my greatest aspirations. It has been both an honor and a privilege to study in such an inspiring academic environment.*

*I would like to express my deepest gratitude to my supervisors, Professor Orazio Baglieri and Professor Lucia Tsantilis, for their invaluable guidance, continuous encouragement, insightful advice, and unwavering support throughout the course of this research. Their expertise, patience, and constructive feedback have been instrumental in the successful completion of this thesis. I am sincerely grateful for the opportunity to learn from them.*

*I would also like to extend my sincere appreciation to Dott. Joseph Nicolas La Macchia, member of Department of Environment, Land and Infrastructure Engineering (DIATI), Politecnico di Torino, for his guidance, technical assistance, and academic support throughout my graduate studies.*

*My deepest gratitude goes to my family for their unconditional love, patience, encouragement, and unwavering support throughout every stage of my academic journey. I wish to pay a special tribute to the memory of my beloved late father, whose strength, resilience, integrity, and belief in the value of education have profoundly shaped the person I am today. Although he is no longer here to witness this achievement, I believe he would have been proud to see the completion of this milestone, and I dedicate this accomplishment to his cherished memory.*

*Finally, I would like to express my sincere appreciation to everyone who has supported, encouraged, and accompanied me throughout this journey. Whether through academic guidance, professional collaboration, friendship, or personal encouragement, your kindness and support have made this achievement possible. I am deeply grateful to each of you.*

**Abstract**

The durability of asphalt pavements is strongly influenced by the rheological performance of the asphalt binder, particularly in terms of fatigue resistance and self-healing capability. Cyclic traffic loading, aging, and environmental effects progressively weaken the binder structure, leading to microcrack initiation, crack propagation, and ultimately pavement failure. In this context, incorporation of waste plastic represents promising strategy to enhance performance of binder. This thesis investigates the healing and fatigue behavior of asphalt binders modified with recycled waste plastics using the Linear Amplitude Sweep (LAS) approach. A comparative experimental study was conducted on three binders: neat 50/70 penetration grade binder, SBS-modified binder, and neat binder modified with 3.3% waste plastic through the wet mixing. Rheological characterization was performed using a Dynamic Shear Rheometer (DSR), including Frequency Sweep (FS), Linear Amplitude Sweep (LAS), Linear Amplitude Sweep Healing (LASH), and Linear Amplitude Sweep Steric Hardening (LAS-SH) tests. Based on experiments, it has been depicted that recycled plastic waste improves the fatigue and healing performance of binder in comparison to the unmodified type. Overall, the modified binders including plastic-modified and SBS have demonstrated how utilization of plastic can be effective in terms of healing and resistance although the dosage is crucial to prevent brittleness of binder.

## INTRODUCTION

Pavement infrastructure constitutes one of the most essential elements of modern civilization, serving as the foundation for communication networks and transportation systems. Activities such as vehicular travel, freight conveyance, and pedestrian movement would be substantially impeded, if not rendered impractical, in the absence of constructed roadways. This multi-layered structure has profoundly transformed human society by enabling efficient mobility and connectivity. Pavement systems are constructed using various methodologies, determined primarily by the classification of the roadway and the anticipated loading conditions of the specific location. These systems are broadly categorized as either rigid or flexible pavements, each engineered to address functional requirements and environmental constraints. The design of pavement structures represents critical consideration within transport and infrastructure engineering. Such designs must satisfy dual imperatives: ensuring the safety of all road users whilst simultaneously delivering economic viability for stakeholders and funding bodies.

A flexible pavement is a multilayer pavement structure in which the surface and binder courses are composed of asphalt mixtures. The asphalt mixture must satisfy both functional and structural performance requirements. Functionally, it should provide adequate skid resistance, smoothness, and driving comfort, while structurally it must effectively distribute traffic loads to the underlying pavement layers.

Throughout its service life, the pavement is continuously exposed to traffic loading and environmental conditions, both of which significantly influence its long-term performance and durability.

The asphalt mixture used in the surface course is directly subjected to traffic loading and environmental conditions. with vehicle wheels, environmental factors, and atmospheric agents, which can cause significant damage such as rutting, thermal and fatigue cracking, and aging. This can result in poor performance. Therefore, the asphalt binder plays a critical role. Fatigue cracking is a phenomenon that arises when the asphalt binder is subjected to repeated loading and unloading cycles, a condition that is referred to as fatigue. Deformations and cracking of the asphalt binder occur in these conditions. It is imperative that the binder exhibits resistance to these phenomena. Furthermore, the asphalt binder's self-healing capacity is a critical factor, as it is capable of self-repair and restoration. Experts have increasingly acknowledged that the properties of a high-quality binder can be improved by modifying it with external additives, such as plastics, to improve its overall performance.

The widespread global use of plastics was facilitated by the introduction of affordable, efficient, and lightweight products. Nevertheless, the disposal of plastic waste became a source of significant concern as this synthetic innovation became more accessible and cost-effective. Scientists and experts proposed the utilization of waste plastics in a variety of industries, such as the road and infrastructure sector, after conducting extensive research and investigation. Plastics were identified as suitable modifiers for asphalt binders to enhance fatigue resistance and self-healing properties due to their durability, light weight, and ability to enhance flexibility. The objective of this thesis is to perform a comprehensive scientific comparison of three distinct asphalt binders, two modified and one virgin, unmodified neat 50/70 binder. The study examines the fatigue resistance and healing capabilities of these binders. One modified binder is Styrene-Butadiene-Styrene (SBS) and the other class is modified neat50/70 biner with addition of 3.35 percent of SUPERPLASTECO waste recycled plastic through wet mixing.

Various methodologies have been developed to rigorously evaluate the self-healing potential of bituminous binders. Laboratory assessments have primarily employed the Dynamic Shear Rheometer (DSR), which enables the precise application of oscillatory shear to systematically characterize binder response under both linear and nonlinear viscoelastic regimes. Moreover, the integration of the Time–Temperature Superposition Principle (TTSP) allows for the quantification of temperature effects, an essential variable influencing binder performance and healing capacity. Recent research has increasingly emphasized the significance of nonlinear viscoelastic behavior, recognizing that substantial deformation levels may induce structural integrity degradation beyond what can be solely attributed to fatigue damage.

The remainder of this thesis is organized as follows: Chapter 1 presents a comprehensive literature review, focusing on the concepts of fatigue resistance, self-healing mechanisms, healing evaluation methods, and the characterization techniques of modified asphalt binders. Chapter 2 describes the experimental program in detail, including the materials used, testing procedures, methodologies, and experimental protocols adopted throughout the study. Chapter 3 presents and discusses the experimental results, providing a detailed analysis of the findings and their implications for the fatigue and healing performance of modified asphalt binders. Finally, Chapter 4 summarizes the main conclusions of the research and offers recommendations for future studies and potential research directions.

# CHAPTER 1 LITRATURE REVIEW

## 1.1- Concept of fatigue and self-healing of asphalt binder

Fatigue resistance refers to the capacity of an asphalt binder to endure repeated cyclic loading without the initiation of significant damage or cracking. In asphalt pavements, traffic-induced tensile and compressive stress is repeatedly applied, leading to the gradual accumulation of microscopic damage within the binder. Over time, these microcracks propagate and merge, forming macrocracks that culminate in fatigue failure, thereby diminishing the pavement's service life [1]. Asphalt binder is a viscoelastic material, exhibiting both elastic and viscous behavior under cyclic loading. The fatigue process occurs in three distinct stages. The first stage, known as the Linear Viscoelastic stage, is characterized by recoverable deformation without permanent damage. The second stage, the Nonlinear Viscoelastic phase, involves the initiation of microcracks and a gradual reduction in stiffness due to damage accumulation. Finally, the fatigue failure stage is reached when microcracks coalesce into macrocracks, causing a rapid decline in stiffness that ultimately leads to failure [1]. The fatigue performance of asphalt binders is influenced by multiple factors, including the grade and composition of the binder. Binders with higher penetration values generally exhibit greater fatigue resistance, whereas stiffer binders tend to have lower resistance. Additionally, loading conditions play a critical role; higher amplitudes or greater deformation rates accelerate fatigue damage. Finally, temperature variations also significantly affect fatigue performance [1]. To evaluate the fatigue of asphalt binders there are a variety of tests that the one of most famous ones is Linear Amplitude Sweep Test in which predicts fatigue life using increasing strain amplitudes. The Linear Amplitude Sweep (LAS) test, combined with the Viscoelastic Continuum Damage (VECD) model, is currently regarded as the preferred method for fatigue characterization, as it offers reliable life predictions within a relatively short testing duration [2].

Binders can partially recover the fatigue damage which is the consequence of cyclic loading and environmental agents, this capability of binder is known as Self-Healing of asphalt binder.

Although the mechanisms responsible for self-healing in bituminous materials are not yet fully understood, self-healing is generally defined as the inherent capability of bitumen to repair microcracks formed within the binder matrix or at the aggregate–binder interface. During a rest period following damage, the material undergoes a recovery process that partially restores its mechanical properties, such as stiffness and strength, thereby enhancing its fatigue resistance and extending its service life [3]. Self-healing is a multifaceted process influenced by various internal mechanisms within the binder as well as numerous external factors [4]. The self-healing behavior of bituminous materials can be explained through a multi-stage physicochemical process. The first stage involves the closure of microcracks driven by the viscous flow of the binder, followed by the adhesion of the crack surfaces. Subsequently, molecular diffusion and chain randomization across the interface restore the continuity of the material, resulting in the recovery of its mechanical properties and improved resistance to further damage [5]. The self-healing capacity of bituminous materials is significantly influenced by the inherent characteristics of the bitumen, which are directly related to its composition and morphology. Moreover, the incorporation of polymeric modifiers into the bituminous matrix alters the self-healing ability of the resulting material. Specifically, the effects of adding the elastomer Styrene-Butadiene-Styrene (SBS) remain uncertain and are subject to varying interpretations [6]. Temperature plays a crucial role in the self-healing process of bitumen by influencing its viscosity and molecular mobility. As the temperature decreases, the viscosity of the binder increases, thereby reducing its ability to flow and limiting the molecular interdiffusion across cracked surfaces. Consequently, the efficiency of the self-healing process is diminished, leading to a lower recovery of the material's mechanical properties [7]. An increase in temperature corresponds to an enhanced recovery capacity of bitumen. Self-healing can also take place over very short durations, provided that the temperature is sufficiently elevated. At ambient temperature, self-healing occurs as well, although the required time is considerably longer. Numerous studies have aimed to identify the optimal healing temperature for bituminous binders. Some researchers argue that this optimal temperature coincides with the bitumen's softening point, while others suggest a range linked to the phase transition temperature [8]. The effect of the rest period on the self-healing process is primarily attributed to the time-dependent nature of wetting and molecular interdiffusion mechanisms. Extending the rest period allows these physicochemical processes to progress more effectively, thereby enhancing the restoration of the binder's microstructure and improving its mechanical properties, including stiffness and strength. Previous studies have suggested that a rest period approximately ten times longer than the loading duration is generally sufficient to achieve a nearly complete recovery of the material's properties [6]. A high load, and consequently an elevated level of stress or deformation, adversely affects the self-repair capacity [9]. Specifically, self-repair is most effective when the damage is minimal, such as in the presence of micro-cracks [10]. Additionally, ageing and humidity are two other factors that negatively impact the self-repair process. Humidity, in particular, exhibits a greater affinity for the aggregates within the bituminous mixture than for the bitumen itself, which may inhibit the occurrence of self-repair [11]. Fatigue resistance and self-healing are fundamentally linked characteristics of asphalt binders.

Fatigue loading leads to the gradual accumulation of microdamage, while self-healing counteracts this damage by mechanisms such as viscous flow, wetting, and molecular diffusion during rest intervals. The interplay between these two processes governs the overall fatigue performance and longevity of asphalt pavements. Therefore, improving the self-healing capacity of asphalt binders through material modifications or optimized loading conditions presents a promising approach to enhance fatigue resistance and extend pavement durability [12].

## 1.2- Concept of LAS-Steric Hardening

Steric hardening, also known as physical hardening, refers to the reversible increase in asphalt binder stiffness that occurs during storage at constant intermediate or low temperatures without chemical oxidation. The phenomenon results from molecular rearrangement, structural relaxation, and the ordering of binder constituents, and it is reversed upon reheating [13,14,15]. Following cooling, asphalt molecules persist in rearranging to achieve a more thermodynamically stable configuration. The crystallization of paraffinic waxes plays a major role in the stiffness increase observed during physical hardening [16]. Physical hardening is also linked to the progressive aggregation of asphaltene molecules into larger supramolecular assemblies. Steric hardening influences LAS results causing higher initial complex modulus, lower phase angle and increasing elastic response.

## 1.3-Characterization of modified binder

The characterization of modified asphalt binder is performed to evaluate the effects of additives on rheological and mechanical behavior of the base binder. In this study, conventional 50/70 penetration grade bitumen was modified using SBS and

Recycled Low Density Plastic (RLDP). The modified binders were characterized through the Dynamic Shear Rheometer (DSR) testing including Frequency Sweep (FS) test, Linear Amplitude Sweep (LAS), Linear Amplitude Sweep Healing (LASH), and Linear Amplitude Sweep -Steric hardening (LAS-SH) tests. The frequency sweep test was used to characterize linear viscoelastic behavior and construct master curves using time temperature superposition principles

(TTSP) and Christian —Anderson (CA) model. Subsequently LAS, LASH, LAS-SH, tests were conducted to evaluate fatigue resistance, self-healing capability and contribution of steric hardening to the recovery of mechanical properties Together, these characterization techniques provide a comprehensive understanding of the influence of SBS and RLDP modification on the performance of asphalt binders under intermediate service temperatures.

# CHAPTER 2- EXPERIMENTAL INVESTIGATIONS

This chapter provides an overview of the entire experimental program, detailing the materials used, the instrumentation employed, the sample preparation process, and the methodological approach, including the conducted test procedures. The experimental work was performed in the road materials laboratory of the Department of Environmental, Land and Infrastructure Engineering (DIATI) at the Politecnico di Torino, specifically in the rheology room, utilizing the Rotational Shear Rheometer (DSR).

## 2.1-Materials

Bitumen is a complex hydrocarbon-based material composed mainly of high-molecular-weight paraffinic and aromatic constituents. Despite its natural occurrence, the bitumen utilized in road construction is primarily derived from the fractional distillation of crude oil, where it remains as the non-volatile residue after the separation of lighter petroleum fractions [17]. Bitumen binder is classified according to their physical and rheological properties including penetration, viscosity, or performance under different temperatures. The grading systems varies depending on country and applicable standards. The penetration grade of an asphalt binder is defined by the penetration depth of a standard needle under specified test conditions: a temperature of 25°C, a load of 100 g, and a loading duration of 5 seconds. The measured penetration value reflects binder consistency, where lower penetration grades indicate stiffer binders and higher penetration grades indicate softer binders.

In this thesis the unmodified neat binder of 50/70 was selected since it is most used paving binder in Europe for highways and urban road [18,19].

Another bituminous biner that was used in this thesis investigation is Styrene–Butadiene–Styrene (SBS) a polymer-modified bitumen in which a thermoplastic elastomer is incorporated into conventional asphalt to improve its rheological and mechanical properties. The SBS polymer consists of two rigid polystyrene end blocks and a flexible polybutadiene mid-block, which interact with bitumen to form a three-dimensional elastic network. This network improves the elasticity and viscoelastic behavior of the binder, resulting in increased resistance to rutting, fatigue cracking, low temperature thermal cracking and improved aging resistance [35,36]. Lastly RLDP modified binder (3.35% Recycled Low Density Plastic) that was produced in laboratory by utilization of specific amount of Neat 50/70 binder modified with a polymeric compound sourced from hard plastic waste. Such a polymeric compound was supplied in granules of 4-6mm, and it is commercially known as SUPERPLAST ECO. The measurements and mixing procedure will be discussed in detail in next chapters.

Figure 2.1-SUPERPLAST ECO plastic granules

The three binders described above were investigated to provide a comprehensive comparison of their rheological behavior. A series of rheological tests were conducted to evaluate and compare their fatigue resistance and self-healing performance.

## 2.2- Instruments

Instruments that have been consumed in this thesis were related to two distinct phase one of which linked to preparation stage that involves warming of binders by oven, mixing procedure to create 3.35% modified binder , for mentioned phase the required equipment are: oven, silicon molds, blanch, high shear mixer machine, fridge, sieve number 0.8, cutter , infrared thermometer. After specimen preparation, the following equipment was used to perform the rheological tests.: cutter, blanch, oven, fridge, rotational dynamic shear or DSR model 302 made by Anton Paar company. Using 8mm parallel plates within an environmentally controlled Peltier system that maintains temperature stability within ±0.1°C, while keeping a 2.0 mm gap and ensuring uniform adhesion between the binder and the plates.

Figure 2.2.1 -Dynamic Shear Rheometer (DSR), MCR 302 Anton Paar

It consists of two plates: an upper plate, which is a cylindrical shaft that can move up and down and may come into different models; in my experiment, the model PP08 was used. PP08 applies rotational torque to the sample; meanwhile, the bottom plate is fixed and positioned horizontally, serving as the surface on which the sample is placed.


Figure2.2.2-PP08 and bottom plate

The machine operates in a way that enables the measurement of the material's rheological properties. It features a black hood used to maintain thermal balance. The DSR is connected to an external cryostat to cool the system during testing. A computer is also used to run the Rheoplus software, monitor data, and conduct tests.

## 2.3- Mixing procedure and challenges

The objective of the mixing process is to alter the properties of the neat binder to improve the mechanical performance of the asphalt binder. This modification is accomplished through a controlled mixing procedure, utilizing specialized equipment and distinct methodologies. The methodologies can be classified as either wet or dry, contingent upon the stage at which the plastic material is incorporated.

In the wet method (the method that was used in this thesis), recycled waste plastic is incorporated directly into hot asphalt binder under controlled temperature and high-shear mixing conditions prior to mixing with aggregates. The plastic particles soften and interact with the binder by absorbing its lighter fractions forming a homogenous polymer modified binder with enhanced rheological properties, improved fatigue and rutting resistance, and increased durability [37,38,39].

The Neat 50/70 and SBS-modified binders were available to use; however, the most challenging aspect of the experimental program was the production of the plastic-modified asphalt binder. During the initial trial, a plastic content of 6.6 % was incorporated into the binder. Under the selected mixing conditions, the plastic particles did not melt or disperse adequately, resulting in an inhomogeneous blend and unsuccessful modification of the binder. The failure of the first mixing attempt is illustrated in the following figure, which highlights the presence of unmelted plastic particles and the lack of a uniform binder matrix.

Figure2.3.1 – plastics on sieve shows mixing failure

figure 2.3.2– unmelted plastics during mixing

As shown in the figures above, the plastic particles were not properly incorporated into the asphalt binder, with most of the material remaining on the sieve after the mixing process. This inadequate dispersion indicated that the initial mixing procedure was unsuccessful and required further optimization to ensure the production of a homogeneous plastic-modified binder.

To overcome this issue and improve the mixing efficiency, two modifications were implemented. The first modification involved reducing the size of the plastic particles by manually cutting them into smaller pieces; although, this process was labor-intensive, it was considered necessary to facilitate melting and enhance the interaction between the plastic and the binder.

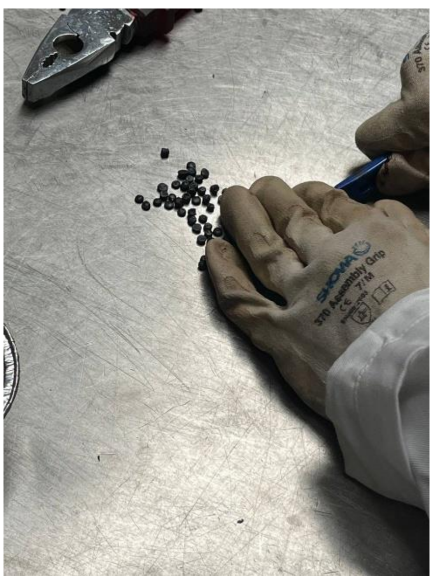

Figure2.3.3 – Cutting plastic pellets manually

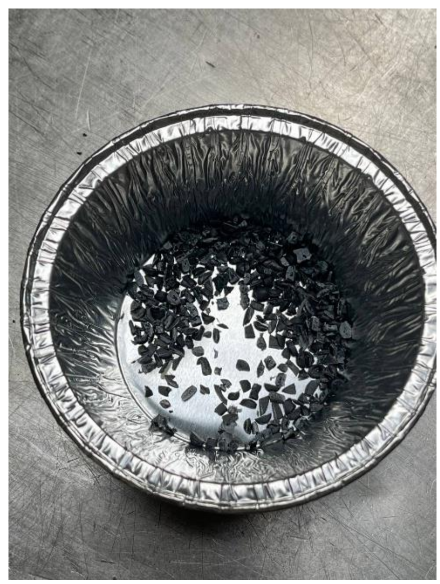

Figure 2.3.4-Dimension of plastic pellets after cutting

The second alteration was reduction of plastic dosage from 6.6% to 3.35% which is almost half of previous dosage. By calculating the exact amount which was used in this experiment was 15.1 gram for 450 grams of neat 50/70 penetration graded binder. The experimental procedure consisted of following main steps: First, the Neat 50/70 asphalt binder was preheated in an oven at 180°C for 2 hours and 30 minutes, during this stage in order to achieve a suitable viscosity the binder was mixed manually by a long cylindrical shaft that was placed in binder's can. In the next step, plastic pellets were added to the binder and by using a medium-high shear mixer (Silverson) operating at 5000 RPM and 1.5 AMPS with initial temperature of 135°C, Plastics were gradually incorporated into the binder at a low percentage while mixing continued. The process of adding plastic continued for 10 minutes. Upon completion; meanwhile, the temperature of the mixture was constantly measuring by an infrared thermometer to make sure about accuracy of procedure, the temperature had increased to 183°C, indicating a positive outcome especially in contrast to a previous trial where temperature loss of 25°C was observed every 5 minutes.

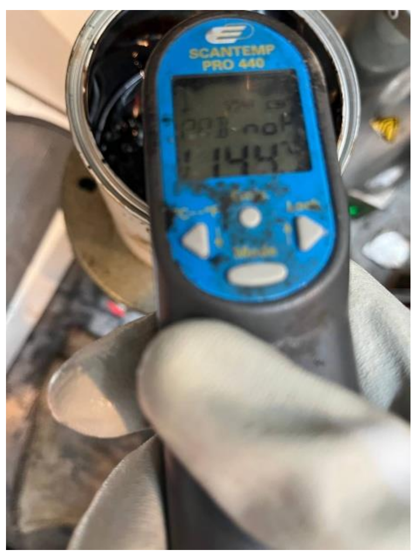


Figure 2.3.5-Measuring mixture temperature by gun thermometer

Then the mixture was allowed to blend thoroughly for an additional 15 minutes, resulting in a total mixing time of 25 minutes as shown below, exhibiting a uniform and homogenous texture.

Figure2.3.6 -Homogenous mixing blend

In the final step, the mixture was cooled at room temperature. This involved preparing the cans and beam molds, which were subsequently filled with the mixture then the mixture was left to cool down within the molds at room temperature for 15 minutes before being transferred to a refrigerator.

Figure2.3.7 -Preparation of beam samples

Afterward, the samples were demolded, wrapped in aluminum foils  and stored for subsequent testing.

Figure 2.3.8-Demolded beam sample

## 2.4- Sample preparation

Neat binder 50-70 was heated in oven with temperature of 180℃ for time interval of two hours and thirty minutes so that the binder gets enough warm and homogenous. Then the binders are poured into silicon molds and left for few minutes in room temperature to cool and then they were transferred to fridge and then removed and demolding was done.

For rheological testing, sample preparation is a prerequisite. During this process, one of the beam samples was cut using a cutter and weighed. The specimen weight was maintained between 0.230 and 0.250 grams. For all tests, a binder weight of 0.245 grams was used consistently across all three binder types: Neat, SBS, RLDP 3.35%.


Figure2.4.1 -Beam sample and cutter

Figure2.4.2 -weighing the sample for the test

After the plastic samples were cut and accurately weighed, the prepared samples were transferred to oven for heating. For the Neat 50/70 asphalt binder, the sample was conditioned at 130°C, following a 5-minute interval protocol consisting of 5 minutes in the oven, 5 minutes at room temperature, and 5 minutes in a refrigerator. In contrast, the modified binders, including the SBS and 3.35%RLDP, were conditioned at 150°C and using a 10-minute interval protocol, comprising 10 minutes in the oven, 10 minutes at room temperature, and 10 minutes in a refrigerator for each stage. The longer conditioning time and higher temperature adopted for the modified binders, were necessary to accommodate their increased viscosity and to ensure adequate thermal equilibration compared with the neat binder.

Figure2.4.3 - Binder specimen during the cooling period after removal from oven

At this stage, the DSR was prepared in advance, with the temperature set to 45°C. Once the sample was removed from the refrigerator, it was placed in the DSR machine and excess binder was carefully removed using a spatula, the black hood was lowered to maintain thermal equilibrium, and the test was initiated.

Figure2.4.5 -Trimming the asphalt binder specimen

## 2.5- Methodological approach

The methodological approach in this thesis integrates experimental protocols and analytical modelling to thoroughly evaluate fatigue and self-healing behavior in bituminous binders. The experimental tests aimed at isolating the truly self-healing capacity of the binders, were conducted under oscillatory conditions with deformation control. To investigate the behavior of binder under small and large amplitude oscillatory conditions the tests are conducted.

### 2.5.1- Frequency Sweep Test

The frequency sweep test is a rheological in which an asphalt binder specimen is subjected to oscillatory shear loading over a range of frequencies while maintaining a constant strain within the linear viscoelastic region. The test measures the complex shear modulus **($G^*$)** and phase angle **($\delta$)**, providing essential information on the binder's stiffness, elasticity, and viscoelastic behavior under different loading conditions. Furthermore, the frequency sweep test serves as the first stage of the Linear Amplitude Sweep (LAS) procedure and provides the linear viscoelastic parameters required for fatigue life prediction based on the Viscoelastic Continuum Damage (VECD) model [20,21,22].

In this part of the thesis by flashing back to Christian-Anderson 1992 summery it is important to note that, Dynamic mechanical analysis, and other methods of viscoelastic testing, are powerful tools in characterizing asphalt binder. However, the interpretation of viscoelastic data can be difficult, and if care is not taken, it can produce misleading conclusions concerning the potential performance of the binders being evaluated.

The master curve, either for creep stiffness or for dynamic complex modulus, is a useful research tool. It can be used to separate time and temperature dependencies, and to evaluate the relaxation processes that occur in a variety of asphalt binder. There are four parameters for the master curve which define its fundamental characteristics: the glassy modulus, the steady-state viscosity, the crossover frequency (or time), and the rheological index. These parameters can be used as input parameters for the prediction of various viscoelastic functions over a wide range of times and temperatures, if the temperature dependency is also known. Indications at this time are that, for mathematical modeling, the temperature dependency can be accurately described by the Williams–Landel–Ferry (WLF) equation at moderate to high temperatures, and an Arrhenius function at low temperatures. A single parameter, Td, defines the temperature dependence through these two functions. Although useful as a research tool, the master curve is not well suited to a direct evaluation of the performance characteristics of asphalt binder. When interpreting the data from a master curve, it should always be kept in mind that it represents the time dependency only at the selected reference temperature and is not indicative of the response at temperatures greatly different from this value. In other words, comparing master curves at a reference temperature of 25°C only gives an indication of the properties at that temperature; the results cannot be generalized to temperatures much higher or lower than this. Similarly, the shift factors only indicate how the master curve is moving with respect to time as the temperature changes. The modulus at a given temperature and loading time is a function of both the master curve and the related shift factors [23].

The formulation below from Christian−Anderson 1992 gives more information in detail about important rheological parameters:

Storage modulus G′, loss modulus G′′ and loss tangent are parameters that are directly related to complex modulus and phase angle and can be calculated through series of relatively simple equations:

$$G'(\omega) = G^*(\omega) \cos \delta$$

While loss modulus is calculated by below formula:

$$G'' (\omega) = G^*(\omega) \sin \delta$$

The storage modulus G′, represents represents the in-phase component of the complex modulus while the loss modulus,G′′, represents the out-of-phase component of the complex modulus.these terms are sometimes misinterpreted as elastic and viscous moduli; in reality elastic component of response only represents part of the loss modulus. In addition to the elastic and viscous response , most real viscoelastic materials exhibit a significant amount of delayed elastic response , which is time dependent but compeletly recoverable. In interpreting the storage and loss moduli it should be kept in mind that both od these parameters reflect a portion of the delayed elastic response.therefore, they cant be restrectly interpreted as elastic and viscous moduli[23].

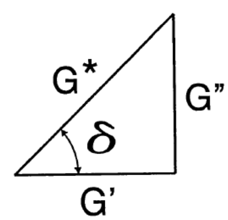


Figuer 2.5.1.1-Relationship between dynamic moduli and phase angle shown shematicly through thr troganometry of a right triangle

Examining the behavior of phase angle as function of frequency, the general shape is sigmoidal. The phase angle at low frequencies, approaches 90° and at very high frequencies 0°. At the crossover frequency, the phase angle generally is very close to 45°[23].

In this research thesis the Frequency sweep test was performed in six different temperature which were 34°C, 28°C, 22°C, 16°C, 10°C, 4°C, while angular frequency was varying between 1 rad/s to 100 rad/s and the strain range was between 1% to 0.01% recording 19 points at each temperature. To guarantee the accuracy of results, for each specimen (Neat, SBS modified binder, 3.35%RLDP modified binder) at least two trials have been performed, and average values were considered for analysis. The variation between repeated measurements remained below 5% for both the complex shear modulus ($G^*$) and phase angle ($\delta$), satisfying the precision requirements specified in AASHTO T 315. By consideration of protocols and principals the tests have been performed with rheometer and then by use of obtained data it is possible to construct master curve. The master curve is constructed to describe the viscoelastic behavior of asphalt binder over a range of loading frequencies and temperatures. Since asphalt binder is thermogeological simple viscoelastic material, its mechanical response depends on both temperature and loading frequency. Master curve combines data obtained at different temperature into a single continues curve using Time–Temperature Superposition Principle (TTSP).

A standard reference temperature must then be selected; generally, 25°C or 0°C is selected [23]. However, the reference temperature of 22°C was selected for this research thesis.

Then shifted with respect to time, until the curve is merged into a single smooth, function [23]. The amount of shifting required at each temperature to form the master curve is of special importance and is called the shift factor a(T). A plot of log a(T) versus temperature is generally prepared in conjunction with the master curve. This type of plot gives a visual indication of how the properties of a viscoelastic material are changing with temperature [23].

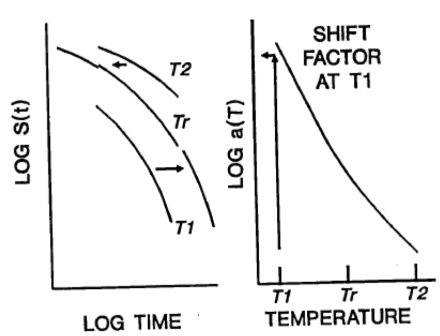


Fgure2.5.1.2-Time temperature superposition

Figure below depicts a typical dynamic master curve where rheological index R is defines as difference between the glassy modulus, Gg, and dynamic complex modulus at the crossover frequency, G(ω0). While the crossover frequency, (ω0), is defined as the frequency at a given temperature where tangent delta is one, at this point the storage and loss moduli are equal. The crossover frequency can be thought of as a hardness parameter, indicating the general consistency of a given asphalt at the selected temperature [23].

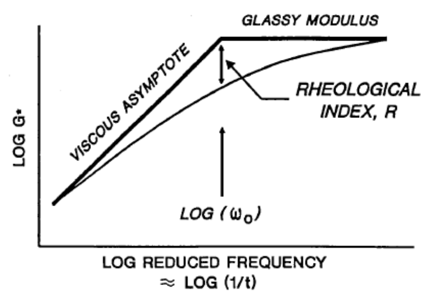


Figure 2.5.1.3-Characteristic parameters of the dynamic master curve

The procedure is continued by calculating shift factor from Williams–Landel–Ferry (WLF) model:

$$\text{Log}(a_T) = -\ C_1(T-T_0)/C_2+(T-T_0)$$

The constants $C_1$ and $C_2$ are empirical parameters determined by the molecular structure of the binder. The derived master curves provide a continuous characterization of binder stiffness over an extensive frequency range spanning from $10^{-4}$ to $10^4$ Hz, thereby enabling the simulation of traffic loading conditions ranging from slow-moving heavy vehicles to high-velocity traffic [24,25].

The Christensen–Anderson (CA) model describes the relationship between the complex modulus and frequency using the following equation:

$$G^*(W) = G_g\left[1 + \left(\frac{W}{W}\right)^{\frac{\log 2}{R}}\right]^{\frac{R}{\log 2}}$$

Where G*(ω) is complex dynamic modulus in, Pa, at frequency ω, rad/s.

In the present study, two reference stiffness values, 5 MPa and 35 MPa, were selected to represent the softening region and the transition region of binder behavior under service conditions, respectively. The corresponding equirigidity temperatures were determined through interpolation of the $|G^*|$-temperature master curves generated using the Christensen–Anderson (CA) rheological model for each binder type, including the neat binder and the RLDP-modified binders containing 3.35% RLDP and SBS modified binder. This parameter directly indicates the binder's temperature sensitivity and performance grade:

- A lower temperature at 5 MPa signifies better flexibility and resistance to low-temperature cracking,
- While a higher temperature at 35 MPa denotes greater stiffness and enhances rutting resistance at elevated service temperatures.

The application of the Christensen–Anderson (CA) model enabled a comprehensive assessment of the modulus evolution and temperature susceptibility of the investigated binders, namely the Neat 50/70 binder and the RLDP-modified binders with 3.35% plastic content and SBS modified binder. By accurately describing the rheological behavior across the investigated temperature range, the CA model established a reliable framework for the subsequent evaluation of fatigue performance using the Linear Amplitude Sweep (LAS) test and self-healing characteristics through the Linear Amplitude Sweep with Healing (LASH) protocol.

### 2.5.2-Linear Amplitude Sweep Test

The fatigue life of the asphalt binders was assessed using the Linear Amplitude Sweep (LAS) test, performed in accordance with the AASHTO TP 101 standard [26]. The LAS methodology provides a rapid and reliable evaluation of fatigue performance by combining linear viscoelastic characterization with progressive damage analysis under increasing strain amplitudes [22]. This method allows for the determination of the material’s fatigue life and the strain level at maximum shear stress, offering essential input parameters for subsequent healing evaluations (LASH tests).

To evaluate the fatigue performance of the investigated asphalt binders, the Linear Amplitude Sweep (LAS) test was conducted using an Anton Paar MCR 301 Dynamic Shear Rheometer (DSR) equipped with 8 mm parallel plates. Prior to testing, the binder specimens were prepared following the sample preparation procedure described in the previous section, ensuring consistent specimen geometry and proper contact between the binder and the testing plates. A 2.0 mm gap was maintained throughout the experiments to comply with the standard LAS testing configuration for asphalt binders. The DSR applied oscillatory shear loading to the specimens, enabling the characterization of their viscoelastic response and fatigue behavior under controlled loading conditions. The use of an 8 mm plate geometry is recommended for intermediate-temperature testing, as it provides accurate measurements while minimizing edge effects and ensuring a uniform stress distribution across the specimen.

The test temperature was set at 15°C and 20°C, representative of intermediate pavement service conditions.

Linear Amplitude Sweep Test or fatigue test is consists of two consecutive stages: stage one is linked to frequency sweep, where binder is subjected to oscillatory loading at a constant strain amplitude of 0.1% over a range of frequencies, where 12 points are recorded five points at frequencies of 0.2, 0.4, 0.6, 0.8, 1 Hz and five points at frequencies of 2, 4, 6, 8, 10 Hz and lastly two points at frequencies of 20 and 30 Hz, this stage is conducted to determine its linear viscoelastic properties such as G* and phase angle . This phase provides input for Viscoelastic Continuum Damage (VECD) model.

While second stage is related to Amplitude Sweep, following the frequency sweep, the binder is subjected to oscillatory loading at a constant frequency of 10Hz while the strain amplitude is increased linearly from 0.1% to 30% over approximately 3100 loading cycles. In this phase the binder progressively damages until failure.

### 2.5.3- LAS-Healing Test

The Linear Amplitude Sweep with Healing (LASH) test is an advanced rheological procedure developed to evaluate the intrinsic self-healing capability of asphalt binders. The methodology extends the conventional LAS test by incorporating a controlled rest period between two loading sequences, allowing the binder to recover part of the accumulated fatigue damage through molecular diffusion and viscous flow. The extent of recovery is quantified by comparing the fatigue response before and after the healing period, providing valuable information on the binder's ability to restore its mechanical properties under conditions representative of intermittent traffic loading. Consequently, the LASH test offers a comprehensive assessment of both fatigue resistance and self-healing performance and has become an effective tool for evaluating conventional and modified asphalt binders [40,27,22].

LAS-Healing Test consists of three phases; the first phase is, the initial damage phase or LAS loading where the binder was subjected to oscillatory shear at a constant strain amplitude corresponding to maximum strain as determined from the LAS test, with a frequency of 10 Hz. This phase was conducted until a predefined damage threshold was attained, typically characterized by a 30% reduction in the initial complex modulus ($G_0$*). This approach ensured consistent damage levels across all binder samples, thereby establishing uniform conditions for subsequent healing analysis. While second phase includes a rest period without loading which is also known as healing phase Following the initial loading stage, the specimen was allowed to rest undisturbed for 30 minutes at the same temperatures (15°C and 20°C). During this period, no external deformation was applied, permitting the material to undergo molecular diffusion, flow, and reconnection at micro-crack interfaces. This process is representative of field rest conditions, such as traffic pauses or nighttime cooling cycles, during which self-healing mechanisms may take place [28,29,30]. And lastly reloading or second LAS loading phase.

To conduct the test procedure using a Dynamic Shear Rheometer (DSR) equipped with 8 mm parallel plates and a 2 mm gap, following the same specimen preparation procedure used for the LAS test is necessary.

### 2.5.4- LAS-Steric Hardening Test

The phenomenon of steric hardening, also referred to as physical or structural hardening, describes the time-dependent increase in stiffness of bituminous binders when maintained at rest under constant temperature in the absence of external loading. This behavior is primarily attributed to molecular reorientation, wax crystallization, and gradual structural rearrangement within the colloidal system of bitumen, rather than to true recovery of fatigue-induced damage. In the context of the Linear Amplitude Sweep with Healing (LASH) procedure, the presence of steric hardening can influence the measured stiffness during rest periods and therefore must be carefully accounted for.

To isolate this effect, dedicated steric hardening control tests were conducted to quantify the intrinsic increase in binder stiffness occurring during rest periods, independent of any prior mechanical loading. This approach enables a clear distinction between genuine self-healing associated with crack closure and molecular diffusion and reversible physico-chemical stiffening due to structural reorganization. By correcting for steric hardening effects, the calculated healing efficiency (H) obtained from the LASH procedure more accurately reflects true damage recovery rather than time-dependent physical aging.

The Linear Amplitude Sweep with Steric Hardening (LAS-SH) approach further provides experimental evidence of this phenomenon by quantifying the increase in binder rigidity after a rest period, thereby allowing the reversible contribution of steric hardening to be explicitly identified and separated from fatigue healing mechanisms [28,31,32,25,33].

In the LAS-SH protocol, the binder specimen is subjected to only one loading sequence following a controlled rest period. Since no fatigue loading is applied prior to the rest period, the test is conducted in the absence of pre-damage, thereby enabling the assessment of the increase in rigidity resulting exclusively from the reversible steric hardening phenomenon rather than from self-healing mechanisms.

The sample preparation and test performance are conducted as previously mentioned for LAS test. This test consists of three stages the first step is related to conditioning of sample while second step is linked to frequency sweep where linear viscoelastic properties are determined and finally Linear Amplitude Sweep (LAS) to evaluate fatigue performance using the VECD approach.

| Material | Test | Temperature | Trials | Rest Time | Trials |
|---|---|---|---|---|---|
| Neat binder 50/70 | Frequency Sweep Test (FS) | T=4-6-10-16-22-28-34°C | --------------- | ------------ | Trial 1 |
| | | | | | Trial 2 |
| | Linear Amplitude Sweep Test (LAS) | T = 15°C | Acceptable | ------------ | Trial 1 |
| | | | Acceptable | | Trial 2 |
| | | T = 20°C | Acceptable | ------------ | Trial 1 |
| | | | Acceptable | | Trial 2 |
| | Linear Amplitude Sweep based Healing (LASH) | T =15°C | Acceptable | 0 Min | Trial 1 |
| | | | Acceptable | | Trial 2 |
| | | | Acceptable | | Trial 3 |
| | | | Acceptable | | Trial 4 |
| | | | Not Acceptable | 30 Min | Trial 1 |
| | | | Acceptable | | Trial 2 |
| | | | Acceptable | | Trial 3 |
| | | | Acceptable | | Trial 4 |
| | | T = 20°C | Acceptable | 0 Min | Trial 1 |
| | | | Acceptable | | Trial 2 |
| | | | Acceptable | | Trial 3 |
| | | | Acceptable | 30 Min | Trial 1 |
| | | | Acceptable | | Trial 2 |
| | Linear Amplitude Sweep with Steric Hardening Test (LAS-SH) | T = 15°C | Acceptable | 30 Min | Trial 1 |
| | | | Acceptable | | Trial 2 |
| | | | Not Acceptable | | Trial 3 |
| | | | Not Acceptable | | Trial 4 |
| | | T = 20°C | Acceptable | 30 Min | Trial 1 |
| | | | Acceptable | | Trial 2 |
| | | | Not Acceptable | | Trial 3 |

Table2.5.4.1 -Data related to Neat 50/70

| Material | Test | Temperature | Trials | Rest Time | Trials |
|---|---|---|---|---|---|
| Neat binder50/70 + 3.3% RLDP | Frequency Sweep Test (FS) | T=4-6-10-16-22-28-34°C | ------------------- | ------------------- | Trial 1 |
| | | | | | Trial 2 |
| | Linear Amplitude Sweep Test (LAS) | T = 15°C | Acceptable | ------------------------ | Trial 1 |
| | | | Acceptable | | Trial 2 |
| | | T = 20°C | Not Acceptable | ------------------------ | Trial 1 |
| | | | Acceptable | | Trial 2 |
| | | | Not Acceptable | | Trial 3 |
| | | | Acceptable | | Trial 4 |
| | Linear Amplitude Sweep based Healing (LASH) | T = 15°C | Not Acceptable | 0 Min | Trial 1 |
| | | | Acceptable | | Trial 2 |
| | | | Not Acceptable | | Trial 3 |
| | | | Not Acceptable | | Trial 4 |
| | | | Acceptable | | Trial 5 |
| | | | Not Acceptable | 30 Min | Trial 1 |
| | | | Acceptable | | Trial 2 |
| | | | Acceptable | | Trial 3 |
| | | T = 20°C | Acceptable | 0 Min | Trial 1 |
| | | | Acceptable | | Trial 2 |
| | | | Acceptable | | Trial 3 |
| | | | Not Acceptable | 30 Min | Trial 1 |
| | | | Not Acceptable | | Trial 2 |
| | | | Acceptable | | Trial 3 |
| | | | Acceptable | | Trial 4 |
| | | | Acceptable | | Trial 5 |
| | | | Acceptable | | Trial 6 |
| | Linear Amplitude Sweep with Steric Hardening Test (LAS-SH) | T = 15°C | Not Acceptable | 30 Min | Trial 1 |
| | | | Acceptable | | Trial 2 |
| | | | Acceptable | | Trial 3 |
| | | T = 20°C | Not Acceptable | 30 Min | Trial 1 |
| | | | Acceptable | | Trial 2 |
| | | | Not Acceptable | | Trial 3 |
| | | | Acceptable | | Trial 4 |

Table 2.5.4.2-Data related to modified binder with 3.3% of RLDP

| Material | Test | Temperature | Trials | Rest Time | Trials |
|---|---|---|---|---|---|
| SBS modified binder | Frequency Sweep Test (FS) | T=4-6-10-16-22-28-34°C | ------------------------ | ------------------- | Trial 1 |
| | | | | | Trial 2 |
| | Linear Amplitude Sweep Test (LAS) | T = 15°C | Not Acceptable | ------------------- | Trial 1 |
| | | | Acceptable | | Trial 2 |
| | | | Not Acceptable | | Trial 3 |
| | | | Acceptable | | Trial 4 |
| | | | Acceptable | | Trial 5 |
| | | | Acceptable | | Trial 6 |
| | | T = 20°C | Not Acceptable | ------------------- | Trial 1 |
| | | | Not Acceptable | | Trial 2 |
| | | | Acceptable | | Trial 3 |
| | | | Acceptable | | Trial 4 |
| | | | Acceptable | | Trial 5 |
| | Linear Amplitude Sweep based Healing (LASH) | T = 15°C | Not Acceptable | 0 Min | Trial 1 |
| | | | Not Acceptable | | Trial 2 |
| | | | Not Acceptable | | Trial 3 |
| | | | Not Acceptable | | Trial 4 |
| | | | Not Acceptable | | Trial 5 |
| | | | Acceptable | | Trial 6 |
| | | | Acceptable | | Trial 7 |
| | | | Not Acceptable | 30 Min | Trial 1 |
| | | | Acceptable | | Trial 2 |
| | | | Not Acceptable | | Trial 3 |
| | | | Not Acceptable | | Trial 4 |
| | | | Acceptable | | Trial 5 |
| | | T = 20°C | Acceptable | 0 Min | Trial 1 |
| | | | Acceptable | | Trial 2 |
| | | | Acceptable | | Trial 3 |
| | | | Not Acceptable | 30 Min | Trial 1 |
| | | | Acceptable | | Trial 2 |
| | | | Acceptable | | Trial 3 |
| | | | Acceptable | | Trial 4 |
| | Linear Amplitude Sweep with Steric Hardening Test (LAS-SH) | T = 15°C | Acceptable | 30 Min | Trial 1 |
| | | | Not Acceptable | | Trial 2 |
| | | | Acceptable | | Trial 3 |
| | | | Acceptable | | Trial 4 |
| | | T = 20°C | Acceptable | 30 Min | Trial 1 |
| | | | Acceptable | | Trial 2 |
| | | | Not Acceptable | | Trial 3 |
| | | | Acceptable | | Trial 4 |

Table 2.5.4.3-Data related to SBS modified binder

# CHAPTER 3-DATA ANALYSIS

This chapter details the processing, analysis, and interpretation of experimental data derived from the rheological characterization of SBS modified binder and recycled low-density polyethylene (RLDP) modified binders, containing 3.35 % by weight. These results are evaluated against the performance benchmarks of a reference Neat 50/70 bitumen. The primary objective is to synthesize findings from various testing protocols into a unified framework that characterizes the viscoelastic properties, fatigue resistance, and healing potential of the investigated materials.

This section is classified in several parts each of which addressing the results, diagrams and analytical numeric that are a link to specific tests which have been performed. In very first part the results obtained from the Frequency Sweep (FS) tests were processed and analyzed to characterize the linear viscoelastic (LVE) behavior of the investigated asphalt binders. The experimental data collected at different temperatures were shifted according to the time–temperature superposition principle (TTSP) and subsequently fitted using the Christensen–Anderson (CA) rheological model to construct the master curves of the complex shear modulus (|G*|) and phase angle (δ). These master curves were then used to determine the fundamental viscoelastic properties of the binders, including stiffness, temperature susceptibility, and the Equi rigidity temperatures corresponding to 5 MPa and 35 MPa. The resulting parameters provide a comprehensive rheological characterization and establish a reliable reference framework for the subsequent evaluation of fatigue performance and self-healing behavior. In addition ,second part is dedicated to Linear Amplitude Sweep results where three different type of biners( Neat, SBS modified binder, modified binder with 3.35%RLDP) are scientifically based on  laboratory tests are compared in terms of fatigue resistance; while , in third part data linked to results of healing performance of Neat and two other modified binders are depicted in order to illustrate how effectively each binder has healed under two different conditions one when no rest was given to the specimen and once when it has rested for 30 minutes to have time to recover and perform self-healing, and finally data related to LAS-Steric hardening test that is not representing true recovery but more a physical stiffness.

## 3.1-Linear Viscoelastic Characterization

Linear viscoelastic characterization is a fundamental step in the rheological evaluation of asphalt binders. As it describes the material response under small-amplitude oscillatory loading where stress and strain remain linearly proportional [23]. and independent of loading amplitude , this characterization commonly is performed through Frequency Sweep test using a dynamic shear (DSR), in which the complex shear modulus ($|G^*|$) and phase angle ($\delta$) are measured over a range of loading frequencies , while maintaining a constant strain within the LVE region [20,23].The experimental data are subsequently shifted according to the Time–Temperature Superposition Principle (TTSP) and fitted using rheological models, such as the Christensen–Anderson (CA) model, to construct master curves that comprehensively describe the stiffness and viscoelastic behavior of asphalt binders across a broad range of temperatures and loading conditions.

Frequency sweep tests were performed for each binder, and specimen is explained in previous sections in a temperature range of 4°C to 34°C while the loading frequency spanned from 1 rad/s and 100 rad/s. The table below shows critical data related to Frequency Sweep test for all three-binder type because of perfect convergency of trials data referring to second trial is provided; here $T_0$ representing the reference temperature that in this thesis 22°C was considered.

| CA Model | Neat50/70 (2ND TRIAL) | SBS (2ND TRIAL) | RLDP3.3% (2ND TRIAL) |
|---|---|---|---|
| T0 | 22 | 22 | 22 |
| C1 | 23.9 | 17.9 | 18.2 |
| C2 | 175.9 | 143.9 | 137.8 |
| Log $G_g$ | 5.56 | 5.86 | 5.83 |
| Log W | 2.75 | 2.44 | 2.19 |
| R | 1.32 | 1.75 | 1.82 |

Table 3.1.1-Data related to frequency sweep test for Neat, SBS, modified binder with 3.35% RLDP

The frequency sweep data, shifted according to the Time–Temperature Superposition Principle, were fitted using the Christensen–Anderson (CA) model to describe the viscoelastic transition region of the binders. The resulting model parameters demonstrated a high degree of consistency among the RLDP-modified binders, with log $(G_g)$ values of 5.56, 5.86, 5.83 and R values of 1.32, 1.75, 1.82 suggesting similar thermorheological characteristics and structural stability.

In the diagrams below master curves related to three different types of asphalt binders of second trial has been shown.

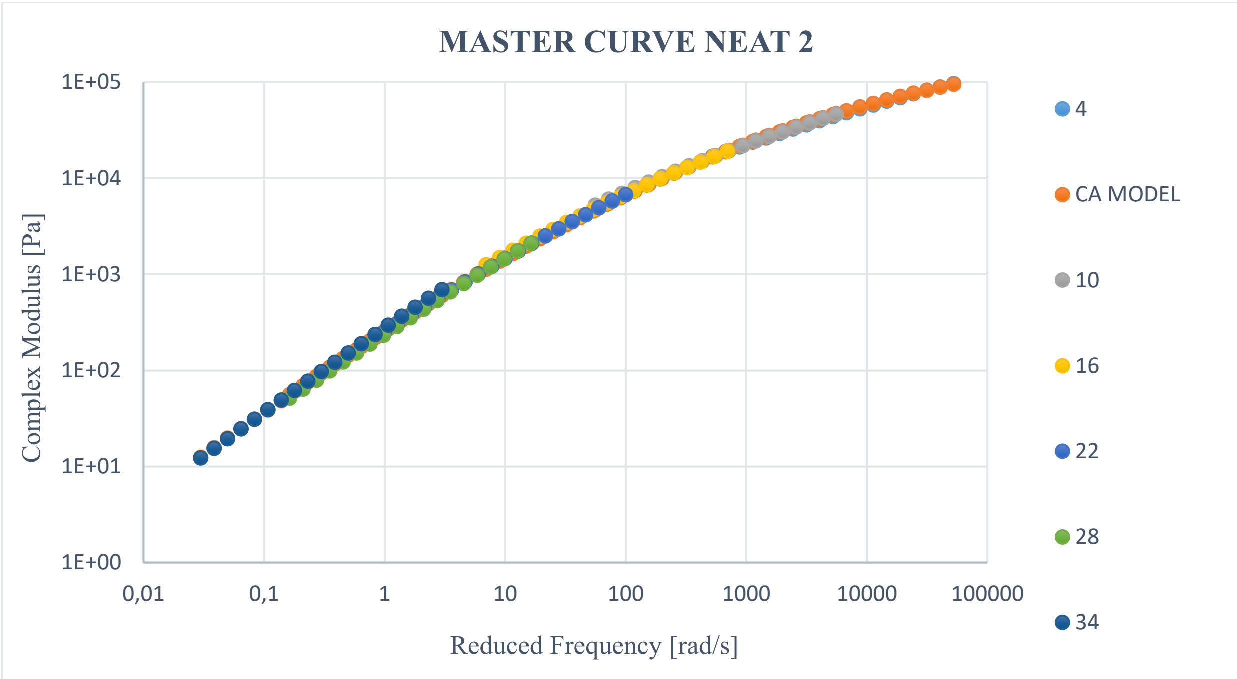


Figure 3.1.1-Master curve of complex modulus and reduced frequency related to Neat 50/70 Trial 2

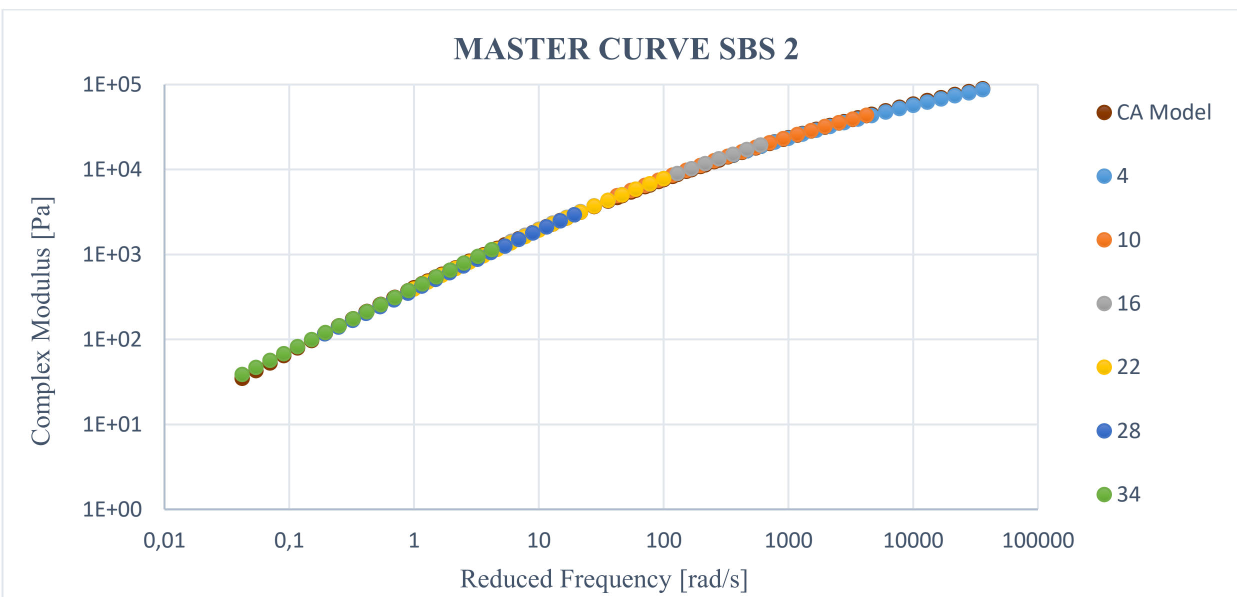


Figure3.1.2 -Master curve of complex modulus and reduced frequency related to SBS modified binder Trial 2

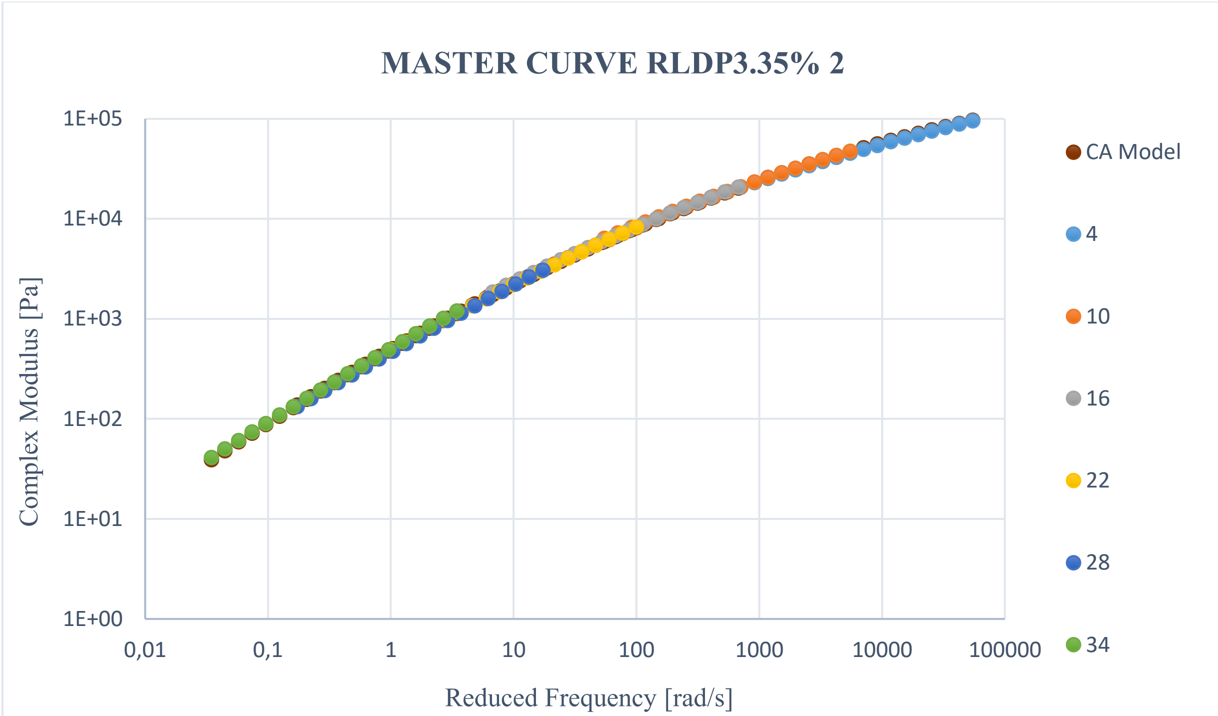


Figure3.1.3 -Master curve of complex modulus and reduced frequency related RLDP3.35% Trial 2

As is shown in above diagrams for all three types of binders Y axis represents the complex modulus in Pascal while X axis demonstrates reduced frequency in radian per seconds; it is evident that the temperature data are perfectly aligned with CA model. At the lowest part of the graph to the topset part of the graph the temperature from highest (34°C) shifts to the lowest temperature (4°C). According to the graphs above by increasing reduced frequency the complex modulus also increases; moreover, the complex modulus has higher values in lower temperature and lower at higher temperatures (at 34°C).

To make a clear comparison between three asphalt binder specimens (Neat, SBS, RLDP3.35%) the master curve below is dedicated which is the average of two trials:

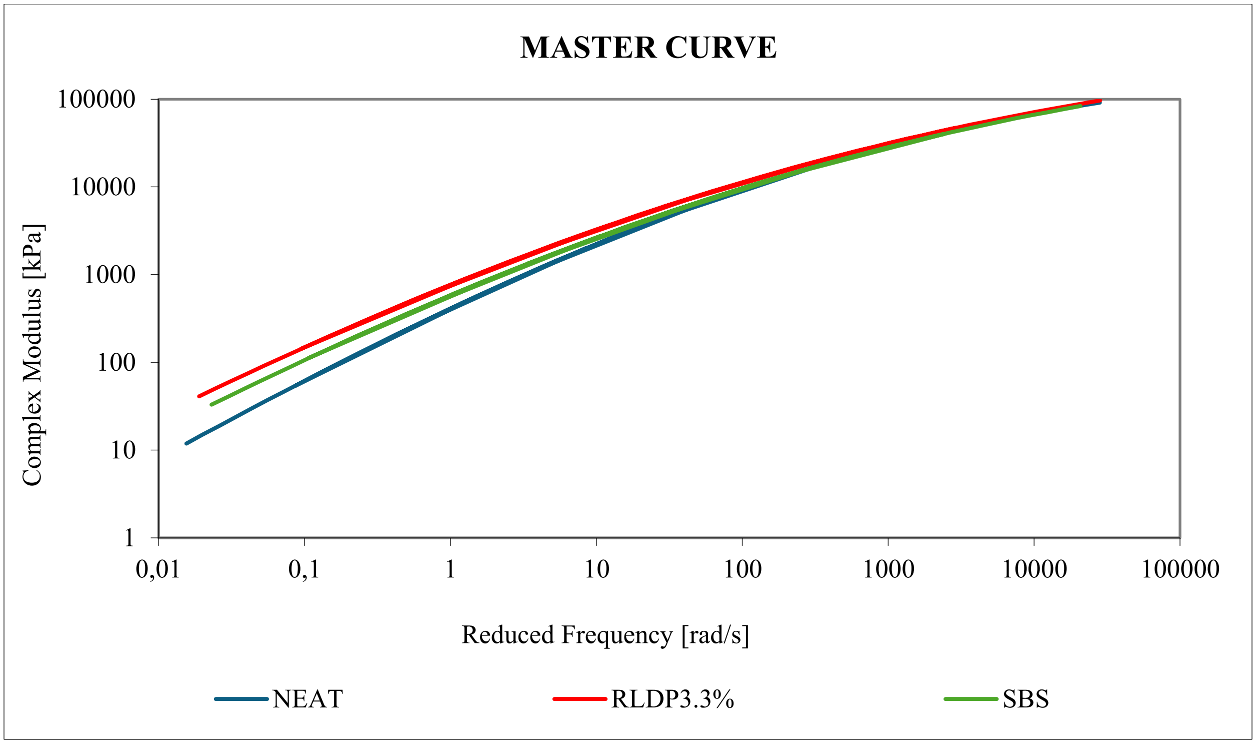


Figure 3.1.4-Master curve of complex modulus and reduced frequency related to average CA model for Neat 50/70, SBS and RLDP3.35%

As is shown in above diagram in all cases the complex modulus ($|G^*|$) is increased by increasing the reduced frequency, reflecting the typical viscoelastic behavior of asphalt binders. The RLDP3.35% modified binder exhibited the highest modules values over the most of frequency range, indicating an increase in stiffness resulting from incorporation of recycled waste plastic. The SBS modified binder also demonstrated enhanced stiffness compared with the neat binder, although to a lesser extent than the RLDP 3.35% modified binder. As is shown in the figure above the difference between the samples are more pronounced at low frequencies, corresponding to high temperature service conditions, suggesting improved resistance to permanent deformation and rutting for the modified binders while at high reduced frequencies, the complex modulus values of the investigated binders became increasingly similar, indicating a diminished influence of SBS and RLDP modification under rapid-loading or low-temperature conditions. Nevertheless, both modifiers enhanced the overall rheological response of the binder while maintaining thermorheological consistency throughout the examined frequency domain.

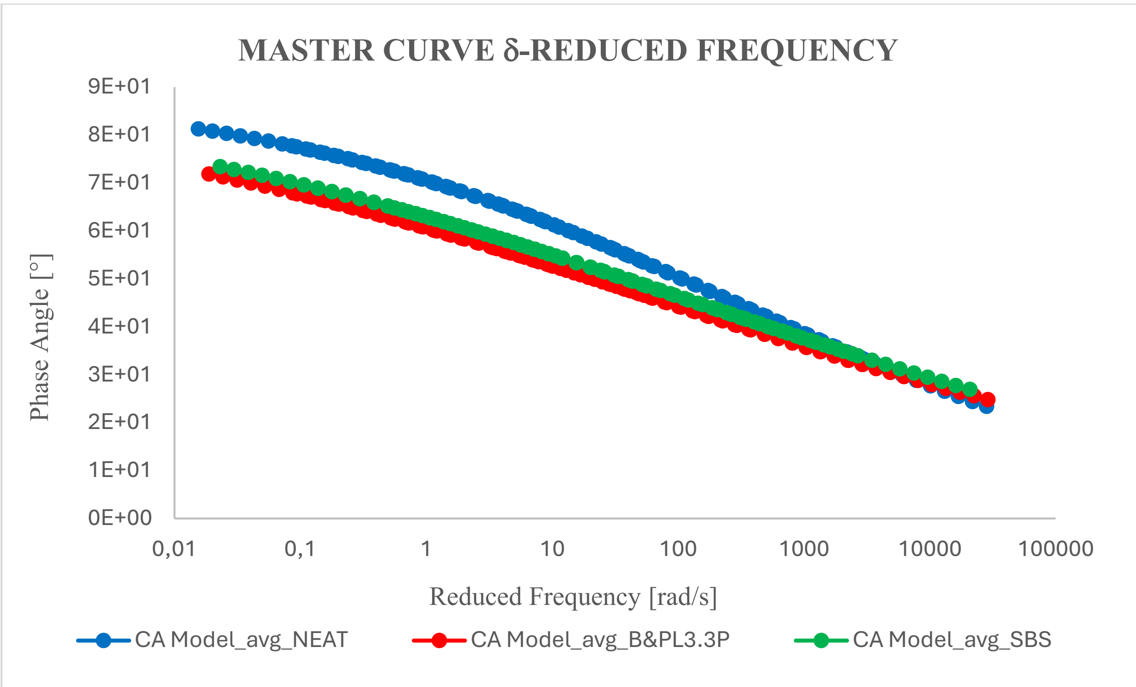


Figure 3.1.5-Master curve of phase angle and reduced frequency related to average CA model for Neat 50/70, SBS and RLDP3.35%

As mentioned previously phase angle is an important factor since it represents the viscoelastic behavior of asphalt binder, the range of 0 to 90 represents pure elastic to pure viscose behavior.

The comparison figure above illustrates that the phase angle for all three binder categories is decreasing by reduction of reduced frequency. The behavior of asphalt binder indicates a gradual transition from a more viscose response at low frequencies to a more elastic response at high frequencies. At low reduced frequencies, the neat binder demonstrates the highest phase angle values (approximately 80°), indicating a predominantly viscous behavior. In contrast, both modified binders exhibit lower phase angles, with the RLDP-modified binder showing the lowest values across most of the frequency spectrum. This indicates that the addition of SBS and RLDP enhances the elastic component of the binder's response, thereby reducing its tendency toward viscous deformation, moreover, in the intermediate frequency range the modifies binders (RLDP3.35% and SBS) continue to exhibit lower phase angles than the neat binder, which indicates the addition of modification substances such as plastics and polymers improved elastic recover and refined resistance to permanent deformation. Among the three binder types RLDP3.35% has shown the lowest phase angle that categorizes it as the best among the three binder types. However, at the end part of the graph where is indicating highest reduced frequency range the binders shows a closely spaced behavior specifically in range of 24° to 27° which is a sign to conclude, the impact of modification of binder becomes less effective under rapid-loading or low-temperature conditions and response of asphalt binders becomes increasingly elastic.

In following part, the black comparison diagram related to Neat50/70, SBS and RLDP3.3% is depicted below :

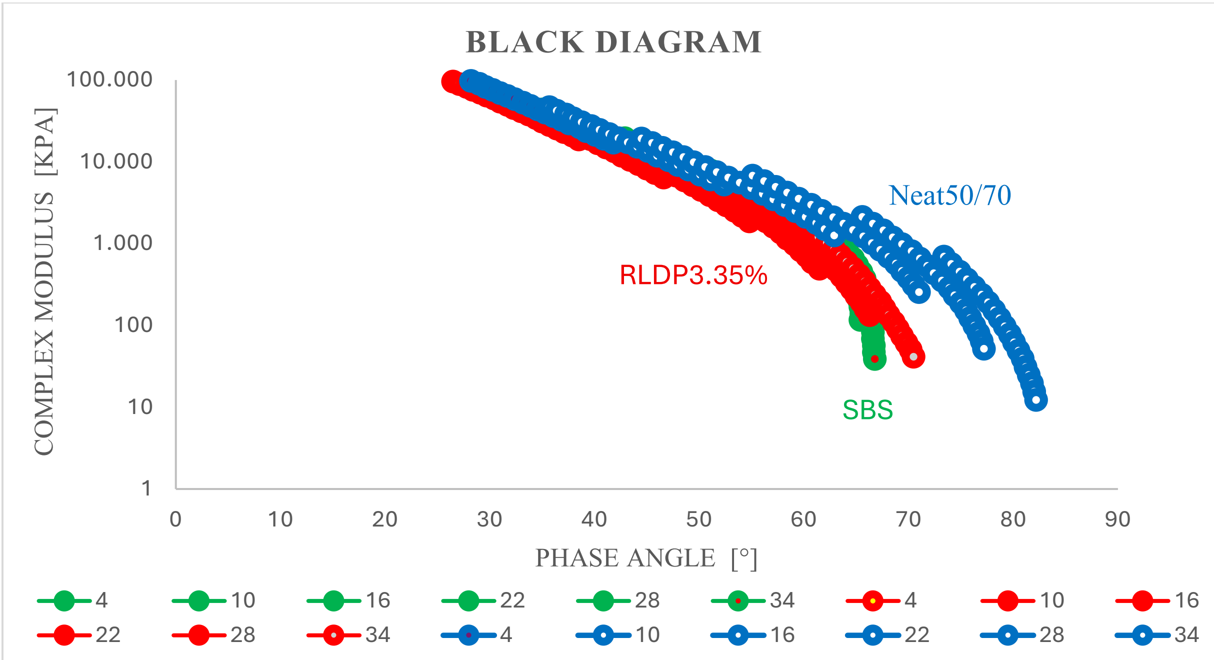


Figure3.1.6 -Black diagram of complex modulus and phase angle

A Black diagram plots the complex shear modulus (|G|) against the phase angle (δ), removing the explicit temperature and frequency axes and allowing comparison of the intrinsic rheological behavior of different asphalt binders [36,23].

Unlike master curve, the black diagram doesn't require time-temperature shifting and is therefore used to assess intrinsic viscoelastic behavior and thermorheological consistency of binders. A smooth continues behavior between G* and δ indicates thermorheologically simple behavior while the deviation from a single curve demonstrates structural changes or effect of polymer modification as is shown at graph above the inward tail is related to SBS modified binder.

### 3.2- Fatigue Resistance

The fatigue performance of the investigated binders was assessed using the Linear Amplitude Sweep (LAS) test, which is designed to characterize the material's resistance to fatigue damage under progressively increasing strain amplitudes. The testing procedure was conducted in accordance with AASHTO TP 101-14 and followed the methodology proposed by De Leonardis (2022). All experiments were performed using an Anton Paar Dynamic Shear Rheometer (DSR) equipped with 8 mm parallel plates and a 2 mm testing gap. To simulate intermediate pavement service conditions, where fatigue cracking is most likely to occur, the LAS tests were carried out at 15 °C and 20 °C. These temperatures were selected to evaluate the influence of binder modification on fatigue resistance under representative in-service conditions.

To ensure the reliability and repeatability of the experimental results, a minimum of two replicate tests were performed for each binder and testing condition. For the neat 50/70 binder, two trials were conducted at both 15 °C and 20 °C, yielding highly consistent and convergent results. Similarly, for the RLDP-modified binder (3.35%), two replicate tests were carried out at 15 °C, demonstrating satisfactory agreement. At 20 °C, four trials were performed, trials 2 and 4 exhibited the highest level of consistency and were therefore considered representative of the material behavior.

A greater number of repetitions was required for the SBS-modified binder due to the increased variability observed during testing. At 15 °C, a total of six LAS tests were conducted, with trials 2, 4, 5, and 6 showing good repeatability and convergence. Likewise, at 20 °C, five trials were performed, among which trials 3, 4, and 5 produced consistent results and were subsequently selected for analysis. This testing approach ensured that the reported fatigue parameters were based on reproducible measurements and accurately reflected the rheological behavior of the investigated binders.

To ensure the robustness and reproducibility of the experimental program, the repeatability of the LAS tests was assessed through a statistical comparison of the corresponding shear stress–strain responses obtained from multiple replicate specimens. A maximum deviation threshold of 5% was adopted as the acceptance criterion for convergence. Only those trials satisfying this requirement were retained for further analysis and interpretation. This quality-control procedure reduced the impact of potential experimental artefacts associated with slight variations in specimen fabrication, sample thickness, trimming accuracy, and contact conditions at the binder–plate interface. As a result, the reported fatigue parameters are considered representative of the true rheological behavior of the investigated binders and provide a reliable basis for subsequent comparative analyses.

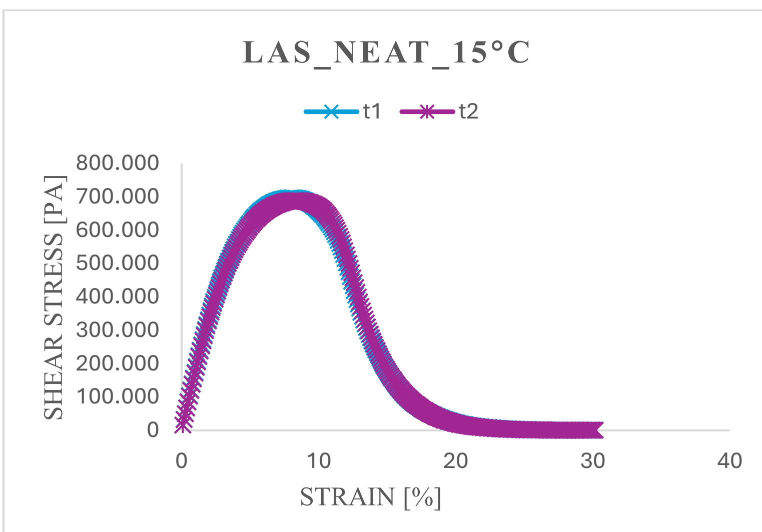


Figure3.2.1 -LAS 15°C stress-strain curves of trials for Neat50/70

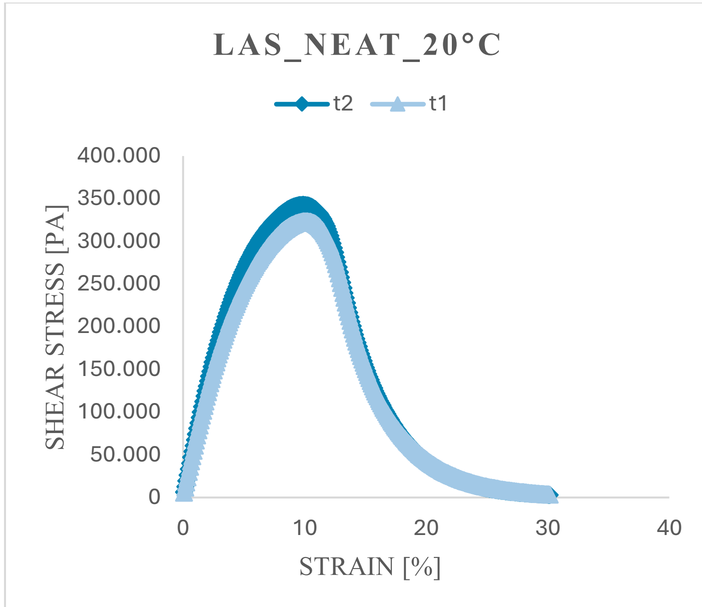


Figure3.2.2 -LAS 20℃ stress-strain curves of trials for Neat 50/70 curves of trials

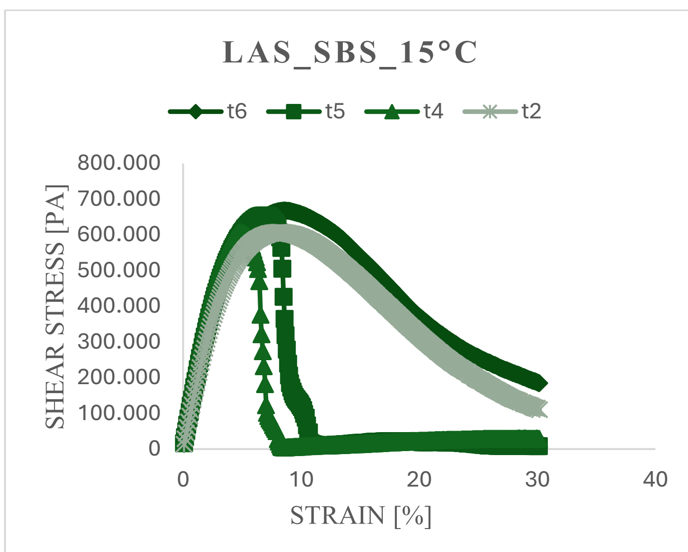


Figure3.2.3 -LAS 15℃ stress-strain curves of trials for SBS modifies binder

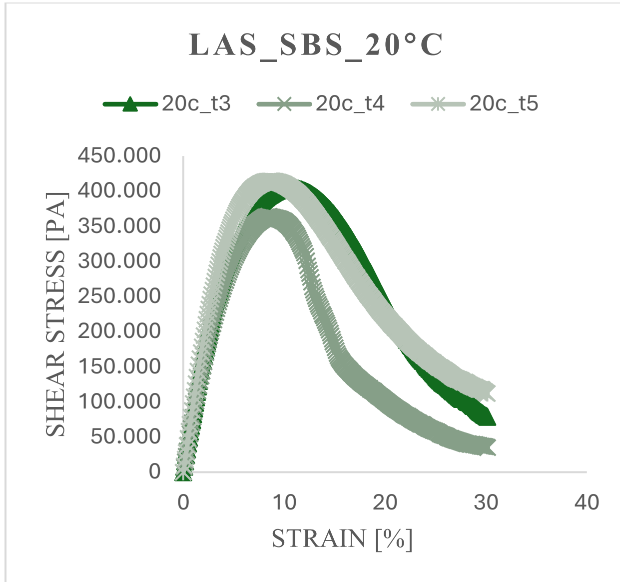


Figure3.2.4 -LAS 20℃ stress-strain curve of trials for SBS modified binder

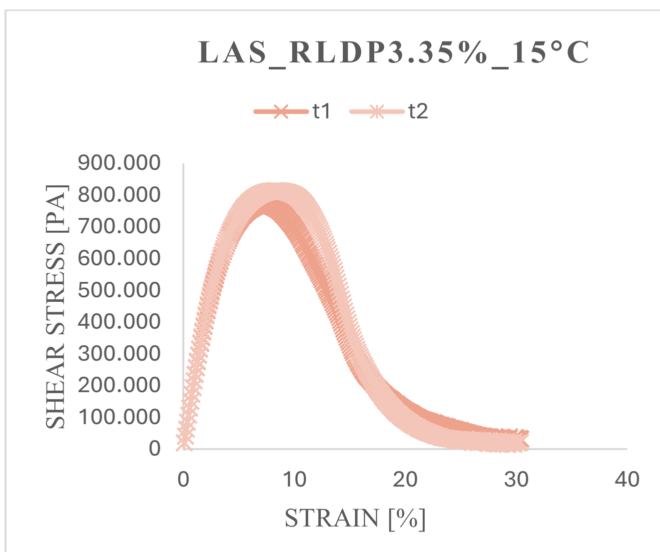


Figure 3.2.5-LAS 15℃ strain-stress curves of trials for RLDP 3.3% modified binder

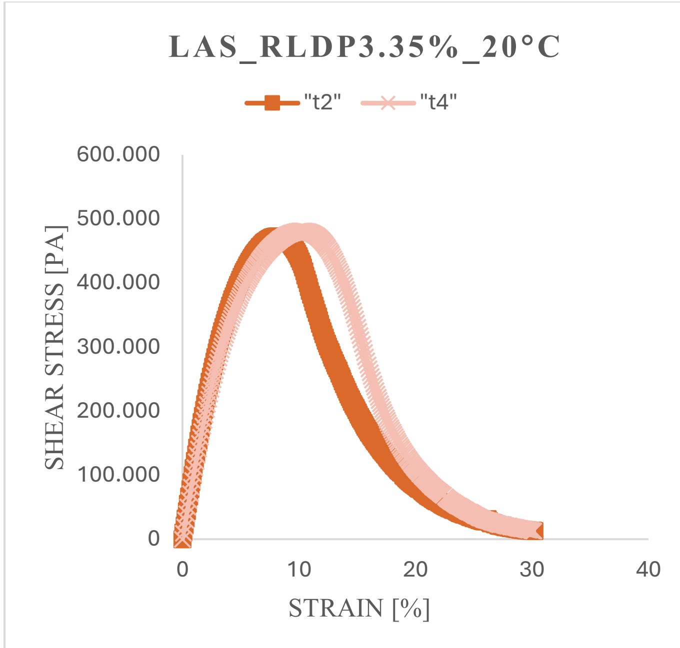


Figure3.2.6 -LAS 20℃ stress-strain curves of trials for RLDP3.35% modified binder

Based on above figures it is evident that for Neat 50/70 and modified binder with 3.35% RLDP the trials display good repeatability for both 15℃ and 20℃ while for SBS modified binder repeatability is not as high as two other binders.

To ensure a consistent comparison among the investigated binders, reference strains were established for the two test temperatures (15°C and 20°C). The reference strains were determined by plotting the average shear stress–strain curves obtained from the acceptable trials for the three binders: Neat 50/70, SBS-modified, and 3.35% RLDP-modified binders.

The strain corresponding to the peak shear stress was identified for each binder, and the average values are presented in the table below. Based on these results, a reference strain of 8% was selected for 15°C, while a reference strain of 10% was adopted for 20°C.

| STRAIN [%] | 15°C | 20°C |
|---|---|---|
| NEAT | 8,162 ~= 8 | 9,97 ~ =10 |
| RLDP3.35% | 7,81 ~ = 8 | 9,52 ~ = 10 |
| SBS | 7,9 ~ = 8 | 9,67 ~ = 10 |

Table 3.2.1-considered reference strains for the given temperature and materials

In graph below a comparison of linked to acceptable trials for two modified asphalt binder categories at 15°C and 20°C are given:

As is illustrated below at temperature of 15°C all trials of RLDP3.3% are placed higher than SBS trials which makes it clear that the modified binder containing 3.35% waste plastic has performed a better resistance than SBS modified binder, it tolerated higher shear stress at same peaks.

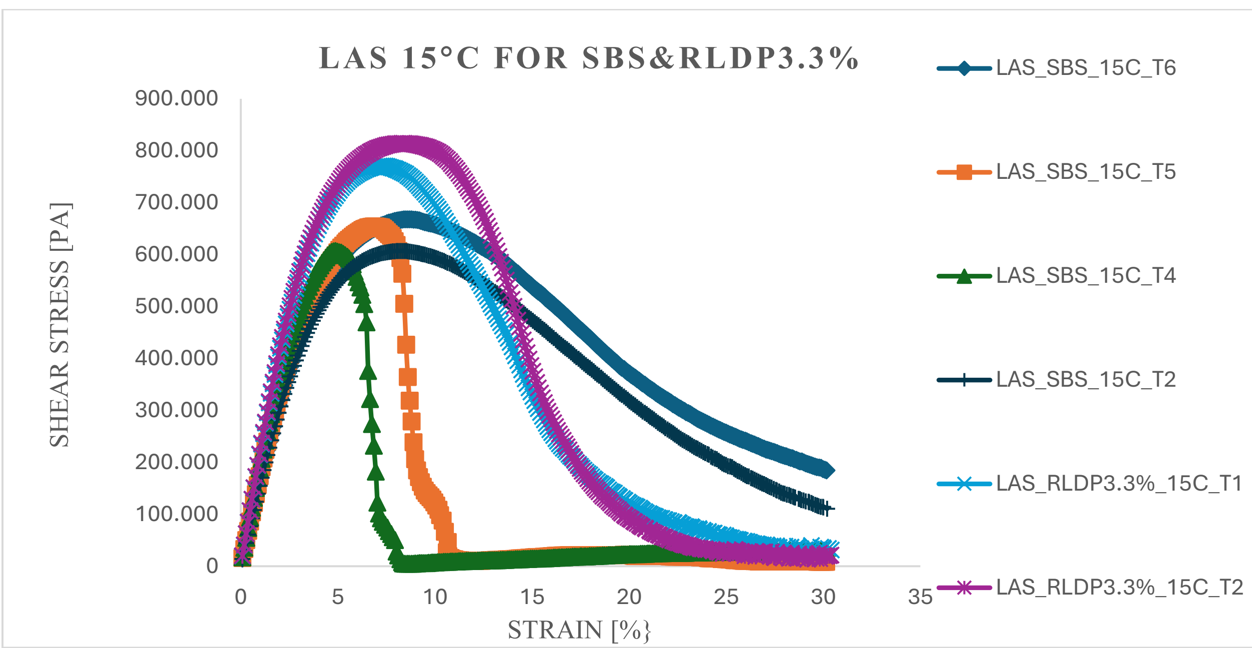


Figure3.2.7 – comparison of LAS 15℃ stress strain curves related to RLDP3.3% modified binder and SBS modified binder

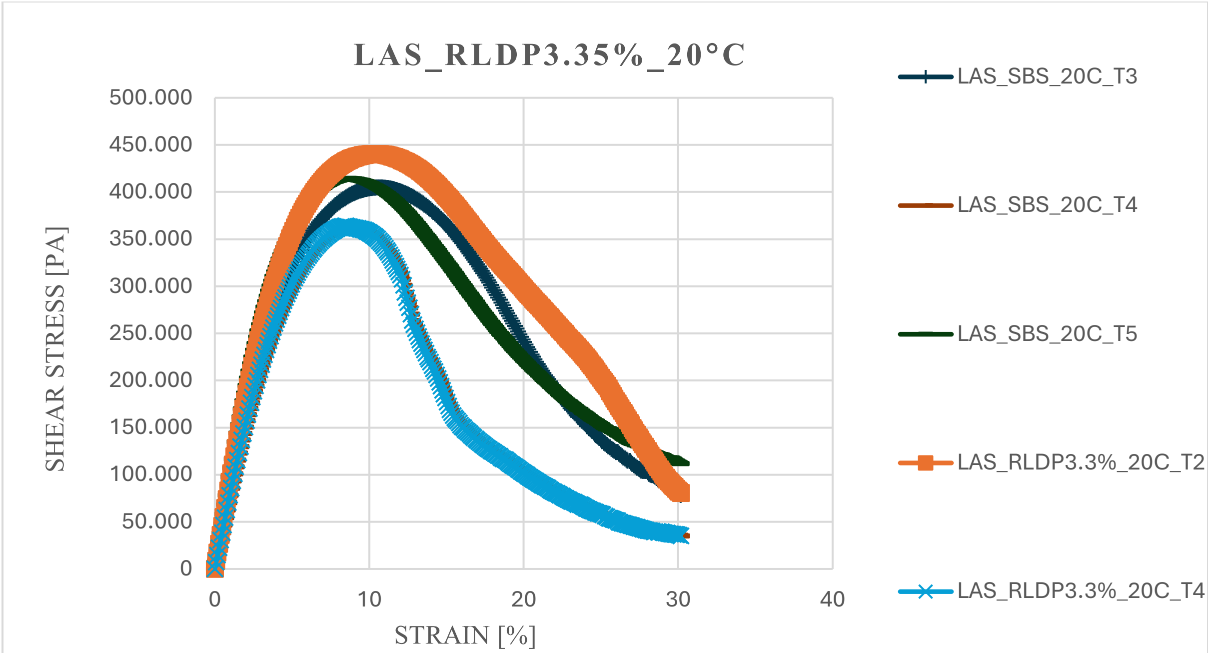


Figure 3.2.8– comparison of LAS 20℃ stress strain curves related to RLDP3.35% modified binder and SBS modified binder

### 3.3 Self-Healing

The Linear Amplitude Sweep with Healing (LASH) tests were performed after determining the peak tensile deformation from the corresponding LAS tests for each binder and testing temperature. Based on the values reported in Table 3.2.1, the deformation threshold at which the first loading phase was interrupted was established for each material. Once this predefined deformation level was reached, a 30-minute rest period was introduced to allow for potential recovery of fatigue-induced damage through self-healing mechanisms. Following the rest period, a second loading phase was applied under the same testing conditions.

Representative comparison plots of the LASH tests conducted with and without the 30-minute rest period at the selected testing temperatures are presented in the following figures.

Figure below shows the first loading phase and second loading phase after 30 minutes rests for acceptable trials for Neat 50/70, SBS modified binder and modified binder with 3.35% RLDP at 15℃ which depicts good repeatability.

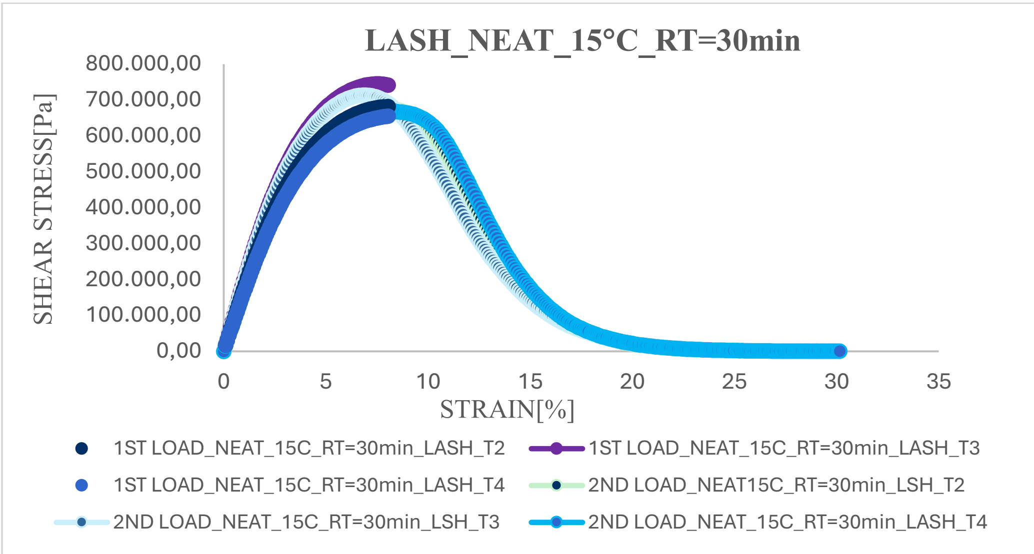


Figure3.3.1 -stress-strain curves related to healing test with 30 minutes rest for Neat50/70 at 15℃

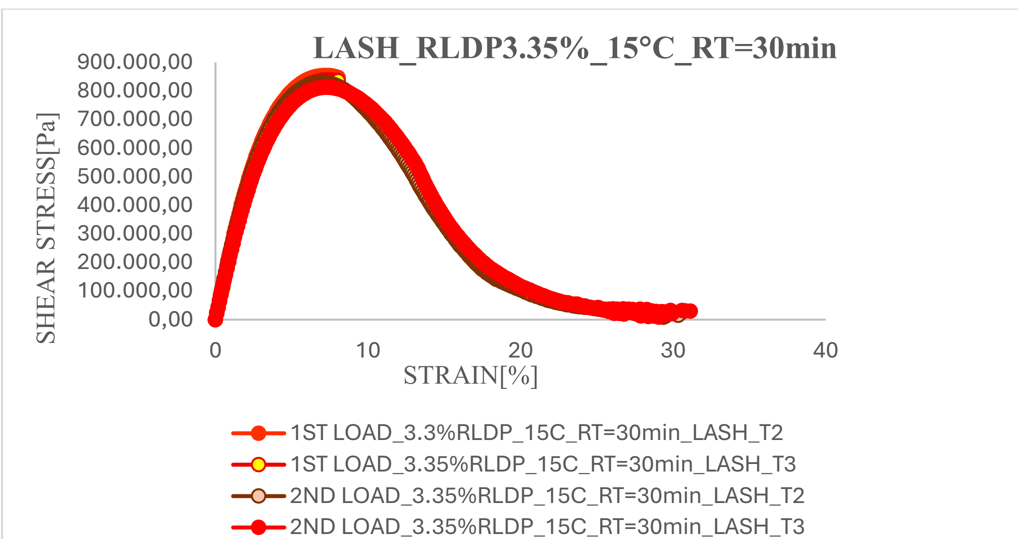


Figure 3.3.2-stress-strain curves related to healing test with 30 minutes rest for RLDP3.3% at 15℃

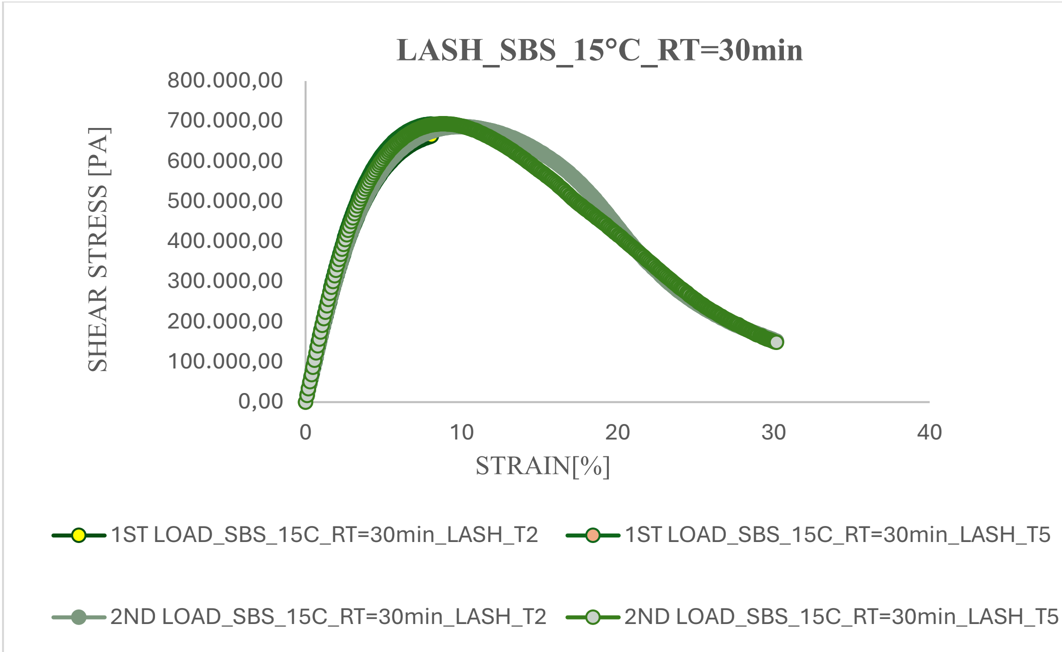


Figure3.3.3 -stress-strain curves related to healing test with 30 minutes rest for RLDP3.3% at 15℃

In the part below the graphic results related to healing test without considering any rest time is shown at 15℃ and 20℃ for three binder classes (Neat50/70, SBS modified binder, modified binder with 3.35% RLDP). By considering the dedicated results below, a high degree of agreement is shown between the trials that proves the accuracy of the results.

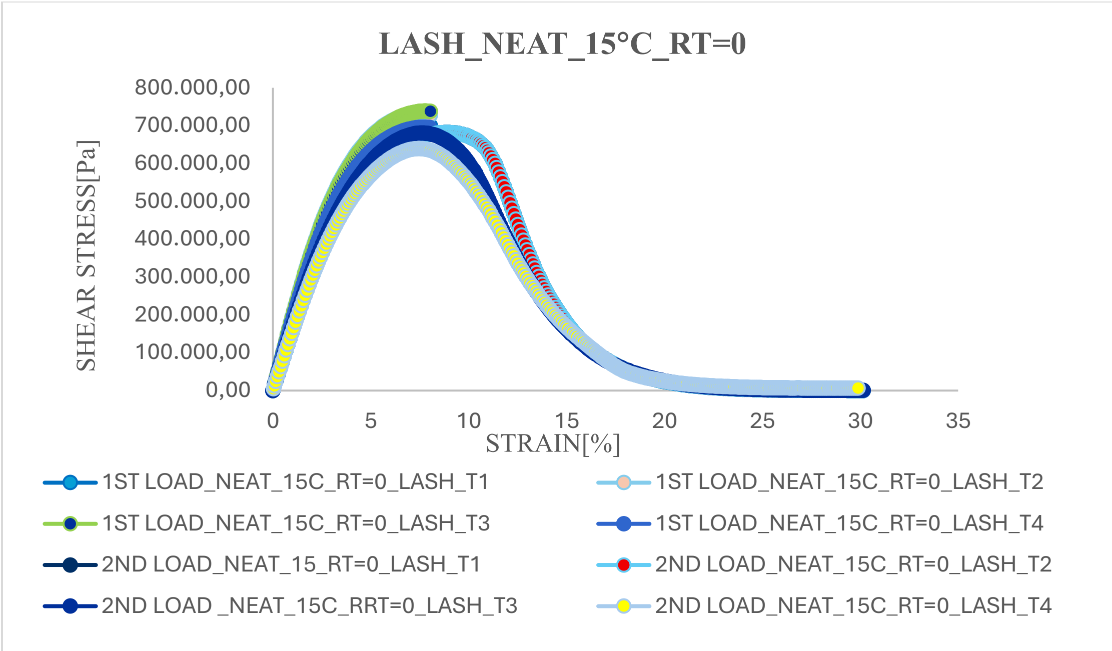


Figure 3.3.4-stress-strain curves related to healing test with 0 minutes rest for Neat at 15℃

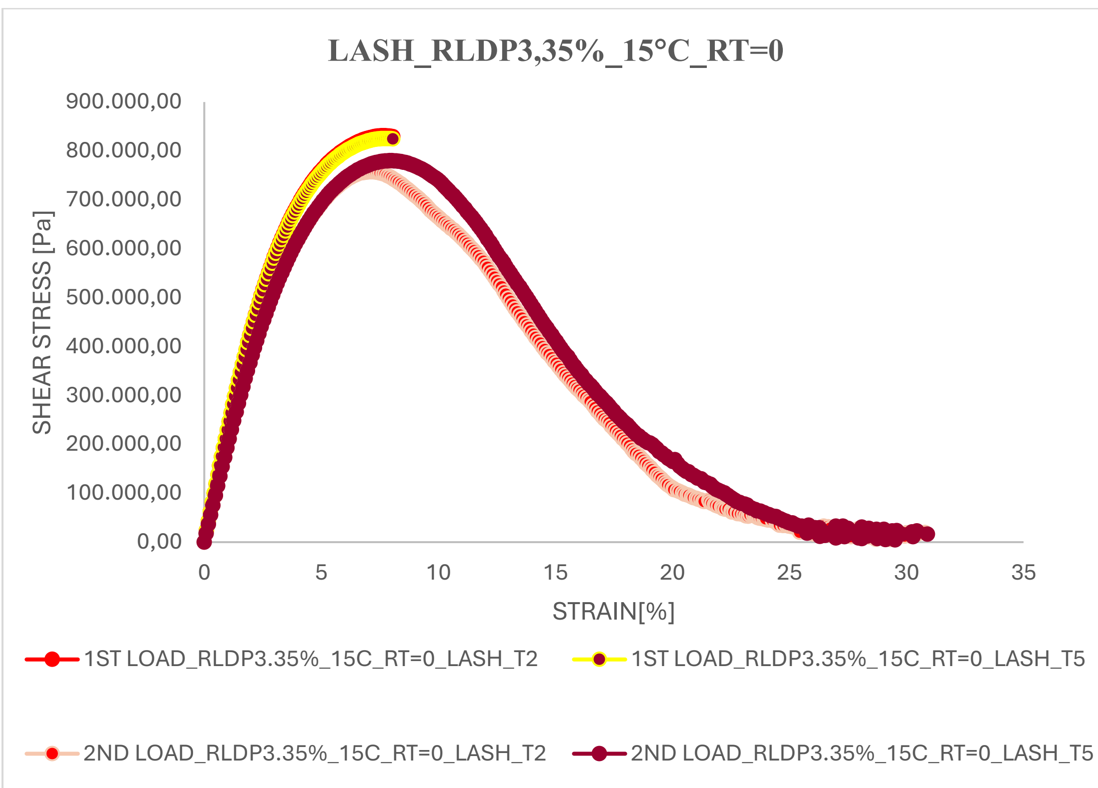


Figure3.3.5 -stress-strain curves related to healing test with 0 minutes rest for RLDP3.3% at 15℃

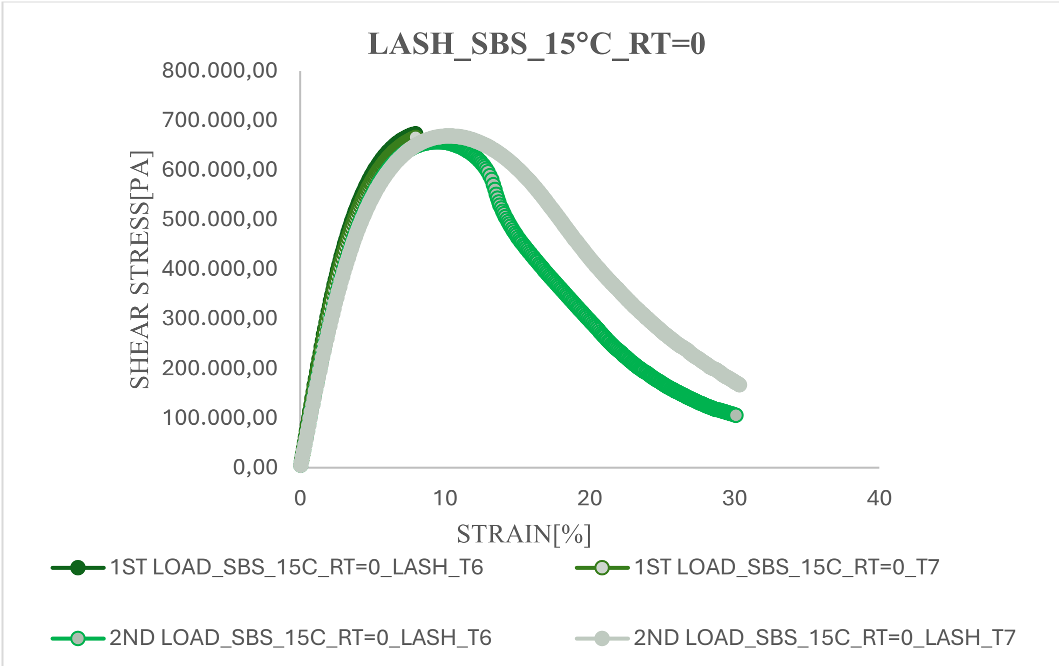


Figure3.3.6 -stress-strain curves related to healing test with 0 minutes rest for SBS modified binder at 15℃

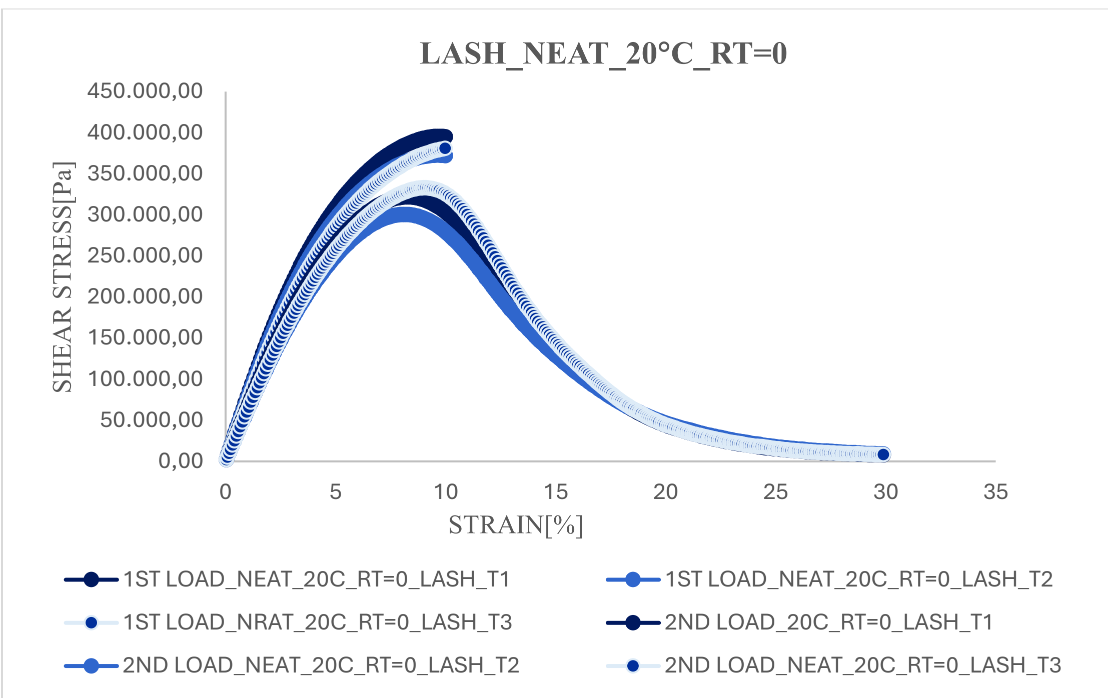


Figure 3.3.7-stress-strain curves related to healing test with 0 minutes rest Neat50/70 at 20℃

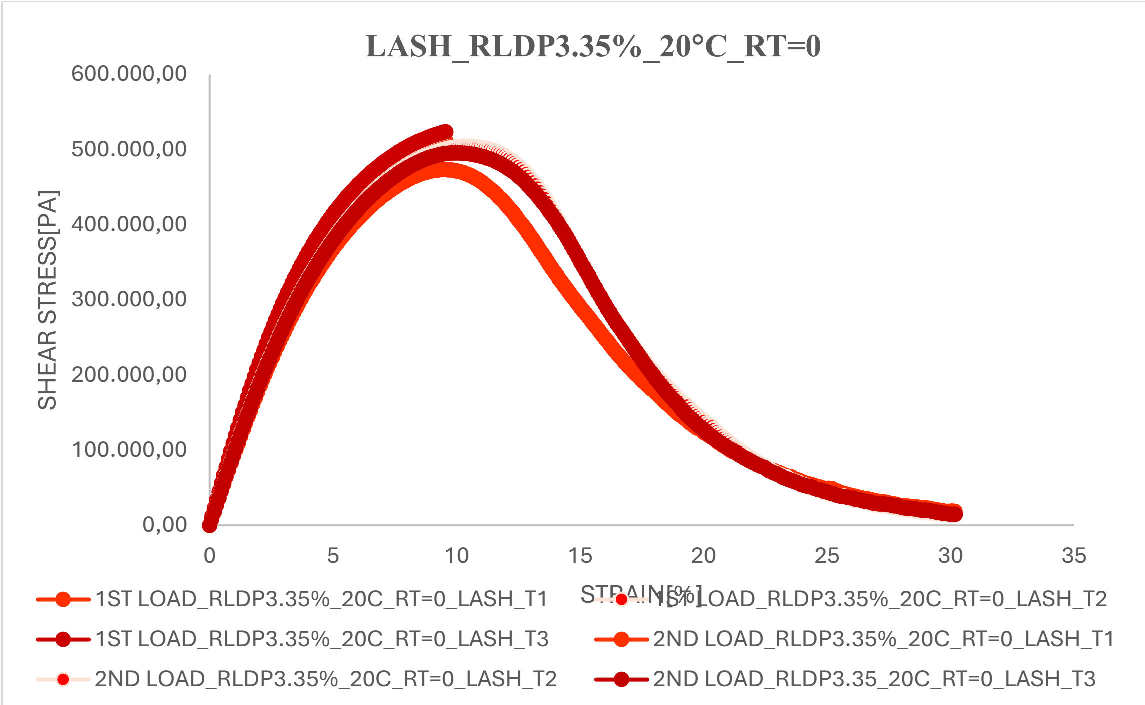


Figure3.3.8 -stress-strain curves related to healing test with 0 minutes rest RLDP3.35% modified binder at 20°C

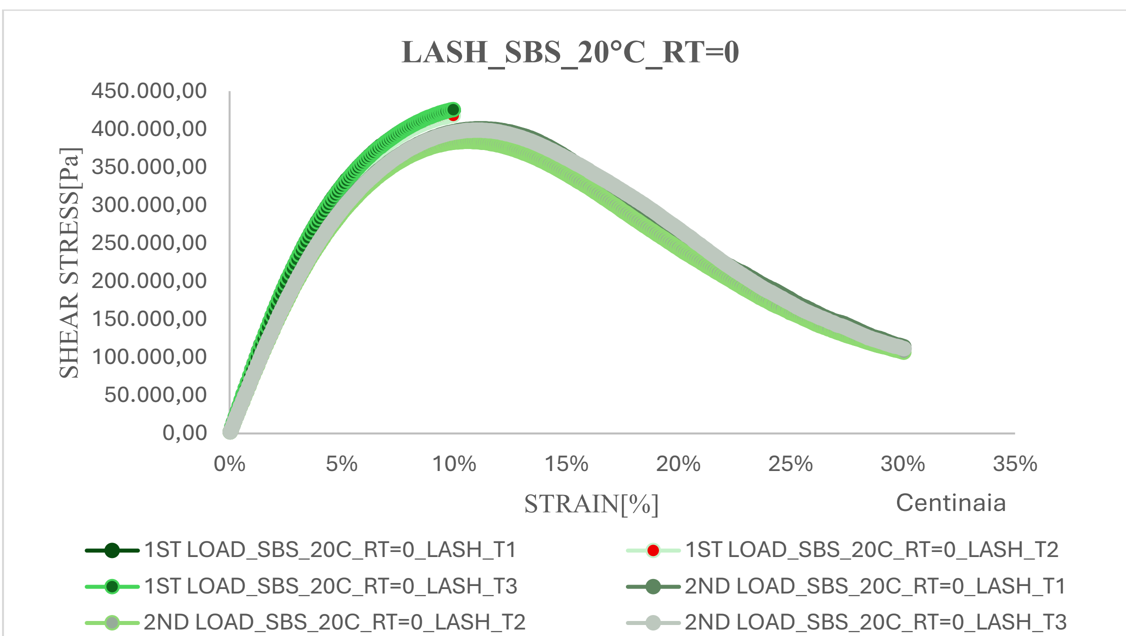


Figure3.3.9 -stress-strain curves related to healing test with 0 minutes rest SBS modified binder at 20°C

The self-healing chapter is continued by comparison of each distinct binder material with itself under two rest period conditions which includes 30 minutes and without rest time. This comparison aids us to understand the level of recovery and the importance of rest time in self-healing properties of asphalt binder.

To start with the Neat50/70 unmodified binder at 15℃ the related figure below shows that the shear stress-strain curve for both rest conditions followed same behavior; although, the curve with 30 minutes rest time has a slightly higher peak than curve with 0 rest time which confirms the positive impact of time on recovery of asphalt binder; nevertheless, that the impact is limited due to low temperature service (15℃) which was not unexpected. The same observations were made for both the SBS-modified binder and the 3.3% RLDP-modified binder.

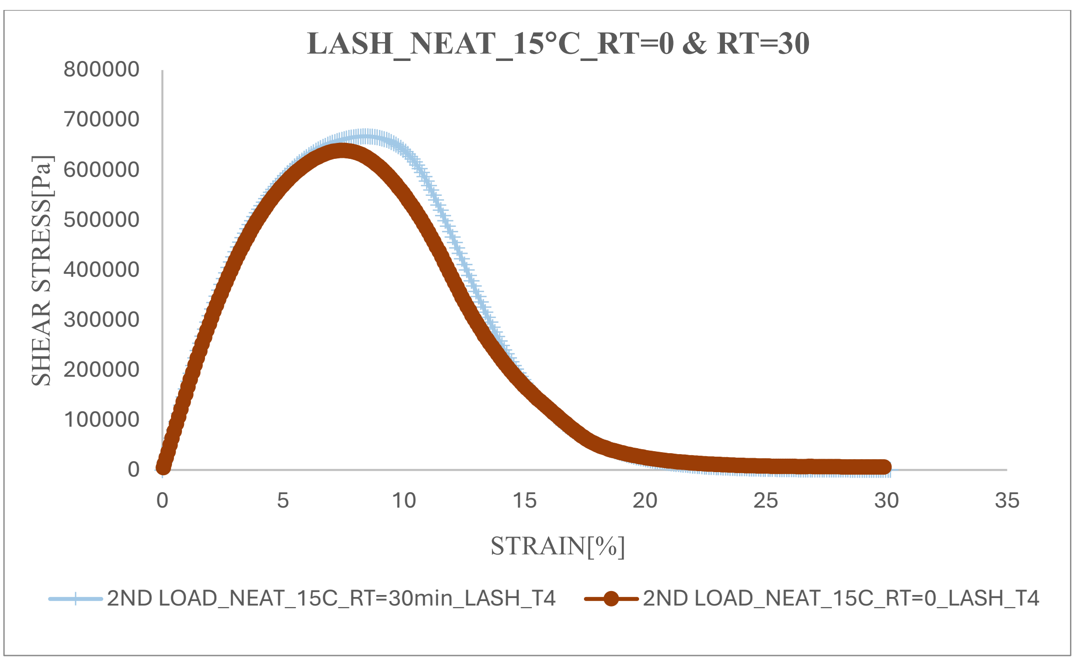


Figure 3.3.10-Comparison of healing with 0 & 30 minutes rest for Neat50/70 at15°C

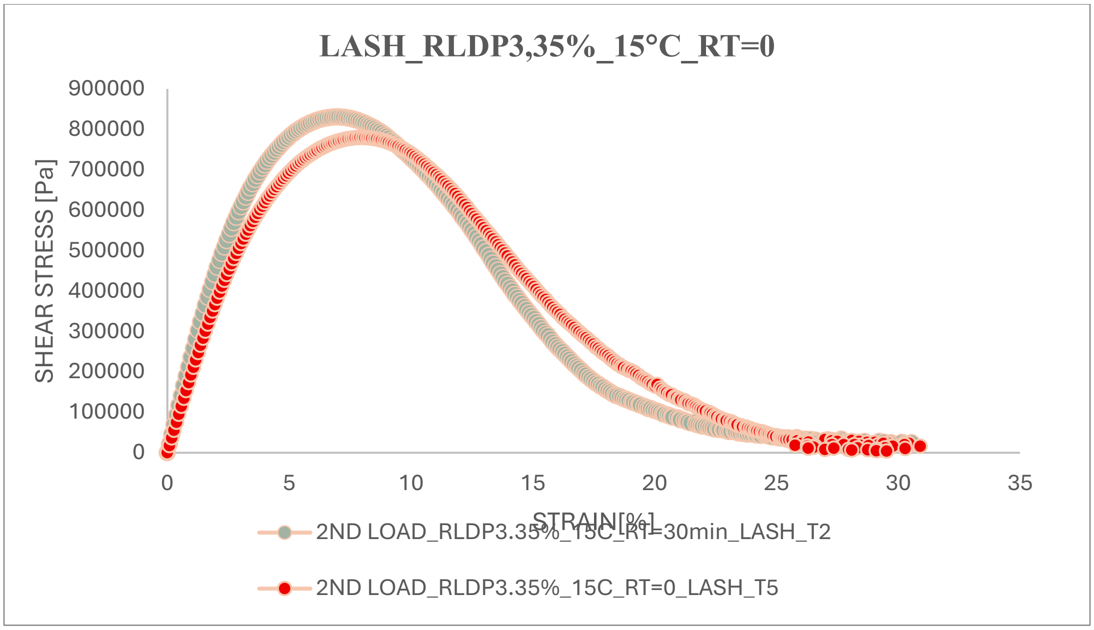


Figure3.3.11 -Comparison of healing with 0 & 30 minutes rest for RLDP3.3% at15°C

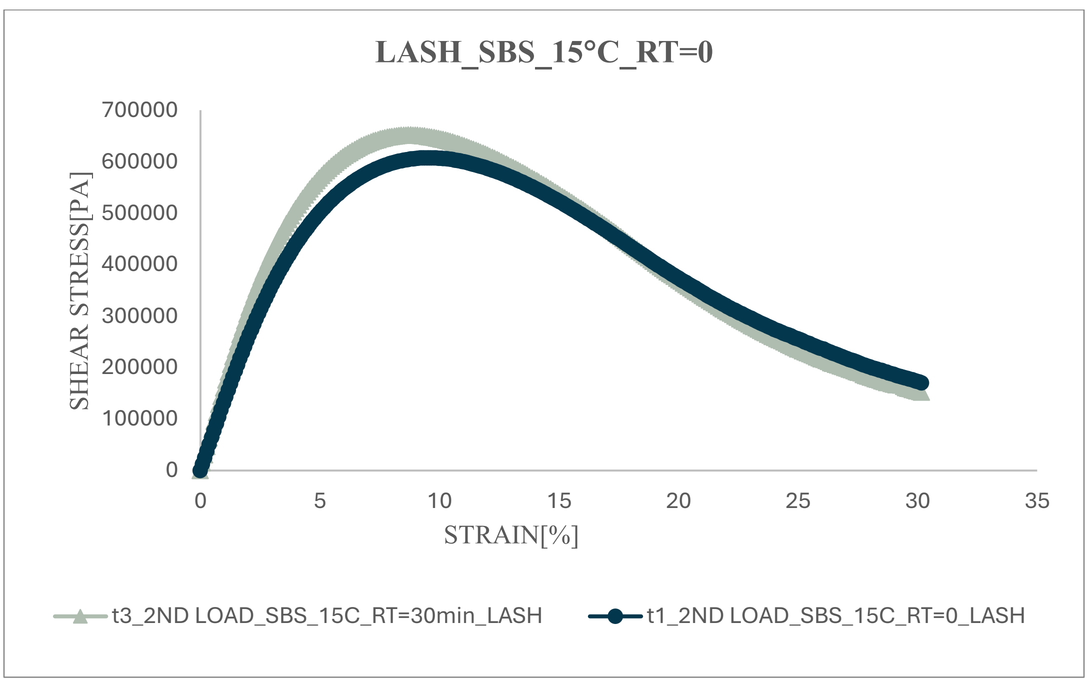


Figure3.3.12 -Comparison of healing with 0 & 30 minutes rest for SBS modified binder at15°C

The following three figures illustrate the LAS-Healing responses for the neat 50/70, SBS-modified, and 3.35% RLDP-modified binders at 20°C under two testing conditions: with no rest period and with a 30-minute rest period. In all cases, the curves corresponding to the 30-minute rest period exhibit higher peak shear stress than those obtained without a rest period, indicating that the recovery interval improves the self-healing performance of the binders. The greater separation between the two curves at 20°C suggests that higher service temperatures enhance healing by increasing molecular mobility and promoting the diffusion processes responsible for mechanical recovery.

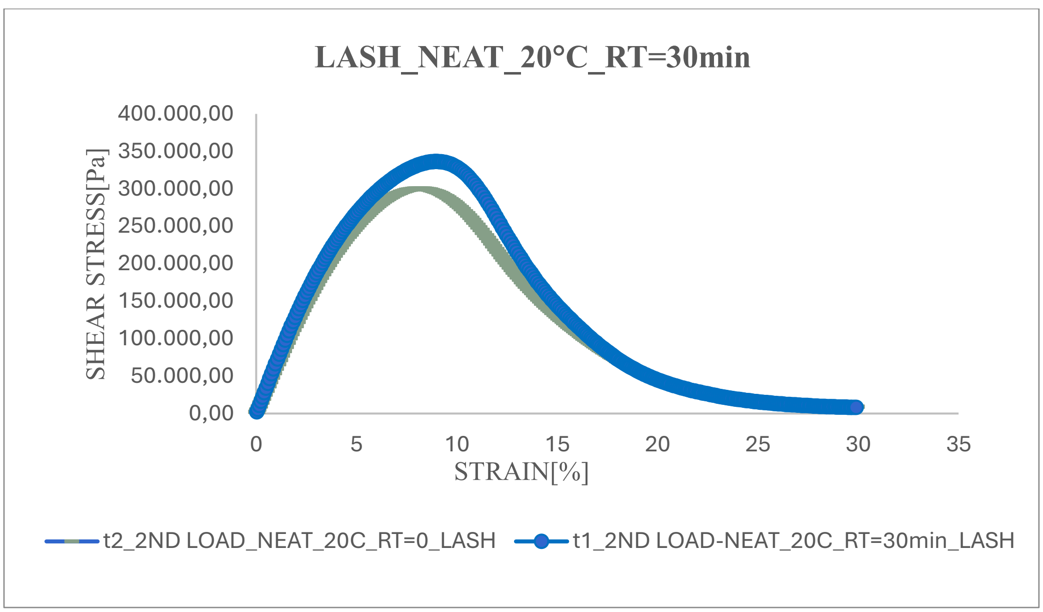


Figure3.3.13 -Comparison of healing with 0 & 30 minutes rest for SBS modified binder at 20°C

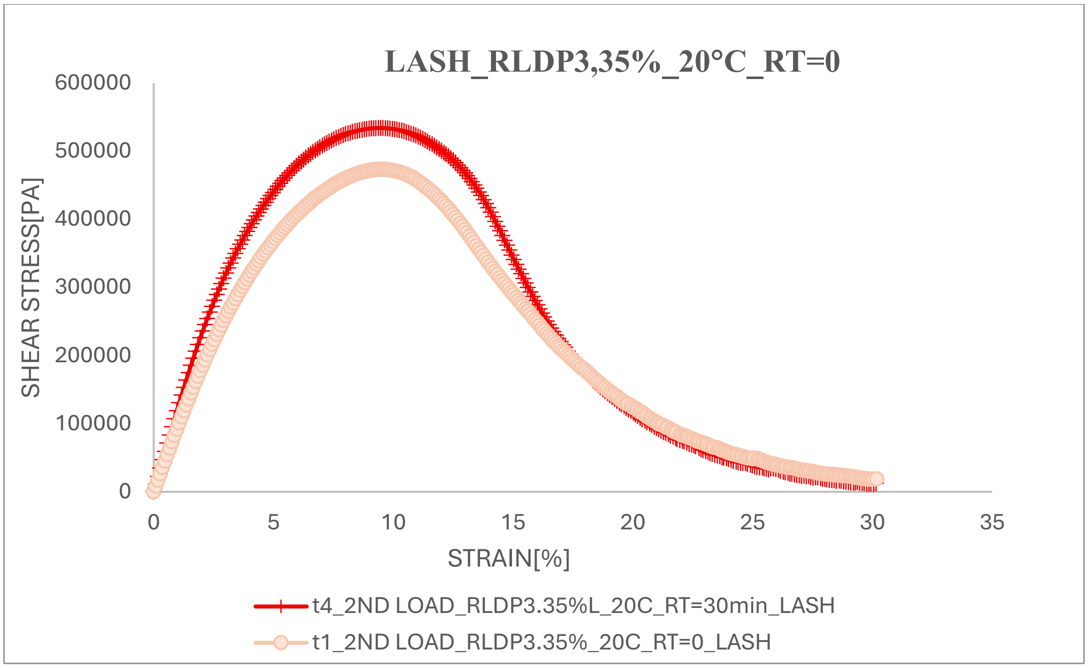


Figure 3.3.14-Comparison of healing with 0 & 30 minutes rest for RLDP3.3% modified binder at 20°C

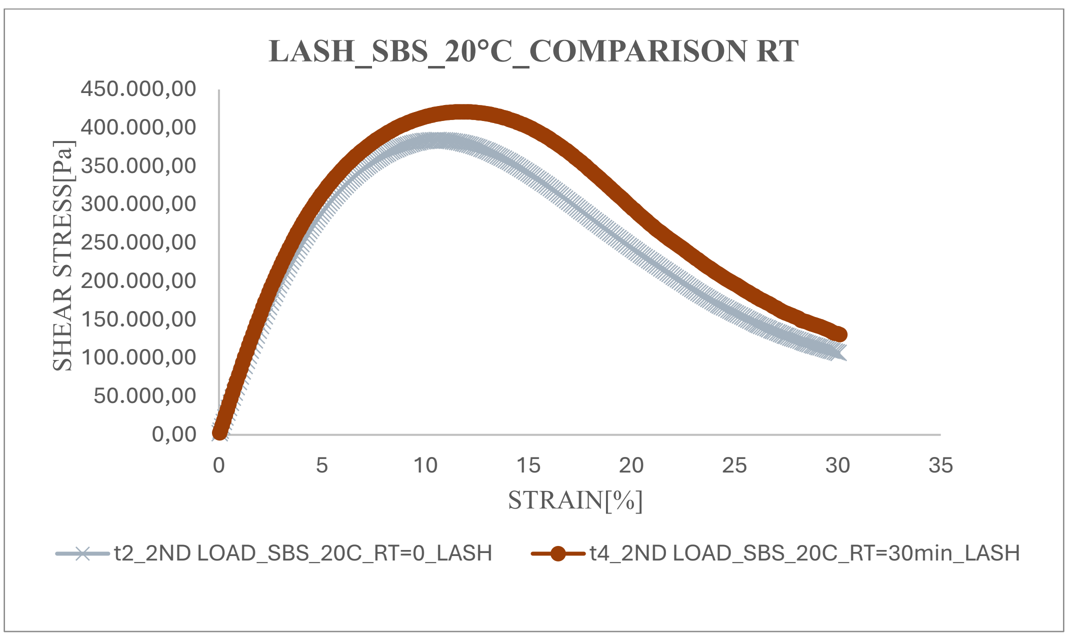


Figure 3.3.15-Comparison of healing with 0 & 30 minutes rest SBS modified binder at 20°C

The given figures below aims to make a comparison between fatigue and healing test at 15c and 20c for different mentioned asphalt binders. As is shown the comparison between accaptable trials demonstrateds that for modified binders at both service tempretures LASH has higher peak than LAS that confirms the healing had occurred. A notable difference was observed in the post-peak behavior of the two modified binders. The 3.35% RLDP-modified binder exhibited a relatively sharper decline in shear stress immediately after reaching the peak, indicating rapid damage propagation and a more brittle failure response. In contrast, the SBS-modified binder displayed a more gradual post-peak stress reduction and a considerably larger area under the stress–strain curve. This behavior suggests that the SBS binder was capable of sustaining load over a wider strain range and absorbing more deformation energy before failure, reflecting greater ductility, toughness, and resistance to fatigue damage. The enhanced post-peak response of the SBS-modified binder can be attributed to the elastic polymer network formed by SBS, which delays crack propagation and promotes stress redistribution during loading. Conversely, although RLDP modification improved the peak strength and self-healing response compared with the neat binder, it did not provide the same level of post-peak ductility as the SBS-modified binder.

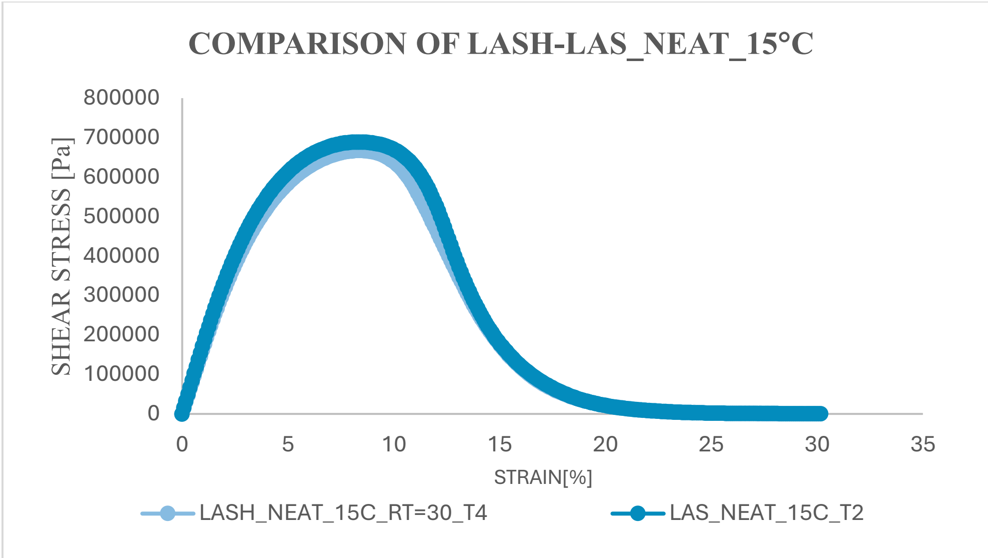


Figure 3.3.16-comparison of LAS and LASH at 30 minutes related to Neat 50/70

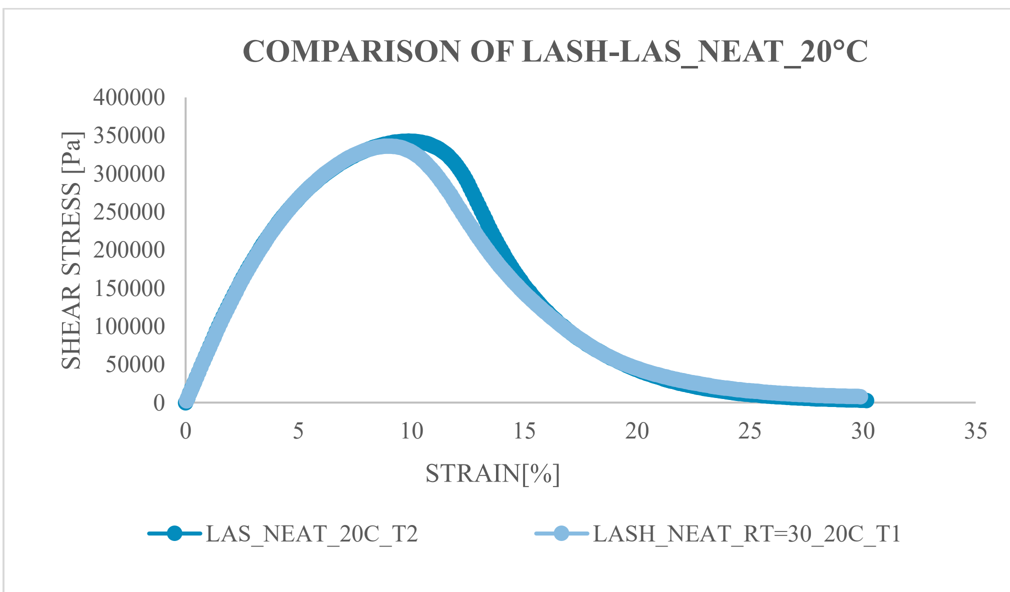


Figure 3.3.17-comparison of LAS and LASH at 30 minutes related to Neat 50/70

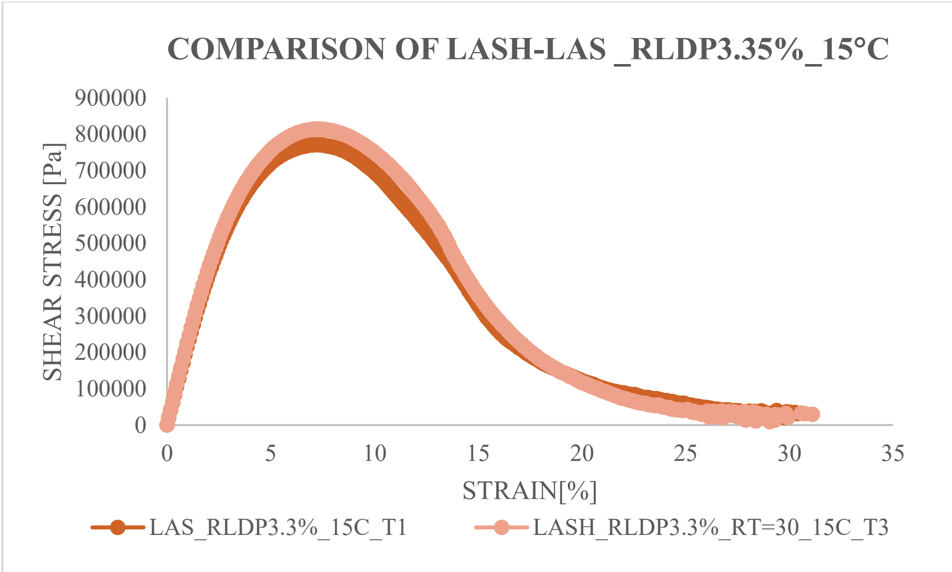


Figure3.3.18 -comparison of LAS and LASH at 30 minutes related to RLDP3.35% modified binder.

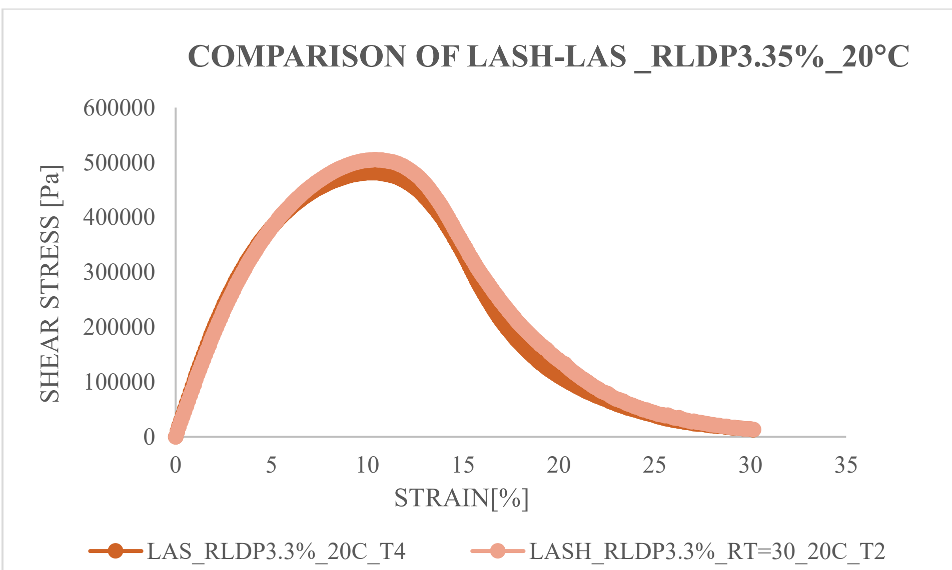


Figure3.3.19 -comparison of LAS and LASH at 30 minutes related to RLDP3.35% modified binder

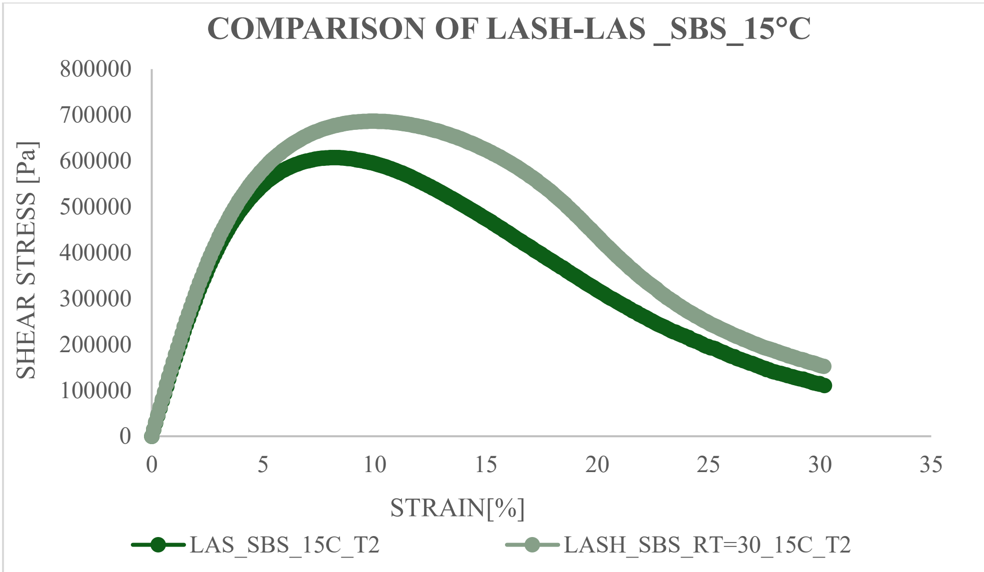


Figure3.3.20 -comparison of LAS and LASH at 30 minutes related to SBS modified binder

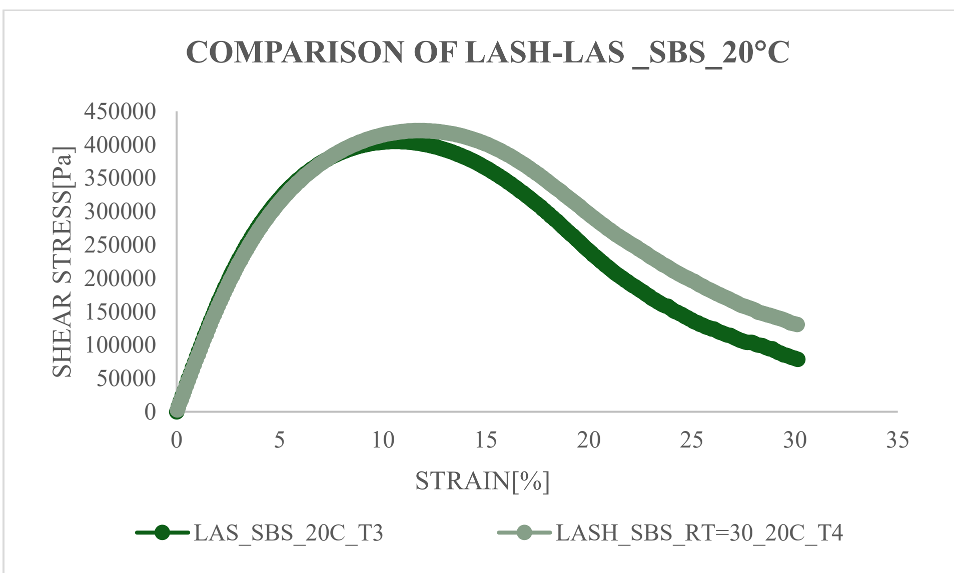


Figure 3.3.21-comparison of LAS and LASH at 30 minutes related to SBS modified binder

### 3.4-LAS-Steric Hardening

Steric hardening is a time-dependent physical phenomenon that occurs during the resting period of asphalt binders and results in an increase in stiffness due to molecular rearrangement, wax crystallization, and structural reorganization within the bituminous matrix. Because steric hardening develops simultaneously with the self-healing process, it can contribute to the apparent recovery of mechanical properties observed after a rest period. Consequently, to accurately assess the intrinsic self-healing capability of asphalt binders, it is essential to separate the stiffness recovery associated with steric hardening from that resulting from actual damage repair mechanisms, such as crack closure and molecular diffusion.

To quantify the influence of steric hardening on the recovery response, Linear Amplitude Sweep with Steric Hardening (LAS-SH) tests were performed on the neat 50/70, SBS-modified, and RLDP-modified (3.35%) binders at 15 °C and 20 °C. Based on the peak tensile deformation values previously determined from the LAS tests, the LAS-SH procedure was designed to evaluate the increase in binder stiffness attributable solely to physical hardening. Unlike the LASH test, which incorporates a rest period after a pre-damage phase to evaluate healing, the LAS-SH test was conducted in the absence of pre-damage, allowing the reversible stiffness increase associated with steric hardening to be isolated and quantified. This approach enabled the differentiation between genuine self-healing and time-dependent physical stiffening, thereby ensuring a more accurate evaluation of the healing efficiency of the investigated binders. Figures below show acceptable trials related to Neat50/70, SBS modified binder, modified binder with 3.35% RLDP .

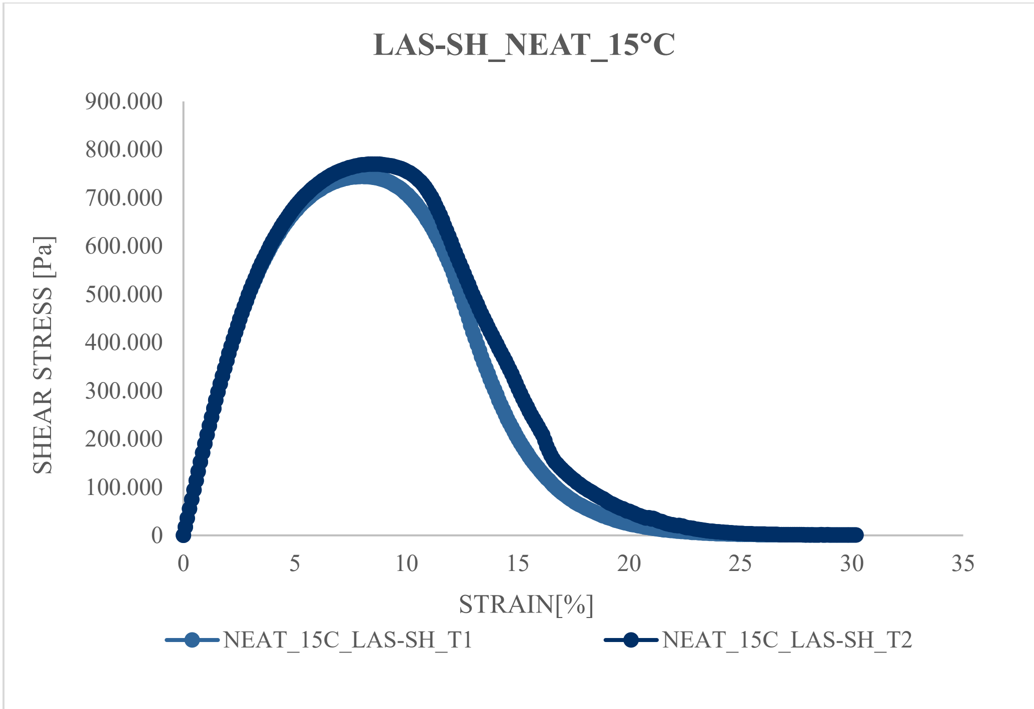


Figure3.4.1 -Stress-strain curves of trials for LAS-SH test related to Neat 50/70 binder

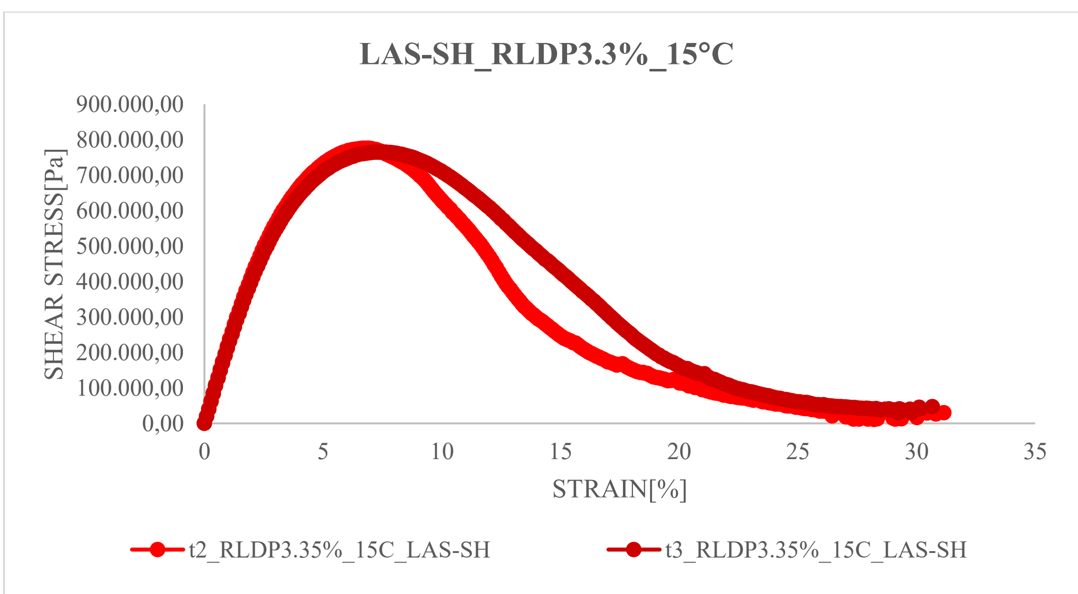


Figure 3.4.2-Stress-strain curves of trials for LAS-SH test related to RLDP3.3% modified binder

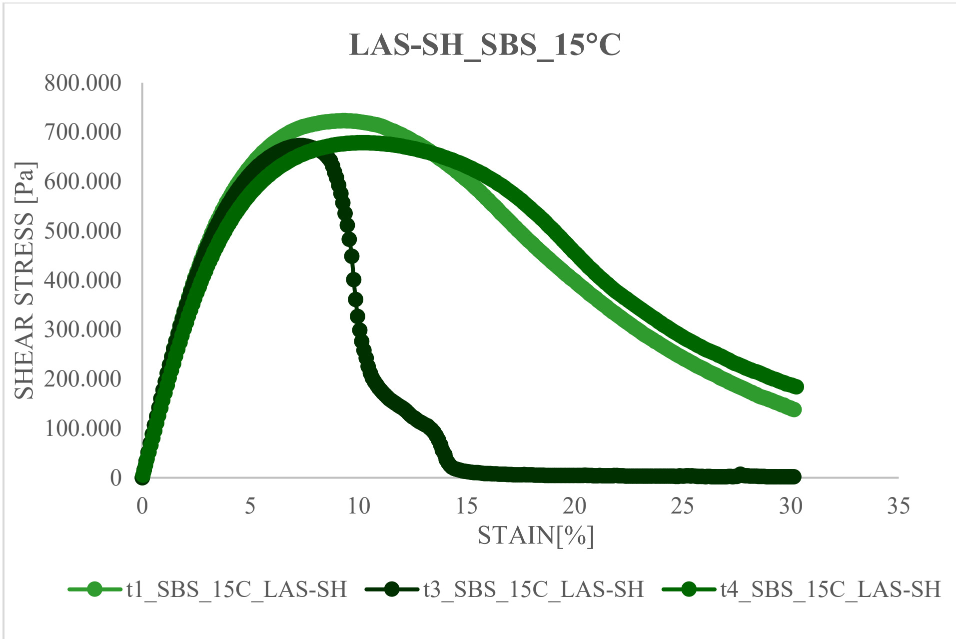


Figure 3.4.3-Stress-strain curves of trials for LAS-SH test related to SBS modified binder

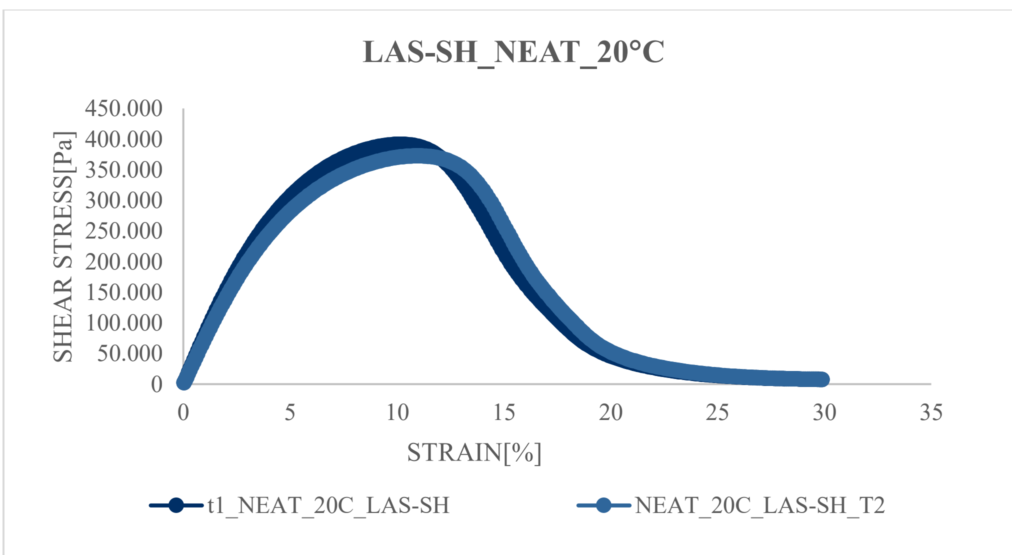


Figure3.4.4 -Stress-strain curves of trials for LAS-SH test related to Neat 50/70 binder

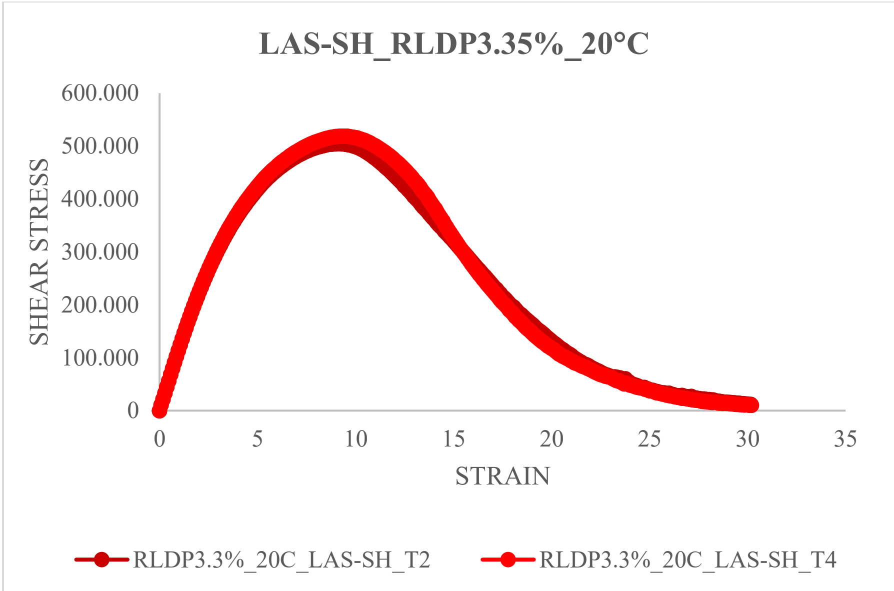


Figure 3.4.5-Stress-strain curves of trials for LAS-SH test related to RLDP3.3% binder

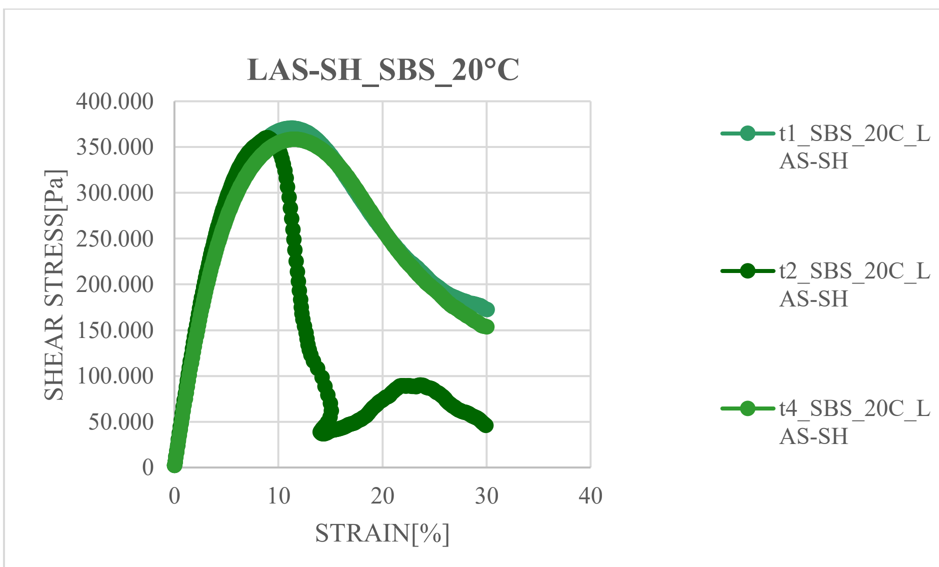


Figure3.4.6 -Stress-strain curves of trials for LAS-SH test related to SBS modified binder

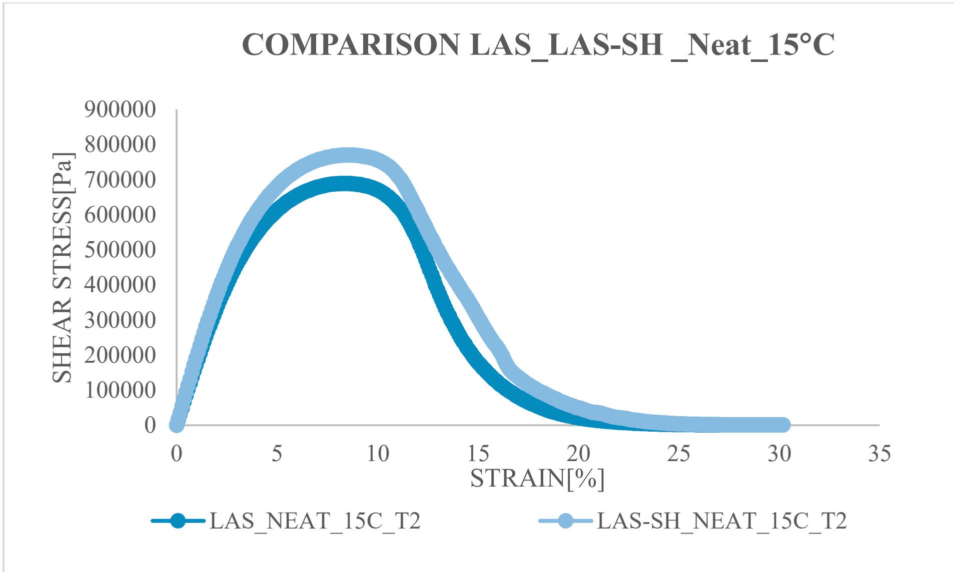


Figure 3.4.7-comparison of LAS and LASH-SH related to Neat 50/70 binder

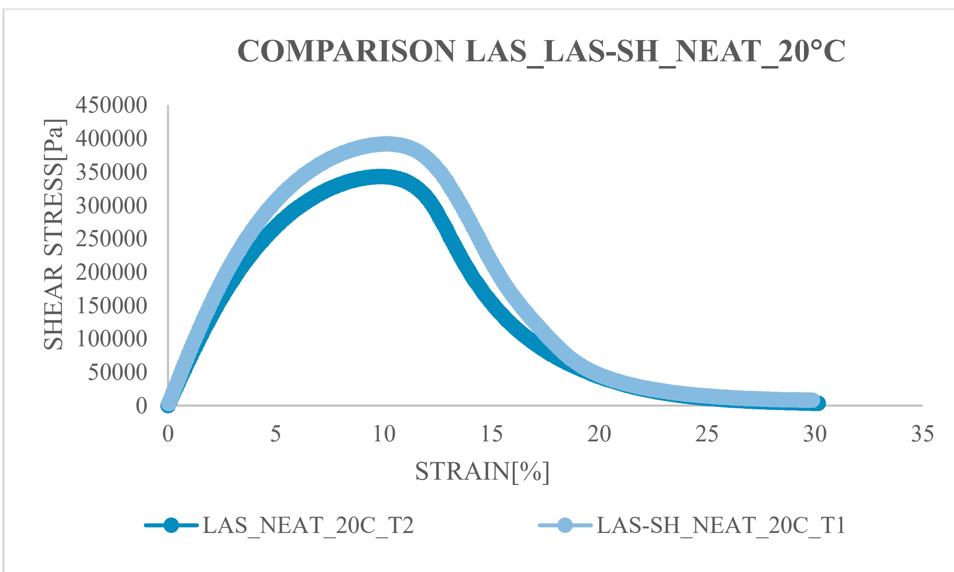


Figure3.4.8 -comparison of LAS and LASH-SH related to Neat 50/70 binder

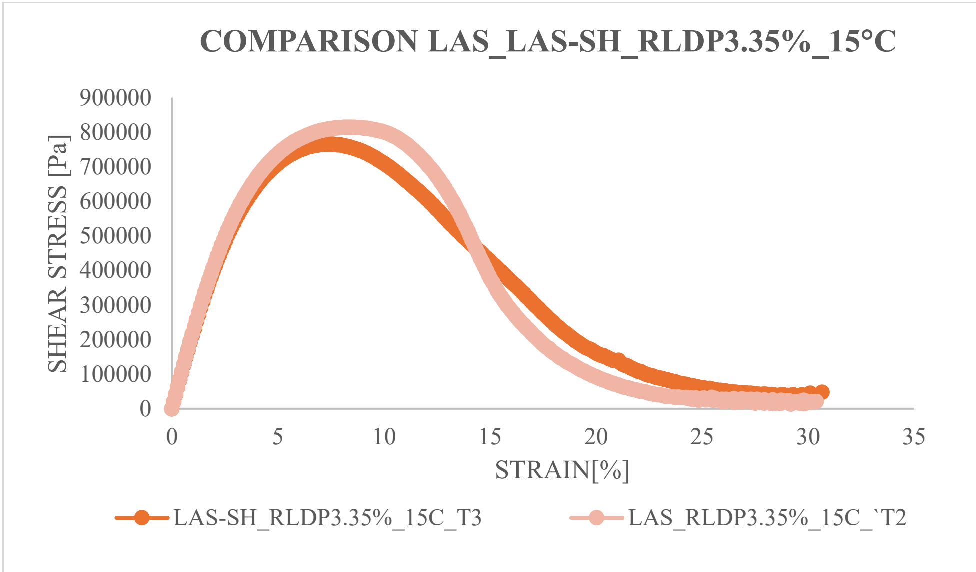


Figure3.4.9 -comparison of LAS and LASH-SH related to RLDP3.35% modified binder

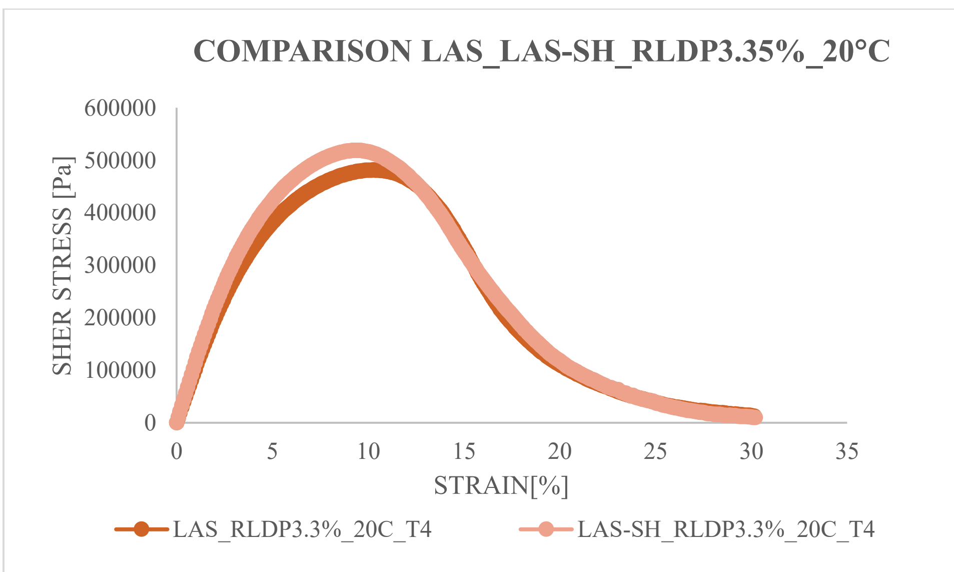


Figure3.4.10 -comparison of LAS and LASH-SH related to RLDP3.35% modified binder

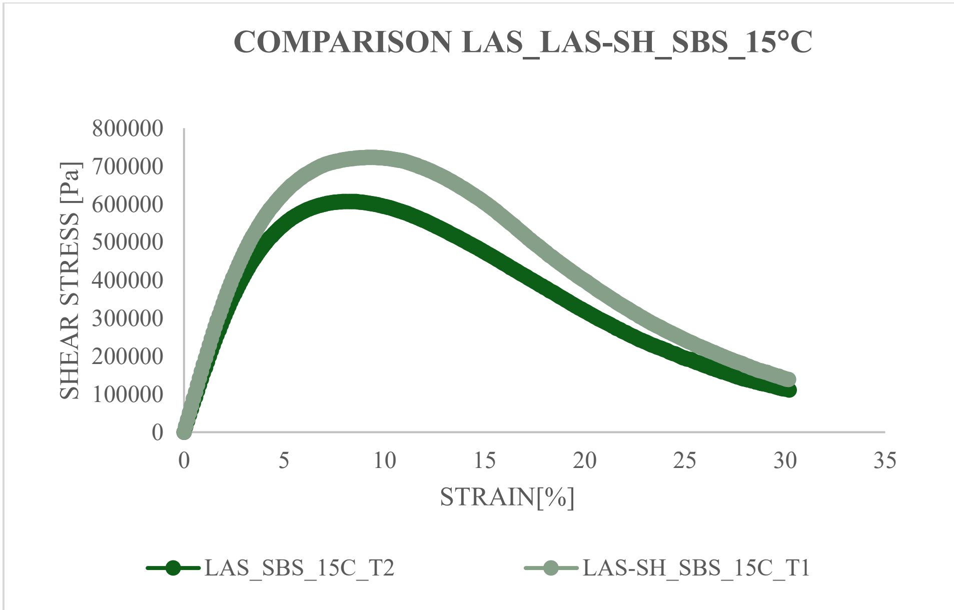


Figure 3.4.11-comparison of LAS and LASH-SH related to SBS modified binder

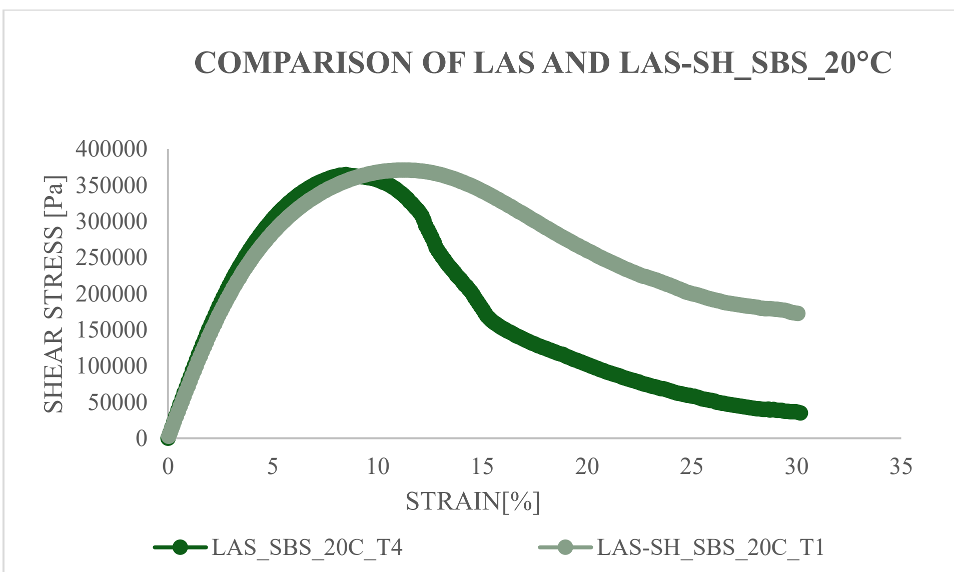


Figure 3.4.12-comparison of LAS and LASH-SH related to SBS modified binder

## 3.5-Data Analysis

Since the Simplified Viscoelastic Continuum Damage (S-VECD) model was not adopted in this study, the quantification of self-healing was performed using two complementary analytical approaches based exclusively on the experimental results obtained from the LAS, LASH, and LAS-SH tests. These methodologies were developed to distinguish the recovery associated with intrinsic healing mechanisms from that resulting from steric hardening, thereby enabling a more accurate assessment of binder recovery following damage and rest periods.

The two approaches differ in both their methodology and objective. The first method evaluates self-healing through the recovery of shear stress at a predefined deformation level, providing a direct measure of the mechanical response regained after the rest period. The second method assesses healing by quantifying improvements in fatigue life using the procedure outlined in AASHTO TP 101, thereby relating recovery to the binder's resistance to fatigue damage accumulation.

Together, these complementary approaches provide a comprehensive evaluation of the healing behavior of the investigated binders and facilitate the assessment of the influence of temperature and binder modification on the recovery process.

To facilitate the subsequent analyses and calculations, a consolidated dataset of averaged results was first established. These tables present the values retained for further evaluation, derived exclusively from trials that satisfied the predefined repeatability and convergence criteria. Only results demonstrating satisfactory experimental consistency and stability were considered, ensuring that the subsequent analyses were based on reliable and representative measurements of binder behavior

table3.5.1 values of reference strains for LAS,LASH,LAS-SH at 15°C and 20°C

| NEAT_LAS_15°C | | |
|---|---|---|
| TRIALS | T | γ |
| | [Pa] | [%] |
| 1 | 696952 | 8,0 |
| 2 | 692652 | 8,0 |
| AVG | 692652 | 8,0 |

| NEAT_LAS_20°C | | |
|---|---|---|
| TRIALS | τ | γ |
| | [Pa] | [%] |
| 1 | 323434 | 10,0 |
| 2 | 342715 | 10,0 |
| AVG | 333075 | 10,0 |

| NEAT_LASH_15°C_RT=30min_1st | | |
|---|---|---|
| TRIALS | T | γ |
| | [Pa] | [%] |
| 2 | 681386 | 8,0 |
| 3 | 742693 | 8,0 |
| 4 | 654412 | 8,0 |
| AVG | 692830 | 8,0 |

| NEAT_LASH_20°C_RT=30min_1st | | |
|---|---|---|
| TRIALS | τ | γ |
| | [Pa] | [%] |
| 1 | 367175 | 10,0 |
| 2 | 369458 | 10,0 |
| AVG | 368317 | 10,0 |

| NEAT_LASH_15°C_RT=30min_2nd | | |
|---|---|---|
| TRIALS | T | γ |
| | [Pa] | [%] |
| 2 | 677184 | 8,0 |
| 3 | 692855 | 8,0 |
| 4 | 666256 | 8,0 |
| AVG | 678765 | 8,0 |

| NEAT_LASH_20°C_RT=30min_2nd | | |
|---|---|---|
| TRIALS | τ | γ |
| | [Pa] | [%] |
| 1 | 328152 | 10,0 |
| 2 | 291787 | 10,0 |
| AVG | 309970 | 10,0 |

| NEAT_LASH_15°C_RT=0min_2nd | | |
|---|---|---|
| TRIALS | T | γ |
| | [Pa] | [%] |
| 1 | 677173 | 8,0 |
| 2 | 637034 | 8,0 |
| 3 | 678607 | 8,0 |
| 4 | 636243 | 8,0 |
| AVG | 657264 | 8 |

| NEAT_LASH_15°C_RT=0min_2nd | | |
|---|---|---|
| | τ | γ |
| | [Pa] | [%] |
| 1 | 3043774 | 10,0 |
| 2 | 279982 | 10,0 |
| 3 | 324947 | 10,0 |
| AVG | 303101 | 10 |

| NEAT_LAS-SH_15°C | | |
|---|---|---|
| TRIALS | τ | γ |
| | [Pa] | [%] |
| 1 | 744449 | 8,0 |
| 2 | 768398 | 8,0 |
| AVG | 756424 | 8,0 |

| NEAT_LAS-SH_20°C | | |
|---|---|---|
| TRIALS | τ | γ |
| | [Pa] | [%] |
| 1 | 391470 | 10,0 |
| 2 | 370060 | 10,0 |
| AVG | 380765 | 10,0 |

table3.5.2 values of reference strains for LAS,LASH,LAS-SH at 15°C and 20°C

| SBS_LAS_15°C | | |
|---|---|---|
| TRIALS | τ | γ |
| | [Pa] | [%] |
| 2 | 607030 | 8,0 |
| 4 | 606931 | 8,0 |
| 5 | 618541 | 8,0 |
| 6 | 665632 | 8,0 |
| AVG | 624534 | 8,0 |

| SBS_LAS_20°C | | |
|---|---|---|
| TRIALS | τ | γ |
| | [Pa] | [%] |
| 3 | 403883 | 10,0 |
| 4 | 357326 | 10,0 |
| 5 | 409634 | 10,0 |
| AVG | 390281 | 10,0 |

| SBS_LASH_15°C_RT=30min_1st | | |
|---|---|---|
| TRIALS | τ | γ |
| | [Pa] | [%] |
| 2 | 662085 | 8,0 |
| 3 | 642810 | 8,0 |
| 4 | 644317 | 8,0 |
| 5 | 692748 | 8,0 |
| AVG | 660490 | 8,0 |

| SBS_LASH_20°C_RT=30min_1st | | |
|---|---|---|
| TRIALS | τ | γ |
| | [Pa] | [%] |
| 2 | 426980 | 10,0 |
| 3 | 432211 | 10,0 |
| 4 | 411366 | 10,0 |
| AVG | 423519 | 10,0 |

| SBS_LASH_15°C_RT=30min_2nd | | |
|---|---|---|
| TRIALS | τ | γ |
| | [Pa] | [%] |
| 2 | 674294 | 8,0 |
| 3 | 648911 | 8,0 |
| 4 | 653711 | 8,0 |
| 5 | 690358 | 8,0 |
| AVG | 666818 | 8,0 |

| SBS_LASH_20°C_RT=30min_2nd | | |
|---|---|---|
| TRIALS | τ | γ |
| | [Pa] | [%] |
| 2 | 403567 | 10,0 |
| 3 | 415198 | 10,0 |
| 4 | 414330 | 10,0 |
| AVG | 411032 | 10,0 |

| SBS_LASH_15°C_RT=0min_2nd | | |
|---|---|---|
| TRIALS | τ | γ |
| | [Pa] | [%] |
| 6 | 648855 | 8,0 |
| 7 | 650719 | 8,0 |
| AVG | 649787 | 8,0 |

| SBS_LASH_20°C_RT=0min_2nd | | |
|---|---|---|
| TRIALS | τ | γ |
| | [Pa] | [%] |
| 1 | 396794 | 10,0 |
| 2 | 382898 | 10,0 |
| 3 | 395835 | 10,0 |
| AVG | 391842 | 10,0 |

| SBS_LAS-SH_15°C | | |
|---|---|---|
| TRIALS | τ | γ |
| | [Pa] | [%] |
| 1 | 717124 | 8,0 |
| 3 | 666503 | 8,0 |
| 4 | 664953 | 8,0 |
| AVG | 682860 | 8,0 |

| SBS_LAS-SH_20°C | | |
|---|---|---|
| TRIALS | τ | γ |
| | [Pa] | [%] |
| 1 | 367378 | 10,0 |
| 2 | 347286 | 10,0 |
| 4 | 354310 | 10,0 |
| AVG | 356325 | 10,0 |

table3.5.3 values of reference strains for LAS,LASH,LAS-SH at 15°C and 20°C

| 3,3%_LAS_15°C | | |
|---|---|---|
| TRIALS | τ | γ |
| | [Pa] | [%] |
| 1 | 764383 | 8,0 |
| 2 | 813732 | 8,0 |
| AVG | 789058 | 8,0 |

| 3,3%_LAS_20°C | | |
|---|---|---|
| TRIALS | τ | γ |
| | [Pa] | [%] |
| 2 | 441912 | 10,0 |
| 4 | 480812 | 10,0 |
| AVG | 461362 | 10,0 |

| 3,3%_LASH_15°C_RT=30min_1st | | |
|---|---|---|
| TRIALS | τ | γ |
| | [Pa] | [%] |
| 2 | 848917 | 8,0 |
| 3 | 837194 | 8,0 |
| AVG | 843056 | 8,0 |

| 3,3%_LASH_20°C_RT=30min_1st | | |
|---|---|---|
| TRIALS | τ | γ |
| | [Pa] | [%] |
| 3 | 531916 | 10,0 |
| 4 | 555935 | 10,0 |
| 5 | 509594 | 10,0 |
| 6 | 527992 | 10,0 |
| AVG | 531359 | 10 |

| 3,3%_LASH_15°C_RT=30min_2nd | | |
|---|---|---|
| TRIALS | τ | γ |
| | [Pa] | [%] |
| 2 | 817389 | 8,0 |
| 3 | 808789 | 8,0 |
| AVG | 813089 | 8,0 |

| 3,3%_LASH_20°C_RT=30min_2nd | | |
|---|---|---|
| TRIALS | τ | γ |
| | [Pa] | [%] |
| 3 | 496428 | 10,0 |
| 4 | 532801 | 1,0 |
| 5 | 503900 | 10,0 |
| 6 | 517365 | 10,0 |
| AVG | 512642 | 10 |

| 3,3%_LASH_15°C_RT=0min_2nd | | |
|---|---|---|
| TRIALS | τ | γ |
| | [Pa] | [%] |
| 2 | 744642 | 8,0 |
| 5 | 779886 | 8,0 |
| AVG | 762264 | 8,0 |

| 3,3%_LASH_20°C_RT=0min_2nd | | |
|---|---|---|
| TRIALS | τ | γ |
| | [Pa] | [%] |
| 1 | 472003 | 10,0 |
| 2 | 503612 | 10,0 |
| | 495821 | 10,0 |
| AVG | 490479 | 10 |

| 3,3%_LAS-SH_15°C | | |
|---|---|---|
| TRIALS | τ | γ |
| | [Pa] | [%] |
| 2 | 748543 | 8,0 |
| 3 | 761999 | 8,0 |
| AVG | 755271 | 8,0 |

| 3,3%_LAS-SH_20°C | | |
|---|---|---|
| TRIALS | τ | γ |
| | [Pa] | [%] |
| 2 | 499419 | 10,0 |
| 4 | 516263 | 10,0 |
| AVG | 507841 | 10,0 |

### 3.5.1- Assessment with Reference Strain

The first analysis method is based on a reference strain established for different temperatures. Specifically, a reference strain of 8% was used at 15°C for Neat50/70, RLDP3.3% modified binder, and SBS modified binder, while a 10% reference strain was applied at 20°C. The choice of reference strain over peak strain is due to significant variability in peak strain observed across trials. This variability makes direct peak-to-peak comparisons unreliable and potentially misleading regarding healing capacity. To ensure consistent evaluation, a reference strain was defined for each temperature, representing the typical strain range at which peak shear stress occurred during the LAS tests.

At the selected reference strain levels, the corresponding shear stress values were extracted from the LAS, LASH, and LAS-SH curves. The LAS curve was considered representative of the undamaged material response, whereas the first loading phase of the LASH test represented the damaged state prior to recovery. The second loading phase of the LASH test, performed after a 30-minute rest period, reflected the recovered condition resulting from the combined effects of self-healing and steric hardening. In addition, the LAS-SH test provided a measure of the stiffness recovery attributable exclusively to steric hardening. By comparing the shear stress values obtained under these different conditions, the overall mechanical recovery following the rest period could be quantified. Subsequently, the contribution of steric hardening, determined from the LAS-SH results, was subtracted from the total recovery observed in the LASH test, thereby isolating the intrinsic self-healing component and enabling a more accurate assessment of the binder's true healing capacity.

In this method a set of formulas was used to calculate healing index of each asphalt binder , where the exact percentage of healing is determined.

$\Delta$Damage = $\tau_{peak}$ (LASH(1ST load) ) – $\tau_{peak}$ (LASH(2nd load)RT=0min )

$\Delta$SH = $\tau_{peak}$(LAS-SH ) – $\tau_{peak}$ (LASH(2nd load)RT=0min )

$\Delta$ (H+SH) = $\tau_{peak}$ (LASH(2ND load)RT=30min ) – $\tau_{peak}$ (LASH(2nd load)RT=0min )

$\Delta H = \Delta (H+SH) - \Delta SH / \Delta$Damage

To start with Neat 50/70 for temperature of 15°C the data related to shear stress at the reference strain is given based on data below and given formula it is possible to calculate the healing index.

| #TRIALS | 15°C NEAT | τ (ref) [pa] | τ (ref ) [MP] | γ (ref) [%] |
|---|---|---|---|---|
| AVG | LAS | 692652 | 0,692652 | 8,00 |
| AVG | LASH 1st Load (RT=30min) | 692830 | 0,692830 | 8,00 |
| AVG | LASH 2nd Load (RT=0min) | 657264 | 0,657264 | 8,00 |
| AVG | LASH 2nd Load (RT=30min) | 682351 | 0,682351 | 8,00 |
| AVG | LAS-SH | 756424 | 0,756424 | 8,00 |

Table3.5.1.1 -Average values of rheological tests related to Neat50/70

$\Delta$Damage = 0.692830 − 0.657264 =0.036

$\Delta SH = 0.756424 - 0.657264 = 0.099$

$\Delta (H+SH) = 0.682351 - 0.657264 = 0.025$

$\Delta H = 0.025 - 0.099 / 0.036 = -2.08$

Based on calculations above the value of −2.08 for Neat 50/70 at 15°C temperature indicates that NO Healing had occurred.

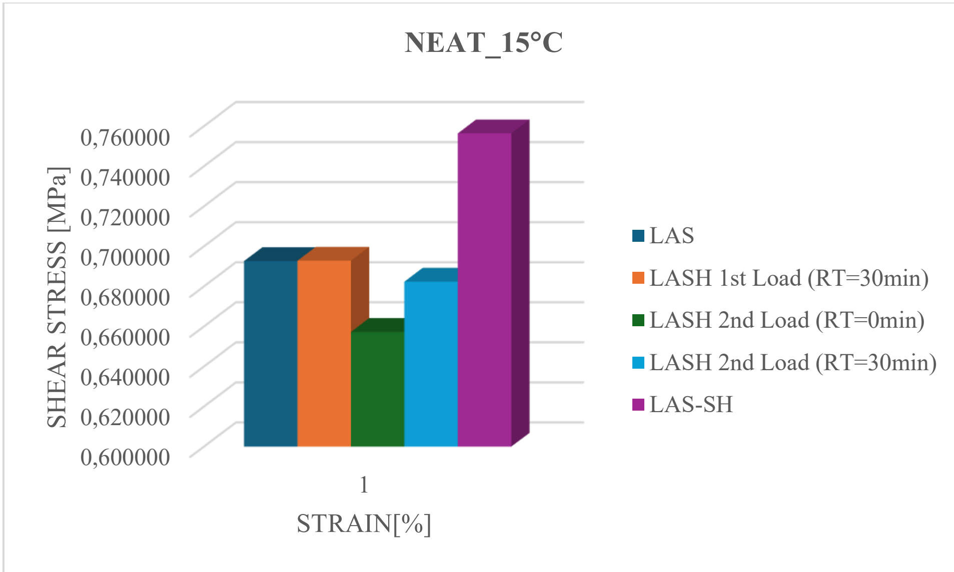


Figure3.5.1.1 -shear stress-strain diagram related to Neat50/70

The calculation was continued for 20°C temperature based on table below

| #TRIALS | 20°C NEAT | τ (ref) [pa] | τ (ref) [MPa] | γ (ref) [%] |
|---|---|---|---|---|
| AVG | LAS | 333075 | 0,333075 | 10,00 |
| AVG | LASH 1st Load (RT=30min) | 368317 | 0,368317 | 10,00 |
| AVG | LASH 2nd Load (RT=0min) | 303101 | 0,303101 | 10,00 |
| AVG | LASH 2nd Load (RT=30min) | 309970 | 0,309970 | 10,00 |
| AVG | LAS-SH | 380765 | 0,380765 | 10,00 |

Table 3.5.1.2-Average values of rheological tests related to Neat50/70

$\Delta$Damage = 0.368317 − 0.303101 = 0.065

$\Delta SH = 0.380765 - 0.303101 = 0.078$

$\Delta$ (H+SH) = 0.368317 − 0.303101 =0.007

$\Delta H = 0.007 - 0.078/0.065 = -1.09$

Based on calculation above the value of −1.09 for Neat 50/70 at 20°C temperature indicates that NO Healing had occurred.

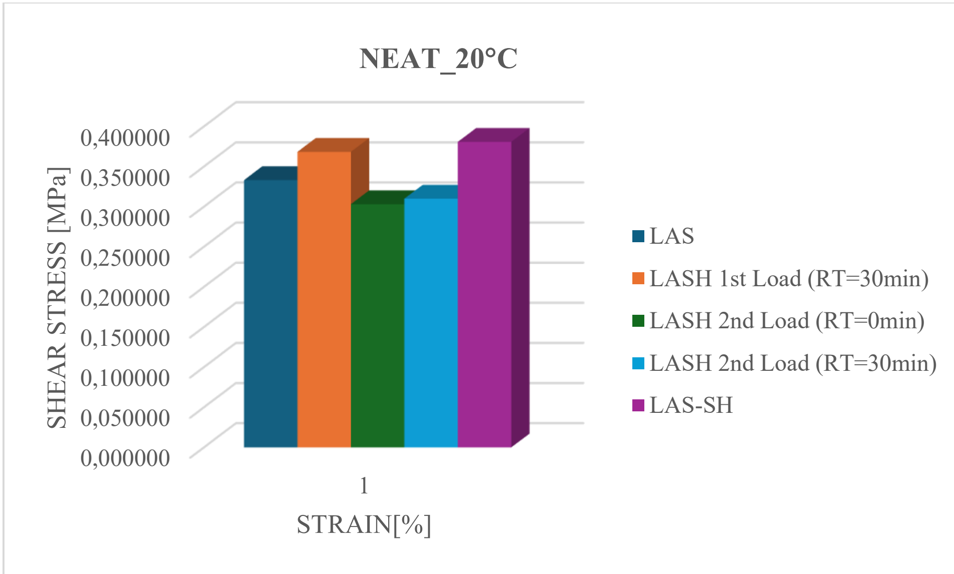


Figure3.5.1.2 -shear stress-strain diagram related to Neat50/70

The absence of a measurable healing response in the neat 50/70 binder is not unexpected. Self-healing in asphalt binders is strongly influenced by temperature, molecular mobility, and rest duration. Under the testing conditions adopted in this study (15°C–20°C and a 30-minute rest period), the recovery observed in the neat binder was insufficient to exceed the contribution of steric hardening, resulting in negligible healing indices. This behavior suggests that the binder's intrinsic healing mechanisms were either inactive or too limited to produce a significant recovery of mechanical properties within the imposed rest period.

In section below the same procedure was conducted for RLDP3.35% modified binder for both 15°C and 20°C.

| #TRIALS | 15°C RLDP3.35% | τ (ref) [pa] | τ (ref) [MP] | γ (at peak) [%] |
|---|---|---|---|---|
| AVG | LAS | 789058 | 0,789058 | 8,00 |
| AVG | LASH 1st Load (RT=30min) | 843056 | 0,843056 | 8,00 |
| AVG | LASH 2nd Load (RT=0min) | 762264 | 0,762264 | 8,00 |
| AVG | LASH 2nd Load (RT=30min) | 813089 | 0,813089 | 8,00 |
| AVG | LAS-SH | 755271 | 0,755271 | 8,00 |

Table3.5.1.3 -shear stress-strain diagram related to Neat50/70

$\Delta$Damage = 0.843056 −0.762264 = 0.081

$\Delta SH = 0.755271 - 0.762264 =$ -0.007

$\Delta$ (H+SH) = $0.813089 - 0.762264$ =0.051

$\Delta H$ =0.051 $- (-0.007)/0.081= 0.716$

Based on calculation above for the RLDP 3.35% modified binder tested at 15°C, a healing index (ΔH) of 0.716 was achieved, indicating that approximately 71.6% of the fatigue-induced damage was recovered during the 30-minute rest period. The contribution from steric hardening was minimal, as reflected by the small negative ΔSH value (−0.007), suggesting that the observed recovery primarily resulted from intrinsic self-healing mechanisms rather than time-dependent physical stiffening. These findings demonstrate the RLDP-modified binder's significant healing capacity at intermediate service temperatures and underscore the effectiveness of the rest period in restoring mechanical properties after fatigue loading.

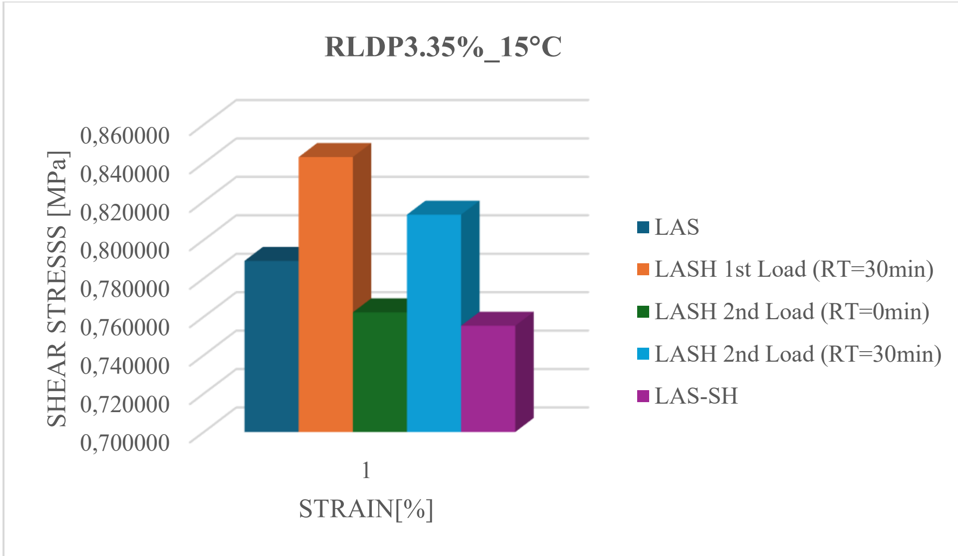


Figure3.5.1.3-shear stress-strain diagram related to RLDP3.35%modified binder

| #TRIALS | 20°C RLDP3.35% | τ (ref) [pa] | τ (ref) [MP] | γ (ref) [%] |
|---|---|---|---|---|
| AVG | LAS | 461362 | 0,461362 | 10,00 |
| AVG | LASH 1st Load (RT=30min) | 531359 | 0,531359 | 10,00 |
| AVG | LASH 2nd Load (RT=0min) | 490479 | 0,490479 | 10,00 |
| AVG | LASH 2nd Load (RT=30min) | 512624 | 0,512624 | 10,00 |
| AVG | LAS-SH | 507841 | 0,507841 | 10,00 |

Table3.5.1.4 -Average values of rheological tests related to RLDP3.3% modified binder

$\Delta$Damage = 0.531359 −0.490479 = 0.041

$\Delta SH = 0.507841 - 0.490479 = 0.017$

$\Delta$ (H+SH) = 0.512624 − 0.490479 =0.022

$\Delta$H =0.022−0.017/= 0.117

Based on the calculated healing indices, the RLDP 3.35% modified binder exhibited a healing index (ΔH) of 0.117 at 20°C, corresponding to a recovery of approximately 11.7% of the fatigue-induced damage. In contrast, the same binder achieved a substantially higher healing index of 0.716 at 15°C, indicating a recovery of approximately 71.6% of the induced damage. This comparison reveals a marked reduction in healing efficiency with increasing temperature. Under the conditions adopted in this study, the RLDP 3.35% binder demonstrated significantly greater self-healing capability at 15°C, while only limited recovery was observed at 20°C. This behavior suggests that the mechanisms governing damage recovery in the modified binder were more effective at the lower testing temperature.

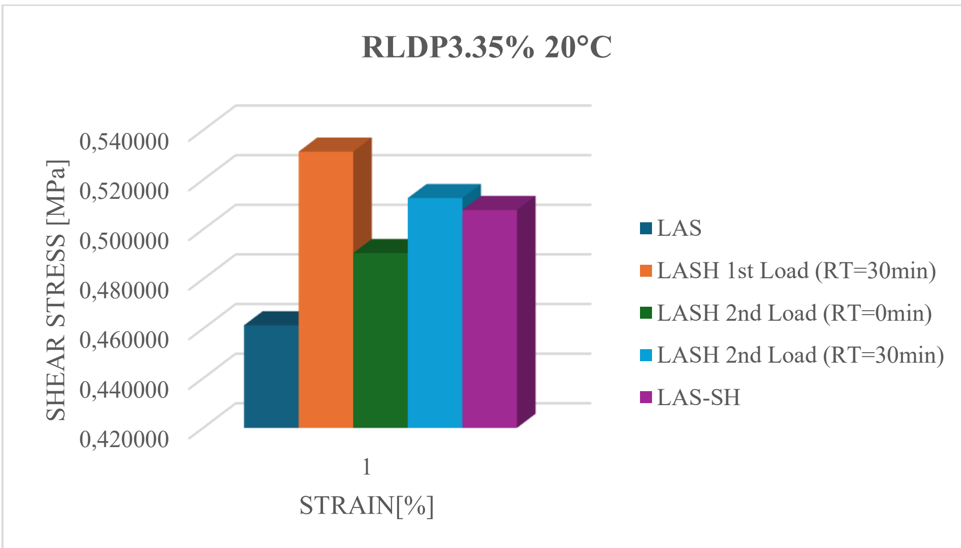


Figure 3.5.1.4-shear stress-strain diagram related to RLDP3.3% modified binder

| #TRIALS | 15°C SBS | τ (ref) [pa] | τ (ref) [MP] | γ (ref) [%] |
|---|---|---|---|---|
| AVG | LAS | 624534 | 0,624534 | 8,00 |
| AVG | LASH 1st Load (RT=30min) | 677417 | 0,677417 | 8,00 |
| AVG | LASH 2nd Load (RT=0min) | 649787 | 0,649787 | 8,00 |
| AVG | LASH 2nd Load (RT=30min) | 682326 | 0,682326 | 8,00 |
| AVG | LAS-SH | 682860 | 0,682860 | 8,00 |

Table3.5.1.5 -Average values of rheological tests related to SBS modified binder

ΔDamage = 0.677417 − 0.649787 = 0.028

ΔSH = 0.682860 − 0.649787= 0.0331

Δ (H+SH) = 0.682326 − 0.649787 =0.0325

ΔH =0.0325−0.0331/0.028= -0.02

Due to above calculation, the obtained healing index for SBS modified binder at 15°C temperature indicates NO Healing had occurred .

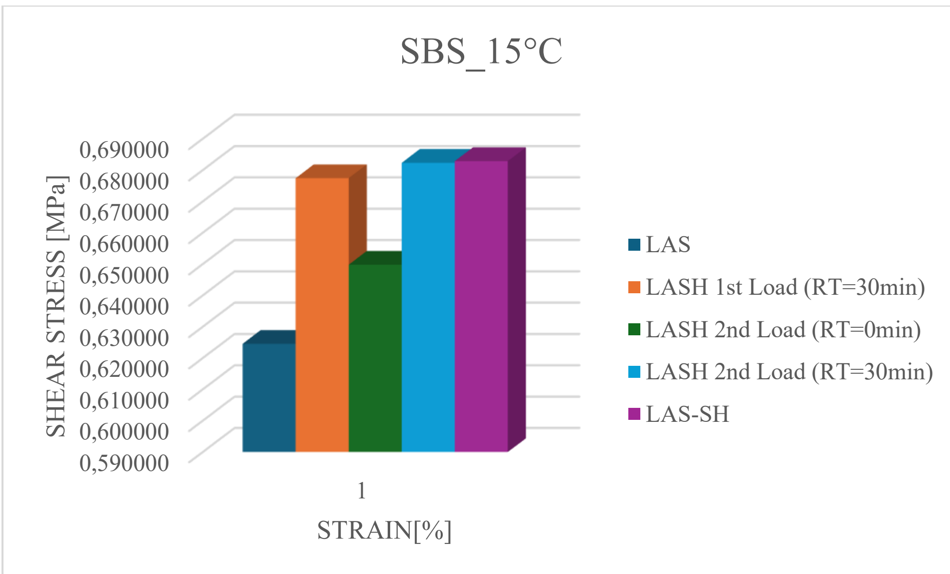


Figure 3.5.1.5-shear stress-strain diagram related to SBS modified binder

| #TRIALS | 20°C SBS | τ (ref) [pa] | τ (ref) [MP] | γ (ref) [%] |
|---|---|---|---|---|
| AVG | LAS | 390281 | 0,390281 | 10,00 |
| AVG | LASH 1st Load (RT=30min) | 423519 | 0,423519 | 10,00 |
| AVG | LASH 2nd Load (RT=0min) | 391842 | 0,391842 | 10,00 |
| AVG | LASH 2nd Load (RT=30min) | 411032 | 0,411032 | 10,00 |
| AVG | LAS-SH | 356325 | 0,356325 | 10,00 |

Table3.5.1.6 -Average values of rheological tests related to SBS modified binder

$\Delta$Damage = 0.423519 − 0.391842 = 0.032

$\Delta$SH = 0.356325 − 0.391842= -0.036

$\Delta$ (H+SH) = 0.411032 − 0.391842 =0.019

$\Delta$H =0.019 − (−0.036) /0. 032= 1.73

The SBS-modified binder exhibited a healing index ($\Delta$H) of 1.73, indicating an exceptionally high recovery capability following the rest period. Although this value exceeds the theoretical limit corresponding to complete recovery of the induced damage, it should not be interpreted as a literal healing of 173%. SBS-modified binders are known to exhibit enhanced elastic recovery due to the presence of a three-dimensional polymer network, which improves their ability to restore mechanical properties after loading [40,41]. Furthermore, polymer modification has been shown to promote damage recovery and crack closure during rest periods[40,42].

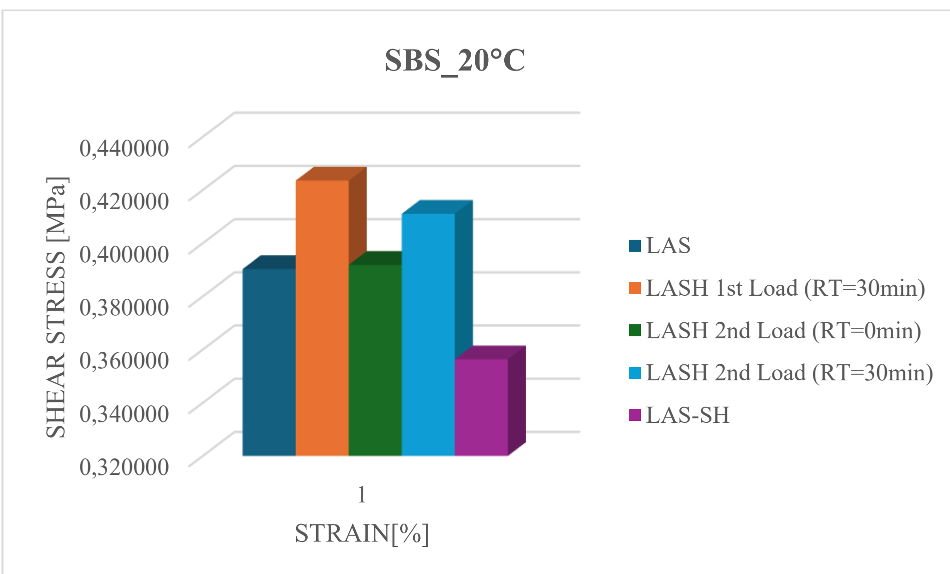


Figure3.5.1.6 -shear stress-strain diagram related to SBS modified binder

### 3.5.2-Analysis based on AASHTO TP101

This test method covers how to determine asphalt binders' resistance to damage by means of cyclic loading employing linearly increasing load amplitudes to accelerate damage. The amplitude sweep is conducted using the Dynamic Shear Rheometer at the intermediate pavement temperature determined from the performance grade (PG) of the asphalt binder according to M 320 [26]. In this method, characteristics of the rate of damage accumulation in the material can be used to indicate the fatigue performance of the asphalt binder given pavement structural conditions and/or expected amount of traffic loading using predictive modeling techniques [26].

According to AASHTO TP101 , a sample is prepared consistently with T 315 (DSR) using the 8-mm parallel plate geometry with a 2-mm gap setting. The sample is tested in shear using a frequency sweep to determine rheological properties. The sample is then tested using a series of oscillatory load cycles at linearly increasing amplitudes at a constant frequency to cause accelerated fatigue damage. The continuum damage approach is used to calculate the fatigue resistance from rheological properties and amplitude sweep results [26].

*Test protocol*—Two types of testing are performed in succession. The first test, a frequency sweep, is designed to obtain information on the rheological properties, and the second test, an amplitude sweep, is intended to measure the damage characteristics of the material [26].

*Frequency sweep*—Frequency sweep test data is used to determine the damage analysis "alpha" parameter. The frequency sweep test is performed at the selected temperature and applies oscillatory shear loading at constant amplitude over a range of loading frequencies. For this test method, the frequency sweep test is selected from the DSR manufacturer's controller software, employing an applied load of 0.1

percent strain over a range of frequencies from 0.2–30 Hz. Data is sampled at the following 12 unique frequencies (all in Hz), Complex shear modulus [|G*|, Pa] and phase angle [d, degrees] are recorded at each frequency [26].

*Amplitude sweep*—The second test is run at the selected temperature using oscillatory shear in strain-control mode at a frequency of 10 Hz. The loading scheme consists of a continuous oscillatory strain sweep. Loading is increased linearly from zero to 30% over the course of 3,100 cycles of loading. Peak shear strain and peak shear stress are recorded every 10 load cycles (1sec), along with phase angle [d, degrees] and dynamic shear modulus [|G*|, Pa] [26].

As is shown in figure below loading cycle is  linear ,because during the amplitude sweep, the strain amplitude increases linearly with time , typically from0.1% to 30% strain over 3100 loading cycles . Therefore, the loading history is continuous linear strain ramp not a staircase.

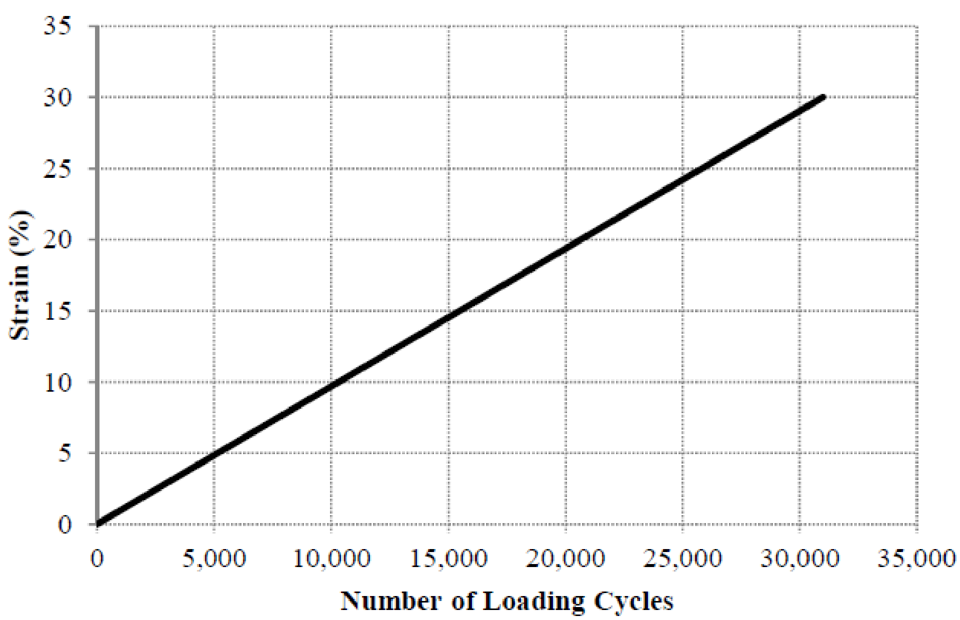

For each measured point, damage accumulation is computed incrementally as:

$$D(t) = \sum_{i=1}^{N} [\pi\gamma\ ^2(C\,i-1\ -Ci)]^{\frac{\alpha}{1+\alpha}}(\,ti\ -ti-1)^{\frac{1}{1+\alpha}}$$

Where

- $|G0*|$is the undamaged modulus (second data point of LAS),
- $\gamma(t)$is the applied shear strain at that measurement,
- $\alpha$=1/$m$ is derived from the frequency sweep master curve, and
- $\Delta t$is the time increment between measurement points.

As the test progresses, the material integrity is expressed through:

$$C(t) = \frac{|G*|(t)}{|G*|initial}$$

Where

- t = testing time

It is important to note that the initial "undamaged" value of |G*| is the second data point, as the first point after change of material condition from rest differs from the undamaged modulus of material at the target loading frequency.

Summation of damage accumulation begins with the first data point. The incremental value of *D*(*t*) at each subsequent point is added to the value of *D*(*t*) from the previous point. This is performed up until the final data point from the test at 30 percent applied strain [26].

For each data point at a given time *t*, values of *C(t)* and *D*(*t*) are recorded (it is assumed that *C,* at *D* (0) is equal to one, and *D* (0) = 0. The relationship between *C(t)* and *D*(*t*) can then be fit to the following power law:

$$C(t) = C_0 - C_1 (D)^\wedge C_2$$

where:

$C_0 = 1$, the initial value of $C$ $C_1$ and $C_2$ = curve-fit coefficients derived through

linearization of the power law adapted from Hintz, et al., in the form shown below:

$$\log (C_0 - C(t)) = \log(C_1) + C_2 \, . \log(D(t))$$

Using the above equation, $C_1$ is calculated as the anti-log of the intercept and $C_2$ is calculated as the slope of line formed as log($C_0$ – C(t)) versus log(*D(t)*). For calculation of both $C_1$ and $C_2$, data corresponding to damages less than 10 are ignored [26].

To calculate fatigue law parameters A and B , first $D_f$ must be calculated, $D_f$ is damage accumulation at time of failure that is obtained by below formula:

$$D(f) = \frac{(C0 - C\ at\ peak\ stress)^{\frac{1}{C2}}}{C1}$$

A is calculated through :

$$A = \frac{f\ (Df)^{\ k}}{k\ (\pi C1C2)^{\ \alpha}}$$

Where

- f = loading frequency (10 Hz),
- k = 1 + (1 – $C_2$) α

Lastly B is achieved through:

B = 2α

Finally, by processing all previous steps calculation of $N_f$ by below formula is conducted:

$$Nf = A * \gamma_{max}^{-B}$$

The tables below show fatigue life in three strain levels 1%, 5% and the peak strain average for LAS, LASH with 30 minutes rest time, LASH with no rest time and LAS-steric hardening for Neat50/70, SBS modified binder, modified binder with 3.35% RLDP. All damage parameters and necessary data related to analysis based on AASHTOTP101 are calculated and gathered in each table separately for 15°C and 20°CC

| | LAS_AVG_15°C_NEAT_(t1, t2) | | |
|---|---|---|---|
| C0 | C1 | | C2 |
| 1,00 | 0,075495 | | 0,33448082 |
| ALPHA | Df | | K |
| 1,548820122 | 345,678 | | 2,03081214 |
| A | B | APPLIED STRAIN | Nf |
| 36587321 | 3,09764 | 1 | 36587320,9 |
| | | 5 | 250134,153 |
| | | 8,162 | 54816,6884 |

Figure3.5.2.1 -AASHTOTP101 damage parameter related to LAS Neat15°C

| | LASH_AVG_15°C_NEAT_RT=30 MIN (t2, t3, t4) | | |
|---|---|---|---|
| C0 | C1 | | C2 |
| 1,00 | 0,075765 | | 0,33581667 |
| ALPHA | Df | | K |
| 1,518842 | 308,7 | | 2,00881183 |
| A | B | APPLIED STRAIN | Nf |
| 24504180 | 3,037684 | 1 | 24504180,2 |
| | | 5 | 184497,283 |
| | | 7,756 | 48618,4833 |

Figure3.5.2.2 -AASHTOTP101 damage parameters related to LASH 30 min rest Neat15°C

| | LASH_AVG_15°C_NEAT_RT=0 MIN (t1, t2, t3, t4) | | |
|---|---|---|---|
| C0 | C1 | | C2 |
| 1,00 | 0,138017 | | 0,25931396 |
| ALPHA | Df | | K |
| 1,557301 | 231,5648 | | 2,15343978 |
| A | B | APPLIED STRAIN | Nf |
| 19020023 | 3,114602 | 1 | 19020023,1 |
| | | 5 | 126531,227 |
| | | 7,851 | 31042,889 |

Figure3.5.2.3 -AASHTOTP101 damage parameters related to LASH 0 min rest Neat15°C

| | LAS-SH_AVG_15°C_NEAT_ (t1, t2) | | |
|---|---|---|---|
| C0 | C1 | | C2 |
| 1,00 | 0,0753 | | 0,33434661 |
| ALPHA | Df | | K |
| 1,58512567 | 360,4699 | | 2,05519179 |
| A | B | APPLIED STRAIN | Nf |
| 48888844 | 3,170251 | 1 | 48888843,9 |
| | | 5 | 297371,383 |
| | | 8,260 | 60566,9754 |

Figure3.5.2.4 -AASHTOTP101 damage parameters related to LAS-SH 30 min rest Neat15°C

| | LAS_AVG_15°C_RLDP3.35%_ (t1, t2) | | |
|---|---|---|---|
| C0 | C1 | | C2 |
| 1,00 | 0,106977306 | | 0,29339003 |
| ALPHA | Df | | K |
| 1,799018428 | 277,2709342 | | 2,271203526 |
| A | B | APPLIED STRAIN | Nf |
| 106028105 | 3,598036856 | 1 | 106028105,3 |
| | | 5 | 323967,2907 |
| | | 7,82 | 64823,14496 |

Figure3.5.2.5 -AASHTOTP101 damage parameters related to LAS modified binder with 3.35%RLDP15°C

| | LASH_AVG_15°C_RLDP3.35%_RT=30 MIN (t2, t3) | | |
|---|---|---|---|
| C0 | C1 | | C2 |
| 1,00 | 0,125059 | | 0,27455526 |
| ALPHA | Df | | K |
| 1,795031 | 207,9096 | | 2,30227886 |
| A | B | APPLIED STRAIN | Nf |
| 52499993 | 3,590063 | 1 | 52499993,3 |
| | | 5 | 162484,984 |
| | | 7,673 | 34928,5422 |

Figure3.5.2.6 -AASHTOTP101 damage parameters related to LASH 30 minutes rest modified binder with 3.35%RLDP15℃

| | LASH_AVG_15°C_RLDP3.35%_RT=0 MIN (t2, t5) | | |
|---|---|---|---|
| C0 | C1 | | C2 |
| 1,00 | 0,175833 | | 0,22615999 |
| ALPHA | Df | | K |
| 1,778806 | 192,0049 | | 2,37651238 |
| A | B | APPLIED STRAIN | Nf |
| 48031493 | 3,557612 | 1 | 48031493,3 |
| | | 5 | 156625,457 |
| | | 7,576 | 35712,5069 |

Figure3.5.2.7 -AASHTOTP101 damage parameters related to LASH 0 minutes rest modified binder with 3.35%RLDP15℃

| | LAS-SH_AVG_15°C_RLDP3.35%_ (t2, t3) | | |
|---|---|---|---|
| C0 | C1 | | C2 |
| 1,00 | 0,106817 | | 0,29624414 |
| | | | |
| ALPHA | Df | | K |
| 1,827845 | 211,1381 | | 2,28646917 |
| | | | |
| A | B | APPLIED STRAIN | Nf |
| 66496886 | 3,65569 | 1 | 66496886,3 |
| | | 5 | 185175,554 |
| | | 7,088 | 51707,113 |

Figure 3.5.2.8-AASHTOTP101 damage parameters related to LAS-SH modified binder with 3.35%RLDP15℃

| | LAS_AVG_15°C_SBS_ (t2, t4, t5) | | |
|---|---|---|---|
| C0 | C1 | | C2 |
| 1,00 | 0,066862 | | 0,40385776 |
| | | | |
| ALPHA | Df | | K |
| 1,682457 | 201,5834 | | 2,00169534 |
| | | | |
| A | B | APPLIED STRAIN | Nf |
| 40459194 | 3,364915 | 1 | 40459194,1 |
| | | 5 | 179904,825 |
| | | 6,677 | 67967,0326 |

Figure 3.5.2.9-AASHTOTP101 damage parameters related to LAS SBS modified binder at 15℃

| | LASH_AVG_15°C_SBS_RT=30 MIN (t2, t5) | | |
|---|---|---|---|
| C0 | C1 | | C2 |
| 1,00 | 0,108102 | | 0,273595386 |
| ALPHA | Df | | K |
| 1,6426577 | 512,0391 | | 2,193316145 |
| A | B | APPLIED STRAIN | Nf |
| 203628657 | 3,285315 | 1 | 203628656,7 |
| | | 5 | 1029205,144 |
| | | 9,431 | 127970,3297 |

Figure3.5.2.9 -AASHTOTP101 damage parameters related to LASH 30 minutes rest SBS modified binder at 15℃

| | LASH_AVG_15°C_SBS_RT=0 MIN (t6, t7) | | |
|---|---|---|---|
| C0 | C1 | | C2 |
| 1,00 | 0,145224792 | | 0,235427485 |
| ALPHA | Df | | K |
| 1,646011335 | 451,5642539 | | 2,258489622 |
| A | B | APPLIED STRAIN | Nf |
| 177336118 | 3,29202267 | 1 | 177336117,8 |
| | | 5 | 886690,5842 |
| | | 9,872 | 94448,03146 |

Figure 3.5.2.10-AASHTOTP101 damage parameters related to LASH 0 minutes rest SBS modified binder at 15℃

| | LAS-SH_AVG_15°C_SBS_ (t1, t3, t4) | | |
|---|---|---|---|
| C0 | C1 | | C2 |
| 1,00 | 0,086856 | | 0,31517256 |
| | | | |
| ALPHA | Df | | K |
| 1,64425475 | 454,7689 | | 2,12588572 |
| | | | |
| A | B | APPLIED STRAIN | Nf |
| 173757585 | 3,288509 | 1 | 173757585 |
| | | 5 | 873724,015 |
| | | 8,960 | 128328,456 |

Figure3.5.2.11 -AASHTOTP101 damage parameters related to LAS-SH 30 minutes rest SBS modified binder at 15°C

| | LAS_AVG_20°C_NEAT_ (t1, t2) | | |
|---|---|---|---|
| C0 | C1 | | C2 |
| 1,00 | 0,050445 | | 0,35730464 |
| | | | |
| ALPHA | Df | | K |
| 1,256092578 | 634,1686 | | 1,8073397 |
| | | | |
| A | B | APPLIED STRAIN | Nf |
| 23742284 | 2,512185 | 1 | 23742284,4 |
| | | 5 | 416466,846 |
| | | 9,97 | 73555,5337 |

Figure 3.5.2.12-AASHTOTP101 damage parameters related to LAS Neat at 20°C

| | LASH_AVG_20°C_NEAT_RT=30 MIN (t1, t2) | | |
|---|---|---|---|
| C0 | C1 | | C2 |
| 1,00 | 0,083632 | | 0,30241166 |
| | | | |
| ALPHA | Df | | K |
| 1,277319 | 379,7252 | | 1,89120397 |
| | | | |
| A | B | APPLIED STRAIN | Nf |
| 10288638 | 2,554639 | 1 | 10288638,3 |
| | | 5 | 168555,199 |
| | | 8,476 | 43775,4818 |

Figure3.5.2.13 -AASHTOTP101 damage parameters related to LASH 30 minutes rest  Neat at 20℃

| | LASH_AVG_20°C_NEAT_RT=0 MIN (t1, t2, t3) | | |
|---|---|---|---|
| C0 | C1 | | C2 |
| 1,00 | 0,12491 | | 0,25292 |
| | | | |
| ALPHA | Df | | K |
| 1,26468 | 296,899 | | 1,945325 |
| | | | |
| A | B | APPLIED STRAIN | Nf |
| 6116554 | 2,529359 | 1 | 6116554 |
| | | 5 | 104366,3 |
| | | 8,458 | 27613 |

Figure 3.5.2.14-AASHTOTP101 damage parameters related to LASH 0 minutes rest Neat at 20℃

| | LAS-SH_AVG_20°C_NEAT_ (t1, t2) | | |
|---|---|---|---|
| C0 | C1 | | C2 |
| 1,00 | 0,054639 | | 0,34854933 |
| ALPHA | Df | | K |
| 1,3122389 | 711,7381 | | 1,8548389 |
| A | B | APPLIED STRAIN | Nf |
| 42575458 | 2,624478 | 1 | 42575458,3 |
| | | 5 | 623344,418 |
| | | 10,570 | 87397,1489 |

Figure3.5.2.15 -AASHTOTP101 damage parameters related to LAS-SH Neat at 20℃

| | LAS_AVG_20°C_RLDP3.35%_(t1, t2) | | |
|---|---|---|---|
| C0 | C1 | | C2 |
| 1,00 | 0,079578 | | 0,31538689 |
| ALPHA | Df | | K |
| 1,54848598 | 439,8182 | | 2,06011551 |
| A | B | APPLIED STRAIN | Nf |
| 79082006 | 3,096972 | 1 | 79082005,7 |
| | | 5 | 541236,612 |
| | | 9,24 | 80936,9178 |

Figure 3.5.2.16-AASHTOTP101 damage parameters related to LAS modified binder with 3.35%RLDP at 20℃

| | LASH_AVG_20°C_RLDP3.35%_RT=30 MIN (t3, t4, t5, t6) | | |
|---|---|---|---|
| C0 | C1 | | C2 |
| 1,00 | 0,092059 | | 0,295015359 |
| ALPHA | Df | | K |
| 1,540759 | 463,5632 | | 2,086284145 |
| A | B | APPLIED STRAIN | Nf |
| 79948255 | 3,081518 | 1 | 79948254,76 |
| | | 5 | 560944,6691 |
| | | 9,579 | 75657,63664 |

Figure 3.5.2.17-AASHTOTP101 damage parameters related to LASH 30 minutes rest modified binder with 3.35%RLDP at 20°C

| | LASH_AVG_20°C_RLDP3.35%_RT=0 MIN (t1, t2, t3) | | |
|---|---|---|---|
| C0 | C1 | | C2 |
| 1,00 | 0,129602 | | 0,247273786 |
| ALPHA | Df | | K |
| 1,555401 | 385,7872 | | 2,170799771 |
| A | B | APPLIED STRAIN | Nf |
| 66614448 | 3,110801 | 1 | 66614448,41 |
| | | 5 | 445873,5435 |
| | | 9,966 | 52169,13759 |

Figure3.5.2.18 -AASHTOTP101 damage parameters related to LASH 0 minutes rest modified binder with 3.35%RLDP at 20°C

| | LAS-SH_AVG_20°C_RLDP3.35%_ (t2, t4) | | |
|---|---|---|---|
| C0 | C1 | | C2 |
| 1,00 | 0,079275 | | 0,31263561 |
| ALPHA | Df | | K |
| 1,53287011 | 462,0484 | | 2,05364156 |
| A | B | APPLIED STRAIN | Nf |
| 72369444 | 3,06574 | 1 | 72369443,8 |
| | | 5 | 520828,54 |
| | | 9,286 | 78075,6504 |

Figure3.5.2.19 -AASHTOTP101 damage parameters related to LAS-SH modified binder with 3.35%RLDP at 20℃

| | LAS_AVG_20°C_SBS_ (t3, t4, t5) | | |
|---|---|---|---|
| C0 | C1 | | C2 |
| 1,00 | 0,068132 | | 0,32542981 |
| ALPHA | Df | | K |
| 1,461315 | 558,8722 | | 1,98579595 |
| A | B | APPLIED STRAIN | Nf |
| 79619404 | 2,922631 | 1 | 79619403,8 |
| | | 5 | 721419,06 |
| | | 9,285 | 118193,941 |

Figure3.5.2.20 -AASHTOTP101 damage parameters related to LAS SBS modified binder at 20℃

| | LASH_AVG_20°C_SBS_RT=30 MIN (t2, t3, t4) | | |
|---|---|---|---|
| C0 | C1 | | C2 |
| 1,00 | 0,068994 | | 0,314055607 |
| ALPHA | Df | | K |
| 1,435823046 | 766,832 | | 1,984944819 |
| A | B | APPLIED STRAIN | Nf |
| 132903555 | 2,871646 | 1 | 132903554,7 |
| | | 5 | 1307200,23 |
| | | 10,717 | 146396,5458 |

Figure 3.5.2.21-AASHTOTP101 damage parameters related to LASH 30 minutes rest SBS modified binder at 20°C

| | LASH_AVG_20°C_SBS_RT=0 MIN (t1, t2, t3) | | |
|---|---|---|---|
| C0 | C1 | | C2 |
| 1,00 | 0,12614 | | 0,23894732 |
| ALPHA | Df | | K |
| 1,437192 | 608,1384 | | 2,09378345 |
| A | B | APPLIED STRAIN | Nf |
| 95568410 | 2,874384 | 1 | 95568409,7 |
| | | 5 | 935849,491 |
| | | 10,943 | 98491,5713 |

Figure 3.5.2.22-AASHTOTP101 damage parameters related to LASH 0 minutes rest SBS modified binder at 20°C

| | LAS-SH_AVG_20°C_SBS_ (t1,t2,t4) | | |
|---|---|---|---|
| C0 | C1 | | C2 |
| 1,00 | 0,060626 | | 0,341895421 |
| ALPHA | Df | | K |
| 1,462640844 | 698,0538 | | 1,962490076 |
| A | B | APPLIED STRAIN | Nf |
| 140214525 | 2,925282 | 1 | 140214525,2 |
| | | 5 | 1265053,381 |
| | | 10,56 | 142183,5144 |

Figure 3.5.2.23-AASHTOTP101 damage parameters related to LAS-SH SBS modified binder at 20°C

In the following part the graphs below depict fatigue life of asphalt binder versus the strain for LAS test at 15°C. The common point about all these graphs is they experience a downward trend which means that by increasing the strain the fatigue life will decrease. According to graphical details below it is evident that for the neat the level consistency between the trials is high while SBS modified binder the repeatability is not as good as neat and 3.35% RLDP modified binder.

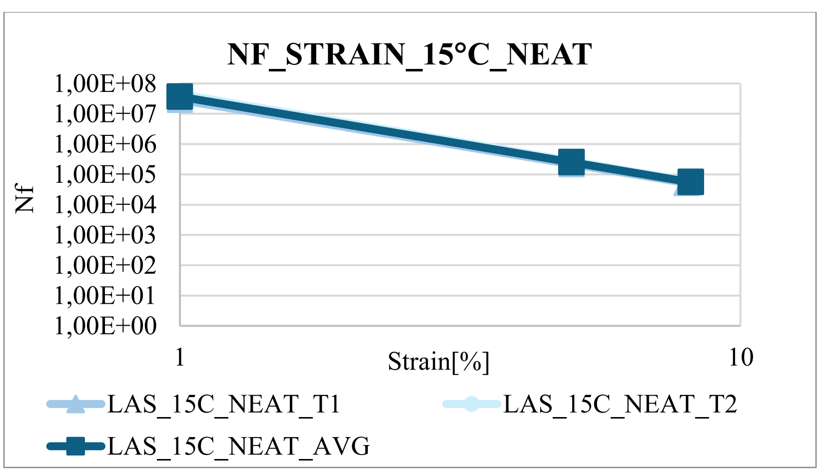


Figure3.5.2.24 -fatigue-strain curve of trials and average for LAS Neat50/70 at 15°C

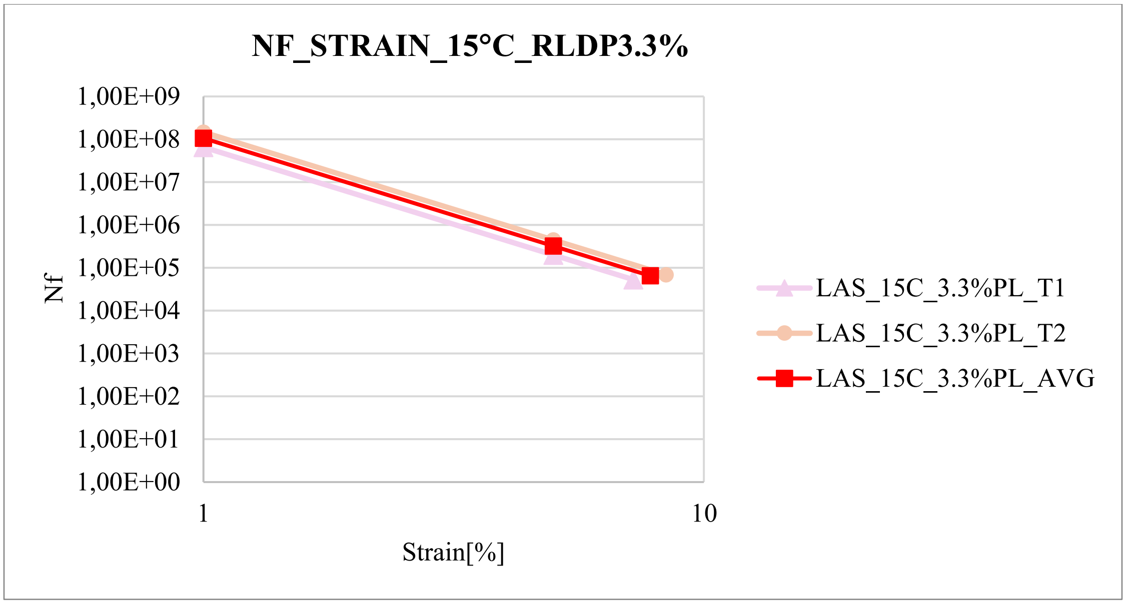


Figure3.5.2.25 -fatigue-strain curve of trials and average for LAS 3.35%RLDP modified binder at 15°C

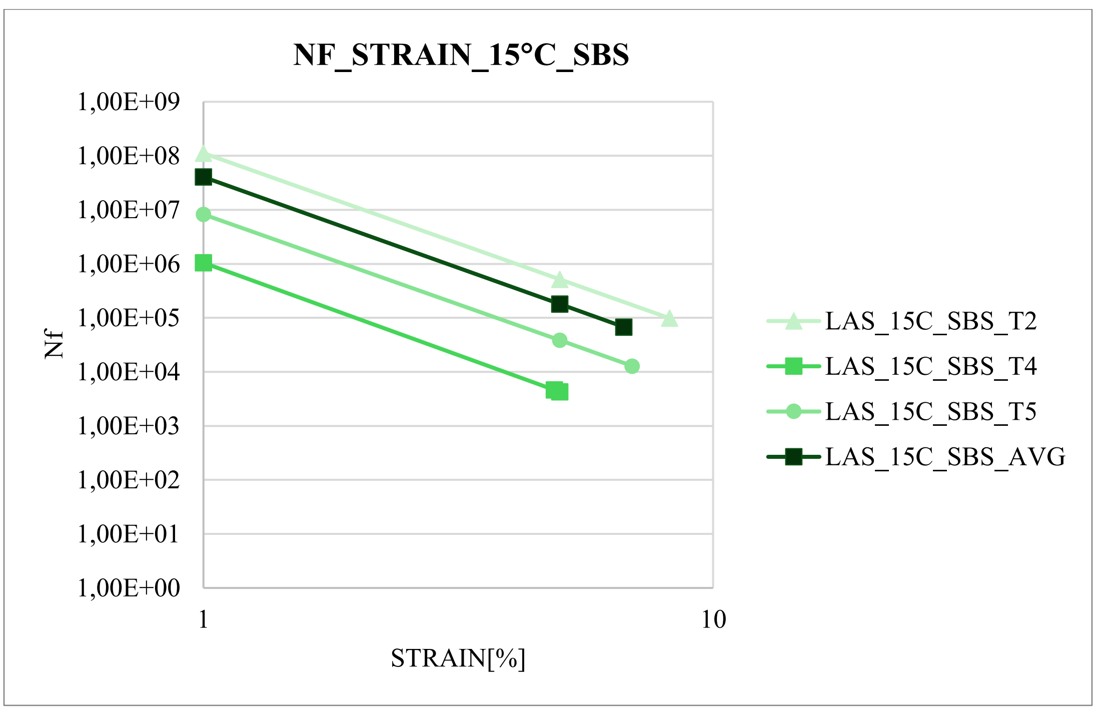


Figure3.5.2.26 -fatigue-strain curve of trials and average for LAS SBS modified binder at 15°C

Figure below presents the fatigue life (Nf) predictions from the LAS test for the neat 50/70 binder, SBS-modified binder, and RLDP 3.35% modified binder at 15°C. For all binders, fatigue life decreased markedly with increasing strain, confirming the anticipated inverse correlation between strain amplitude and fatigue resistance. Among the materials evaluated, the RLDP 3.35% modified binder consistently demonstrated the highest predicted fatigue life, indicating superior resistance to fatigue damage under the test conditions. The SBS-modified binder also exhibited enhanced fatigue performance relative to the neat binder, although its fatigue life was slightly lower than that of the RLDP-modified binder. At elevated strain levels, the fatigue life curves converged, implying that the effect of binder modification diminishes as applied deformation increases and fatigue damage becomes the prevailing failure mechanism.

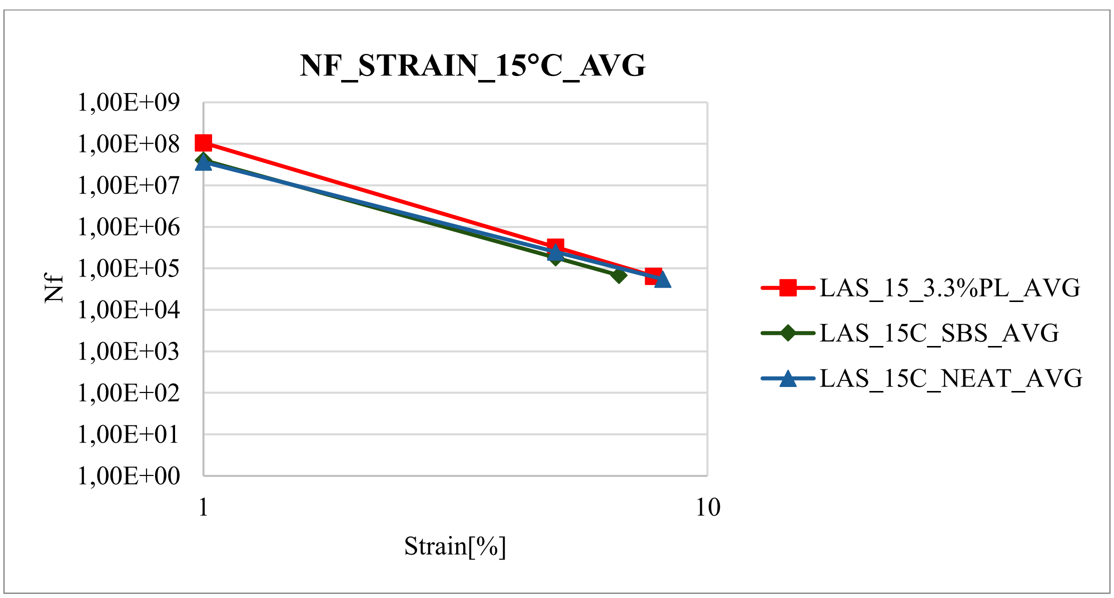


Figure3.5.2.27 – comparison of Neat50/70, SBS modified binder , modified binder with 3.35% RLDP from LAS test at 15°C

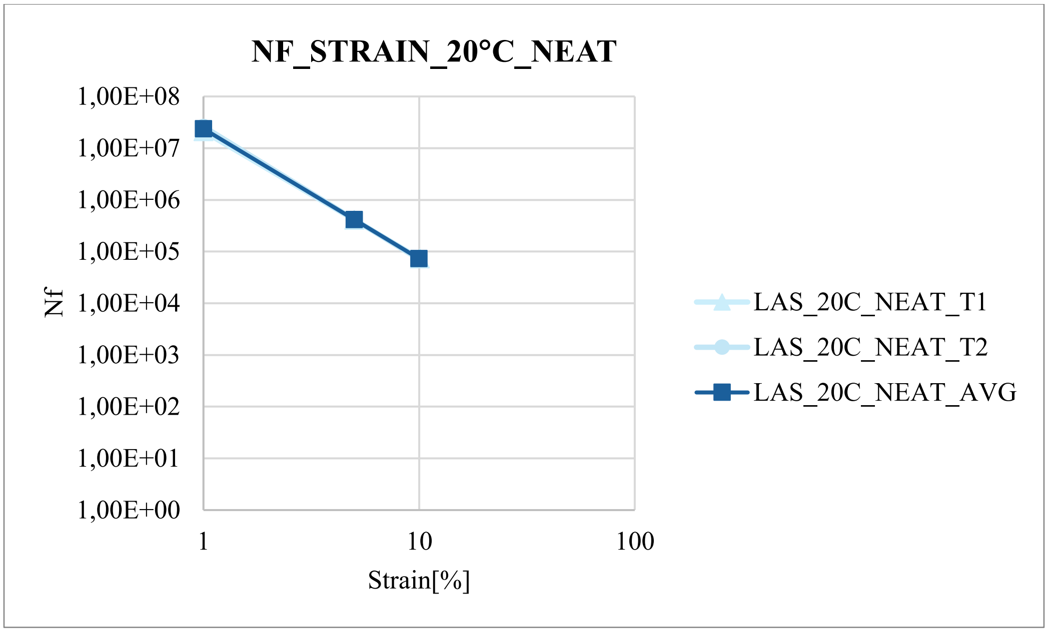


Figure3.5.2.28 -fatigue-strain curve of trials and average for LAS Neat50/70 at 20℃

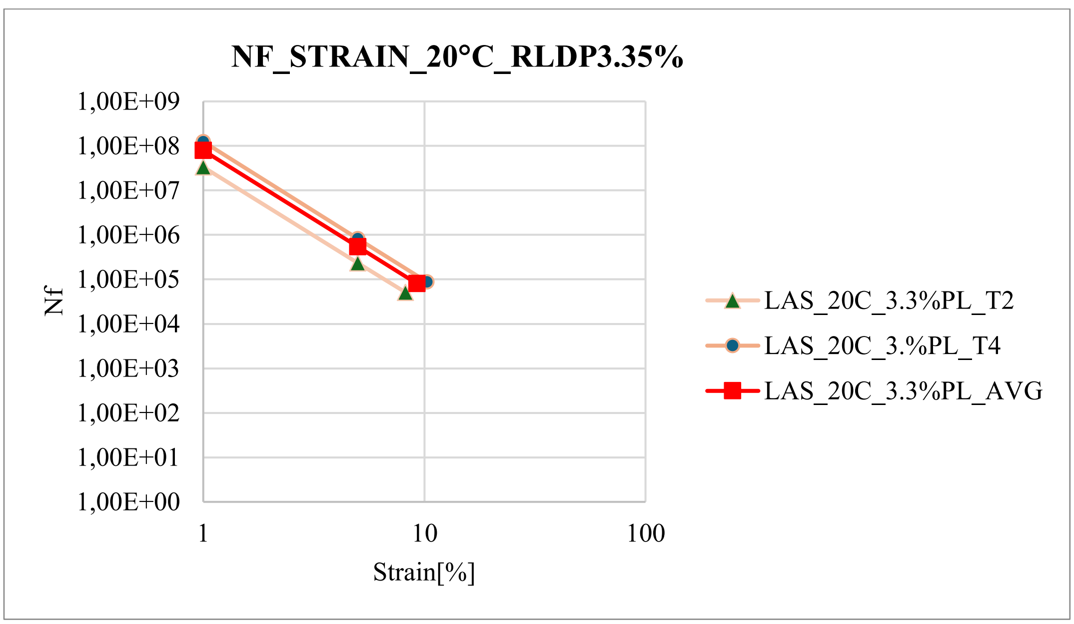


Figure3.5.2.29 -fatigue-strain curve of trials and average for LAS 3.35%RLDP modified binder at 20℃

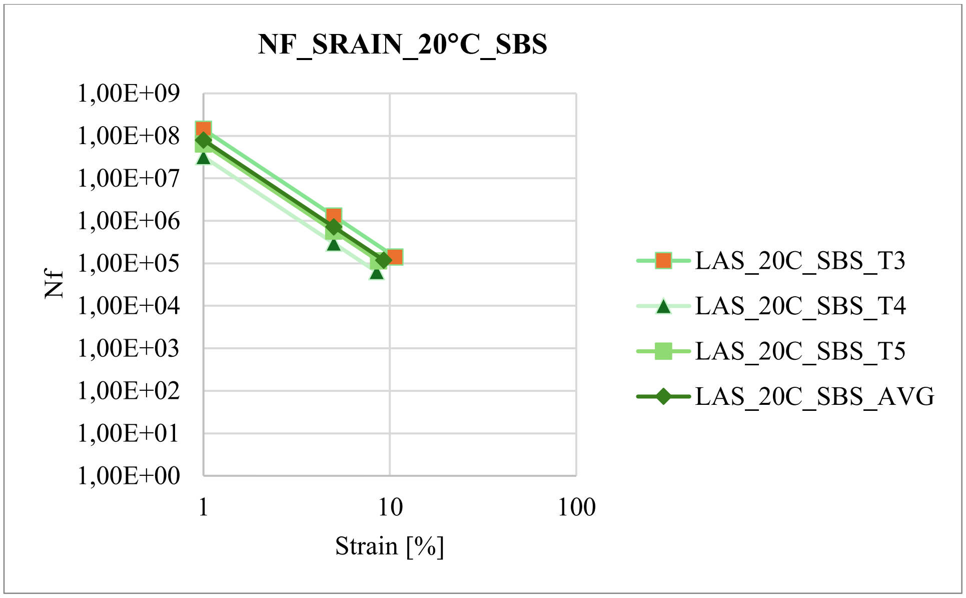


Figure3.5.2.30 -fatigue-strain curve of trials and average for LAS SBS modified binder at 20℃

Figure below presents the predicted fatigue life ($N_f$) as a function of strain for the neat 50/70, SBS-modified, and RLDP 3.35% modified binders at 20°C. As expected, the fatigue life of all binders decreased progressively with increasing strain, reflecting the accelerated accumulation of fatigue damage under higher deformation levels. At low strain, both modified binders exhibited substantially greater fatigue resistance than the neat binder, with the RLDP 3.35% and SBS binders showing comparable fatigue lives. However, as the strain increased, the fatigue life of the RLDP-modified binder decreased more rapidly than that of the SBS-modified binder. At the highest strain level, the SBS-modified binder exhibited the greatest fatigue resistance, while the RLDP 3.35% binder showed the lowest predicted fatigue life among the three materials. These findings suggest that SBS modification provides superior fatigue performance under high strain conditions, whereas RLDP modification is more effective at lower deformation levels.

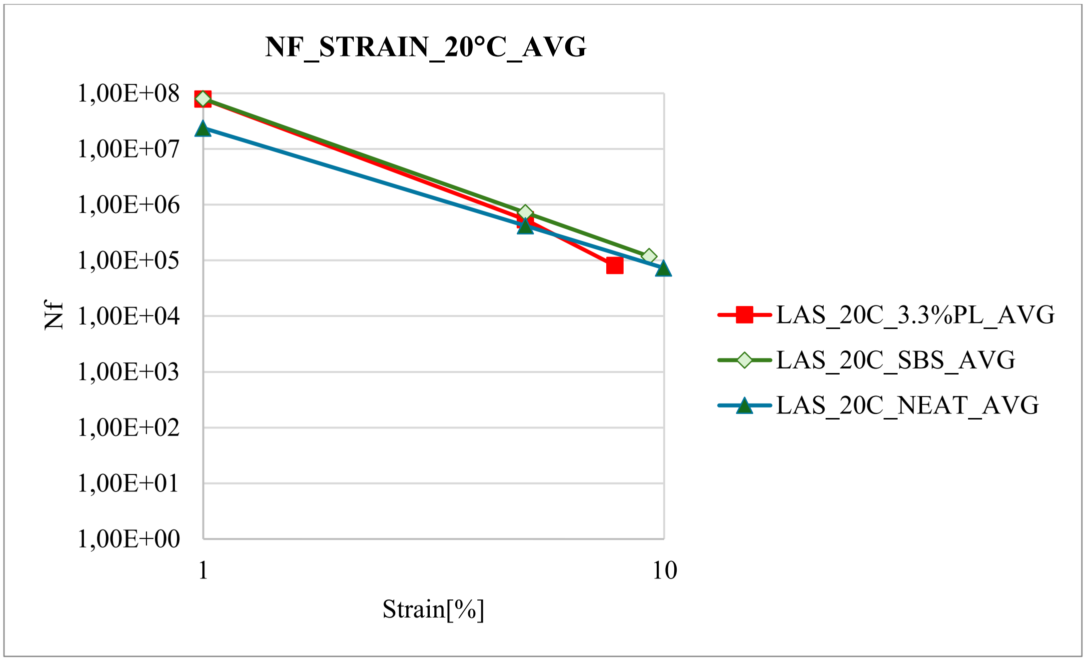


Figure3.5.2.31 -fatigue-strain curve of , average for LAS SBS modified binder , 3.3%RLDP, Neat50/70 at 20℃

The following figures present a comparison of the LAS, LAS-H (30-minute rest period), LASH (without rest period), and LAS-SH test results for each binder. The results are expressed as predicted fatigue life ($N_f$) versus strain, with all four test conditions plotted on a single graph for each binder. The curves are based on the average values obtained from the convergent experimental trials.

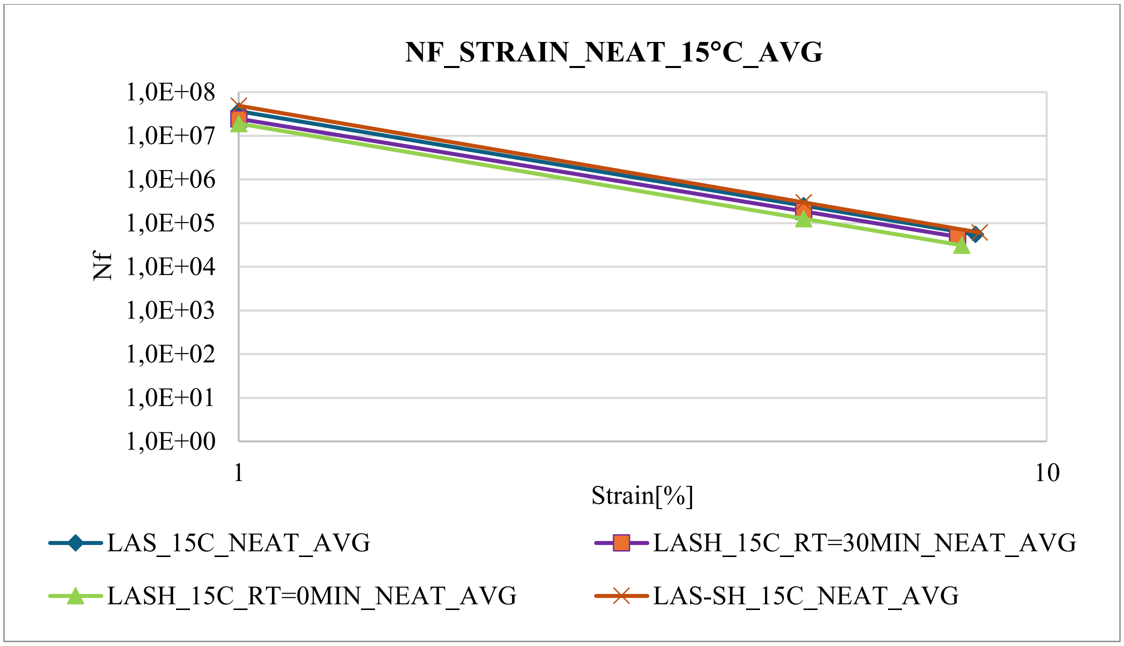


Figure3.5.2.32 -comparison of LAS, LASH RT=30, LASH RT=0, LAS-SH, for Neat50/70 at15℃

According to the above graph for Neat50/70 at 15°C the LAS-Steric hardening has placed at highest fatigue life throughout the investigated strain range showing high molecular reorientation and structural rearrangement. It is followed but LAS test and as expected LASH (healing) with 30 minutes rest places higher than healing without rest although the difference is very slight which is not out of expectation since it is a neat binder without modification. While figure W indicates the data related to RLDP3.35% . As expected, fatigue life decreases progressively with increasing strain, reflecting the accelerated damage accumulation under higher deformation levels. The conventional LAS test exhibited the highest fatigue life throughout the investigated strain range, representing the fatigue resistance of the undamaged material. Both LASH curves showed lower fatigue lives due to the damage introduced during the first loading phase. The introduction of a 30-minute rest period resulted in a slight increase in fatigue life compared with the condition without rest, indicating the occurrence of recovery processes during the rest interval.

Furthermore, the LAS-SH curve consistently exceeded the LASH results, demonstrating that steric hardening contributed to the observed recovery. Overall, the results suggest that the RLDP 3.3% binder possesses a measurable self-healing capability at 15°C, although a portion of the recovery can be attributed to physical hardening phenomena occurring during the rest period.

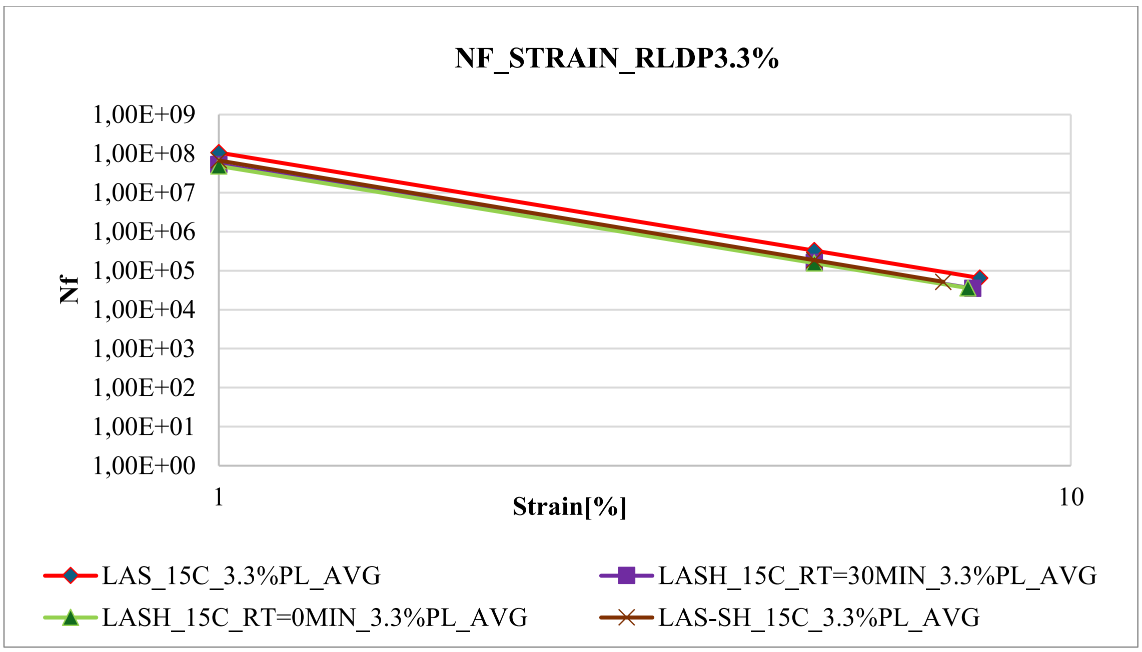


Figure3.5.2.33 -comparison of LAS, LASH RT=30, LASH RT=0, LAS-SH, for modified binder with 3.35%RLDP at15°C

For the SBS-modified binder at 15°C, the LASH test with a 30-minute rest period produced the highest predicted fatigue life ($N_f$) over the investigated strain range. The LASH test without a rest period exhibited slightly lower fatigue life values, indicating that the introduction of a 30-minute recovery period enhanced the binder's ability to recover from fatigue damage. This improvement suggests that the rest period promoted the self-healing process, resulting in increased resistance to fatigue failure. The LAS-SH curve closely followed the LAS-H responses, demonstrating that steric hardening also contributed to the observed recovery in mechanical performance during the rest period. In contrast, the conventional LAS test consistently yielded the lowest fatigue life, reflecting the absence of any recovery mechanism during loading. Overall, these results indicate that the SBS-modified binder exhibits a pronounced recovery capacity, with both self-healing and steric hardening contributing to the improvement in fatigue performance.

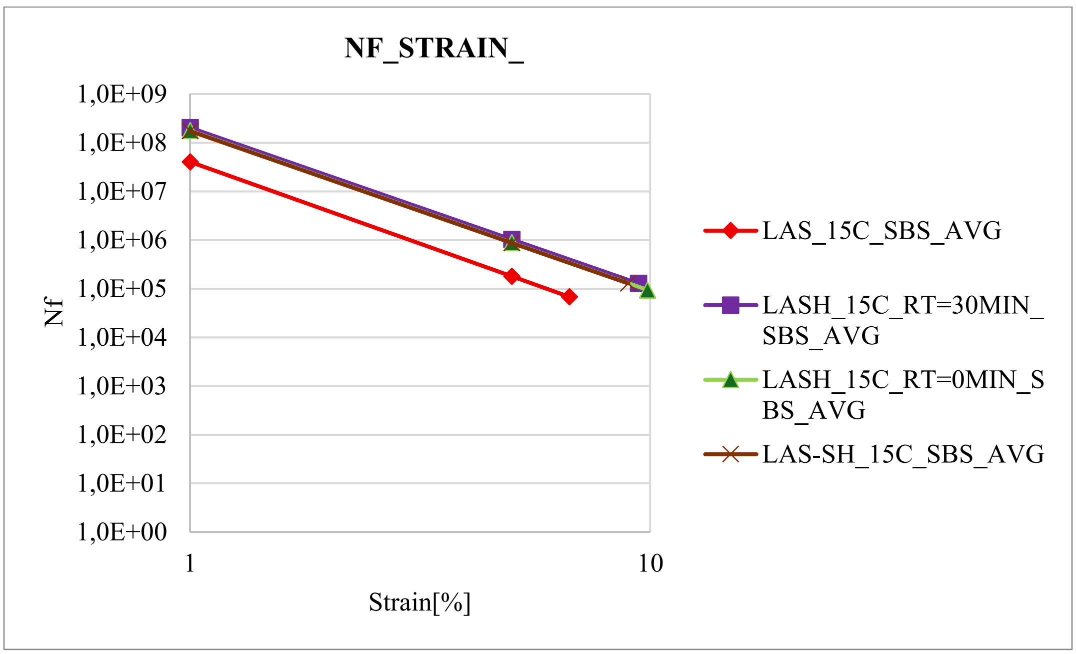


Figure3.5.2.34 -comparison of LAS, LASH RT=30, LASH RT=0, LAS-SH, for SBS modified binder at15°C

The graph below shows the condition of all tests for Neat 50/70 at 20°C which is very similar to Neat’s behavior at 15°C.

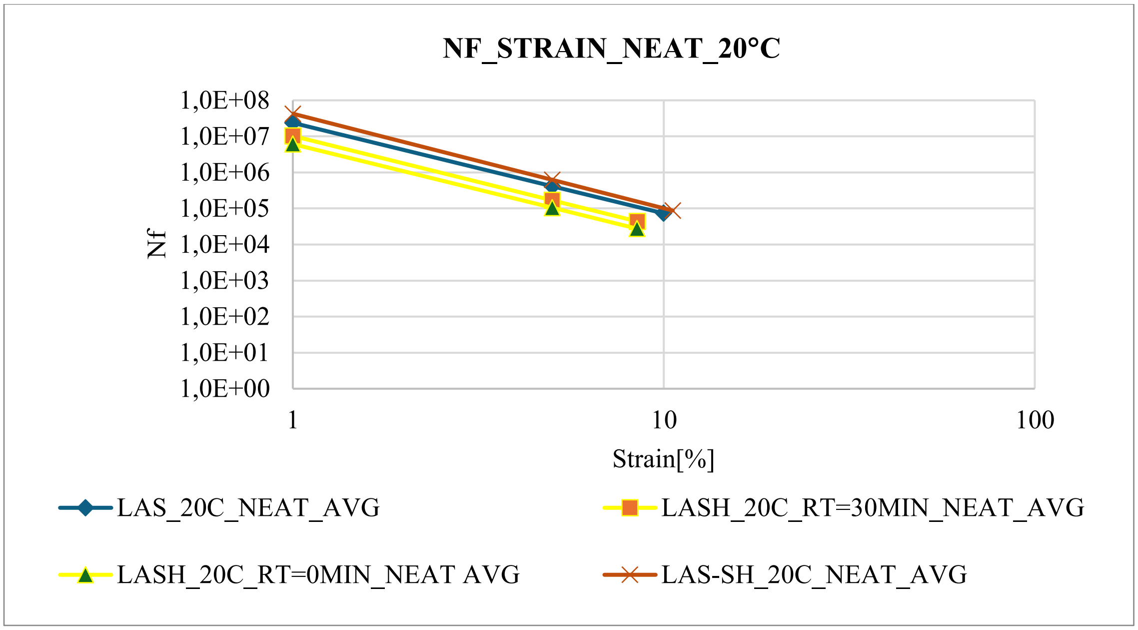


Figure 3.5.2.35-comparison of LAS, LASH RT=30, LASH RT=0, LAS-SH, for Neat 50/70 at 20°C

Although the LASH test with a 30-minute rest period produced the highest predicted fatigue life and the LASH test without rest exhibited the lowest values, the differences among the four curves were relatively small. The close convergence of the LAS, LASH, and LAS-SH curves indicates that the fatigue responses of the RLDP 3.35% modified binder were broadly comparable, suggesting that both the self-healing and steric hardening effects were modest at 20°C.

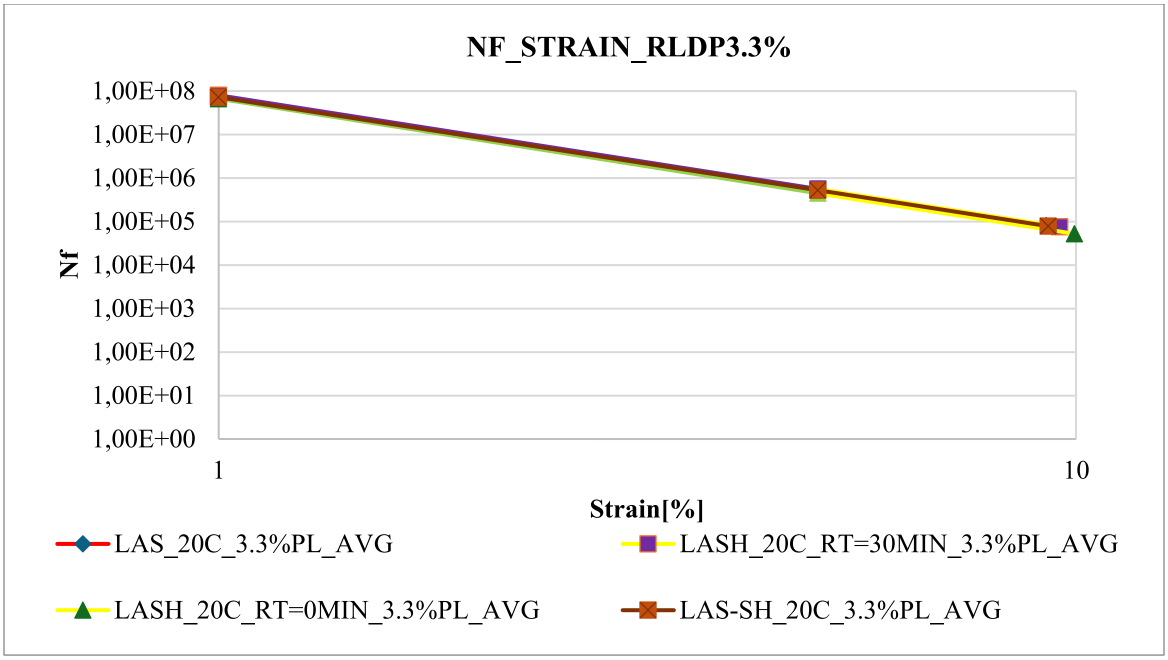


Figure 3.5.2.36-comparison of LAS, LASH RT=30, LASH RT=0, LAS-SH, for modified binder with 3.35%RLDP at 20℃

For the SBS-modified binder at 20°C, the LAS-SH curve exhibited the highest predicted fatigue life, followed by the LAS-H curve, while the conventional LAS test produced the lowest fatigue life. This trend indicates that the rest period improved the fatigue performance of the binder compared with continuous loading, as evidenced by the higher fatigue life obtained from the LAS-H test. However, the superior fatigue life predicted by the LAS-SH test suggests that steric hardening contributed more significantly to the observed mechanical recovery than the self-healing process under the investigated conditions. Consequently, the increase in fatigue resistance during the rest period appears to be strongly influenced by time-dependent physical hardening in addition to intrinsic healing mechanisms.

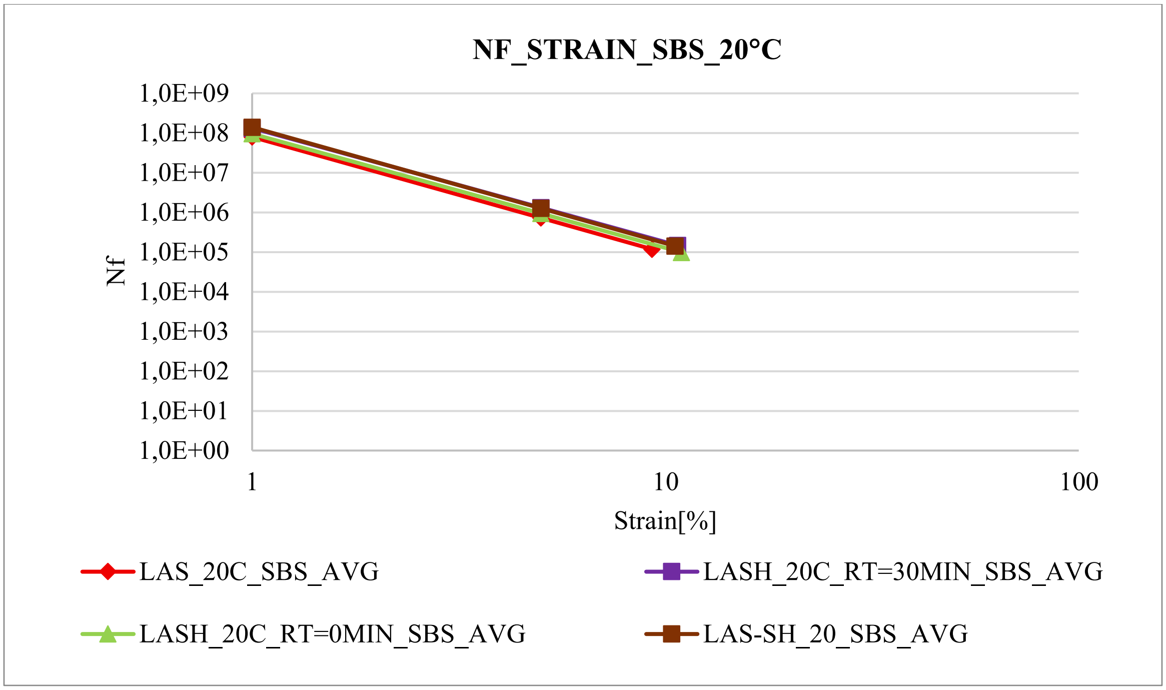


Figure3.5.2.37 -comparison of LAS, LASH RT=30, LASH RT=0, LAS-SH, for modified binder with 3.35%RLDP at15°C

Based on comparison graph above for SBS modified binder at 20°C LAS-Steric hardening and LASH with 30 minutes rest period have been placed significantly close to each other and distant from LASH without rest period which illustrates the good performance of SBS modified binder in terms of healing with rest time at 20°C. To facilitate a consistent comparison among the three asphalt binders, a common reference strain of 5% was selected for the evaluation of the LAS, LAS-H with a 30-minute rest period, LAS-H without a rest period, and LAS-SH tests. According to the AASHTO TP 101 procedure, the fatigue life ($N_f$) is determined at three strain levels: 1%, 5%, and the strain corresponding to the peak shear stress. Since all reported values represent the average of the selected convergent trials, the 5% strain level was adopted as the principal point of comparison because it provides a uniform basis for assessing the fatigue and healing performance of the neat, SBS-modified, and 3.3% RLDP-modified binders. The following tables and figures present the corresponding fatigue life results obtained at both 15°C and 20°C.

| TESTS AT 15C | STRAIN[%] | NF |
|---|---|---|
| LAS_AVG_15C_NEAT_ | 5 | 250134 |
| LAS_AVG_15C_RLDP3.35%_ | 5 | 323967 |
| LAS_AVG_15C_SBS | 5 | 179905 |
| LASH_AVG_15C_NEAT_RT=30 MIN | 5 | 184497 |
| LASH_AVG_15C_RLDP3.35%_RT=30 MIN | 5 | 162485 |
| LASH_AVG_15C_SBS_RT=30 MIN | 5 | 1029205 |
| LASH_AVG_15C_NEAT_RT=0 MIN | 5 | 126531 |
| LASH_AVG_15C_RLDP3.35%_RT=0 MIN | 5 | 156625 |
| LASH_AVG_15C_SBS_RT=0 MIN | 5 | 886691 |
| LAS-SH_AVG_15C_NEAT | 5 | 297371 |
| LAS-SH_AVG_15C_RLDP3.35% | 5 | 185176 |
| LAS-SH_AVG_15C_SBS | 5 | 873724 |

Table 3.5.2.1-Nf values for SBS,3.35%RLDP, Neat with strain of 5% at 15

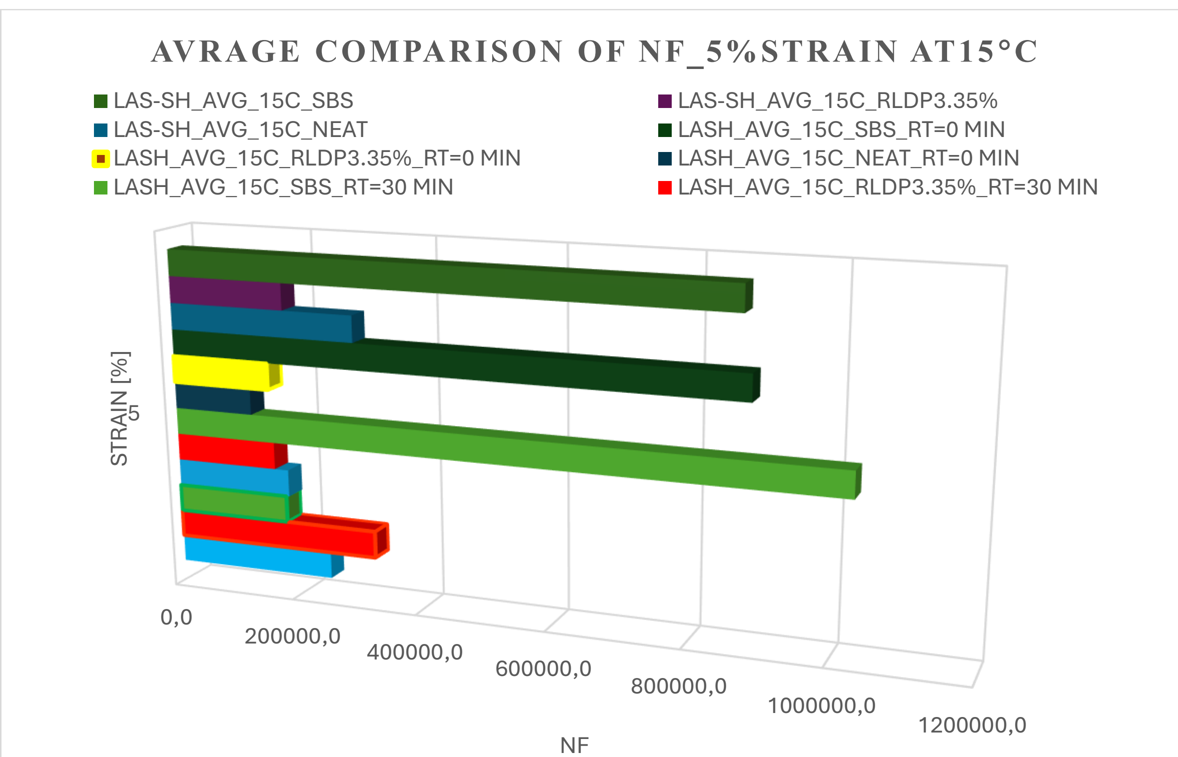


Figure 3.5.2.38-comparison 3 asphalt binders for LAS, LASH RT=30, LASH RT=0 , LAS-SH at 15°C

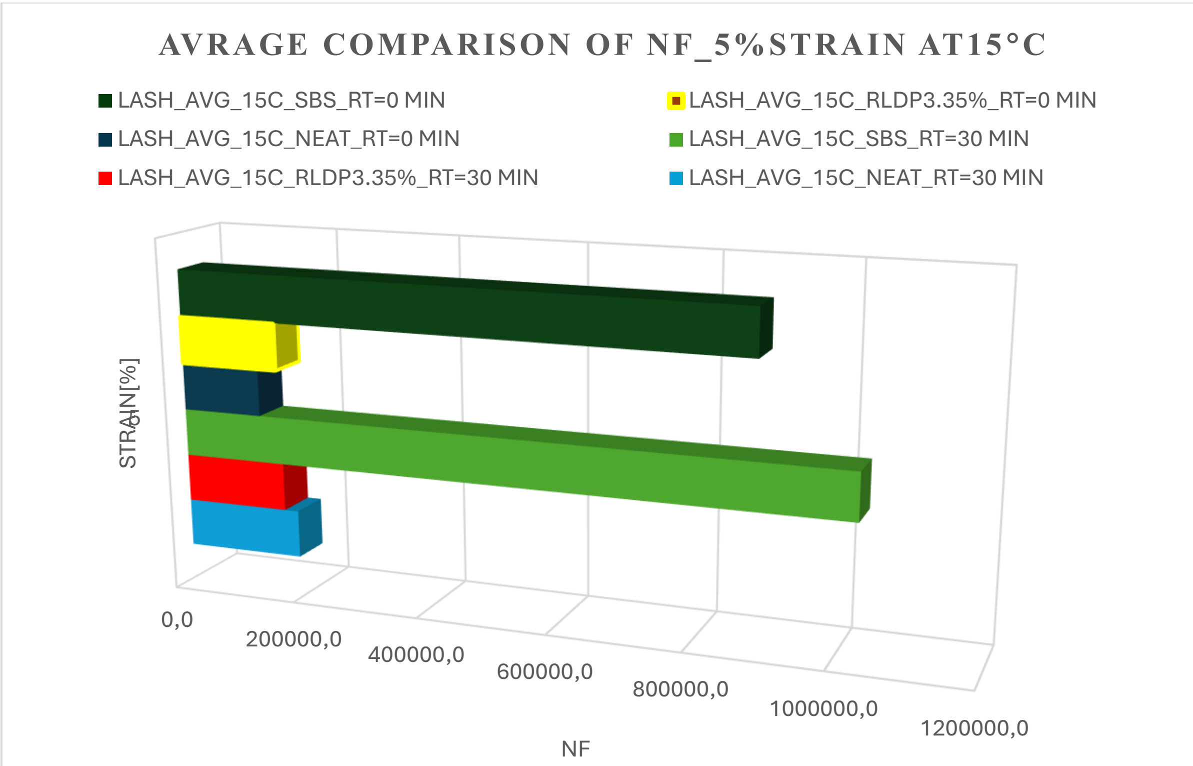


Figure 3.5.2.39-average comparison of NF_5%strain through LASH protocols for SBS, 3.35% RLDP, Neat5070 at 15°C

Figure 3.5.2.39 compares the fatigue life ($N_f$) of the neat 50/70 binder, the SBS-modified binder, and the 3.35% RLDP-modified binder at 15°C based on the selected reference strain of 5%. The results indicate that the SBS-modified binder tested under the LAS-H protocol with a 30-minute rest period exhibited the highest fatigue life among all binders, demonstrating its superior self-healing capability. Furthermore, the SBS-modified binder tested without a rest period still achieved a higher fatigue life than the 3.35% RLDP-modified binder tested with a 30-minute rest period, highlighting the inherent fatigue resistance and recovery potential imparted by SBS modification. As expected, the Neat 50/70 binder tested without a rest period exhibited the lowest fatigue life, reflecting its limited resistance to fatigue damage. Interestingly, the neat binder subjected to a 30-minute rest period achieved a slightly higher fatigue life than the 3.35% RLDP-modified binder under the same healing

condition, suggesting that, at the selected strain level and test temperature, the healing response of the neat binder was comparable to, or marginally greater than, that of the RLDP-modified binder.

| TESTS AT 20C | STRAIN[%] | NF |
|---|---|---|
| LAS_AVG_20C_NEAT_ | 5 | 416467 |
| LAS_AVG_20C_RLDP3.35% | 5 | 541237 |
| LAS_AVG_20C_SBS | 5 | 721419 |
| LASH_AVG_20C_NEAT_RT=30 MIN | 5 | 168555 |
| LASH_AVG_20C_RLDP3.35%_RT=30 MIN | 5 | 560945 |
| LASH_AVG_20C_SBS_RT=30 MIN | 5 | 1307200 |
| LASH_AVG_20C_NEAT_RT=0 MIN | 5 | 104366 |
| LASH_AVG_20C_RLDP3.35%_RT=0 MIN | 5 | 445874 |
| LASH_AVG_20C_SBS_RT=0 MIN | 5 | 935849 |
| LAS-SH_AVG_20C_NEAT | 5 | 623344 |
| LAS-SH_AVG_20C_RLDP3.35% | 5 | 520829 |
| LAS-SH_AVG_20C_SBS | 5 | 1265053 |

Table 3.5.2.2-Nf values for SBS,3.35%RLDP, Neat with strain of 5% at 20℃

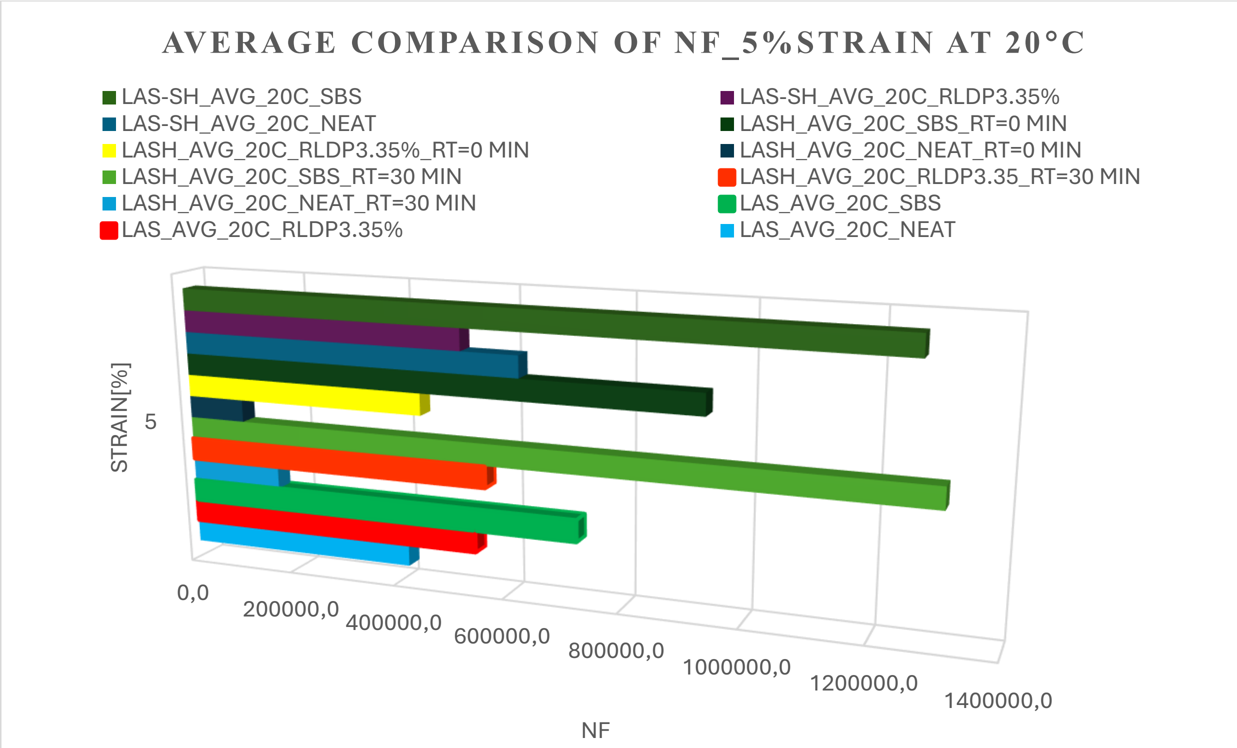


Figure 3.5.2.40average comparison of NF_5%strain for SBS, 3.35% RLDP, Neat5070 at 20C

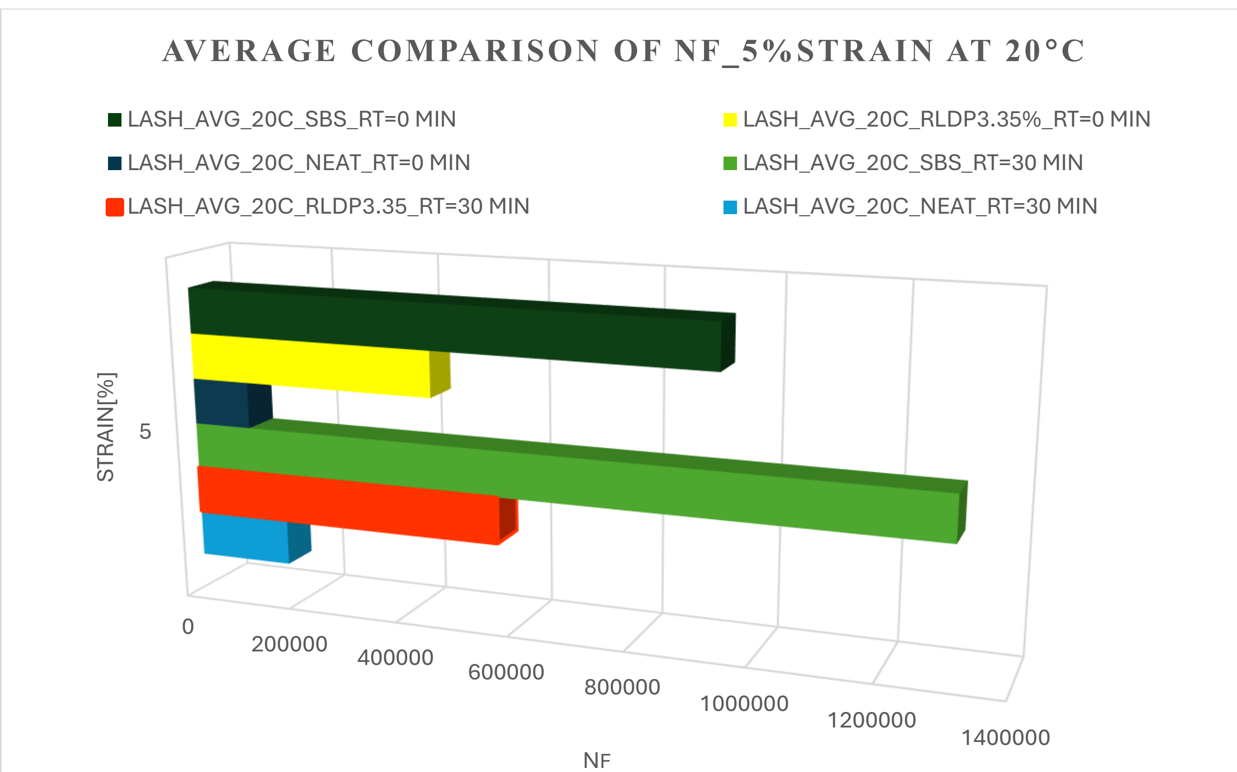


Figure 3.5.2.41-average comparison of NF_5%strain through LASH protocols for SBS, 3.35% RLDP, Neat5070 at 20C

Figure 3.5.2.41 presents the corresponding comparison at 20°C, highlighting the influence of temperature on the fatigue and healing performance of the investigated binders. A significant improvement in fatigue life was observed for both modified binders as the test temperature increased from 15°C to 20°C. Similar to the results obtained at 15°C, the SBS-modified binder subjected to the LAS-H test with a 30-minute rest period exhibited the highest fatigue life among all binders. Furthermore, its fatigue life increased by 27% at 20°C compared with its performance at 15°C, demonstrating the beneficial effect of elevated temperature on its self-healing capability.

An even more pronounced improvement was observed for the 3.35% RLDP-modified binder. Under the LAS-H protocol with a 30-minute rest period, its fatigue life increased by 245.23% relative to the value obtained at 15°C, indicating that the healing efficiency of the RLDP-modified binder was highly temperature dependent. Nevertheless, despite this substantial improvement, the SBS-modified binder continued to exhibit a considerably higher fatigue life than the 3.3% RLDP-modified binder, confirming the superior fatigue resistance and recovery capability provided by SBS modification.

In contrast, the neat 50/70 binder exhibited a different trend. The results obtained from the LAS-H test without a rest period indicated that increasing the temperature from 15°C to 20°C led to a 8.64% reduction in fatigue life. This decrease suggests that, in the absence of a recovery period, the neat binder became more susceptible to fatigue damage at the higher temperature, reflecting its comparatively poor resistance to deformation and limited recovery capacity.

A consistent trend was observed for all binder systems at both test temperatures: specimens subjected to a 30-minute rest period consistently exhibited higher fatigue life than those tested without a rest period. This finding confirms the beneficial role of the recovery interval in promoting the restoration of mechanical properties and enhancing the fatigue performance of asphalt binders through self-healing.

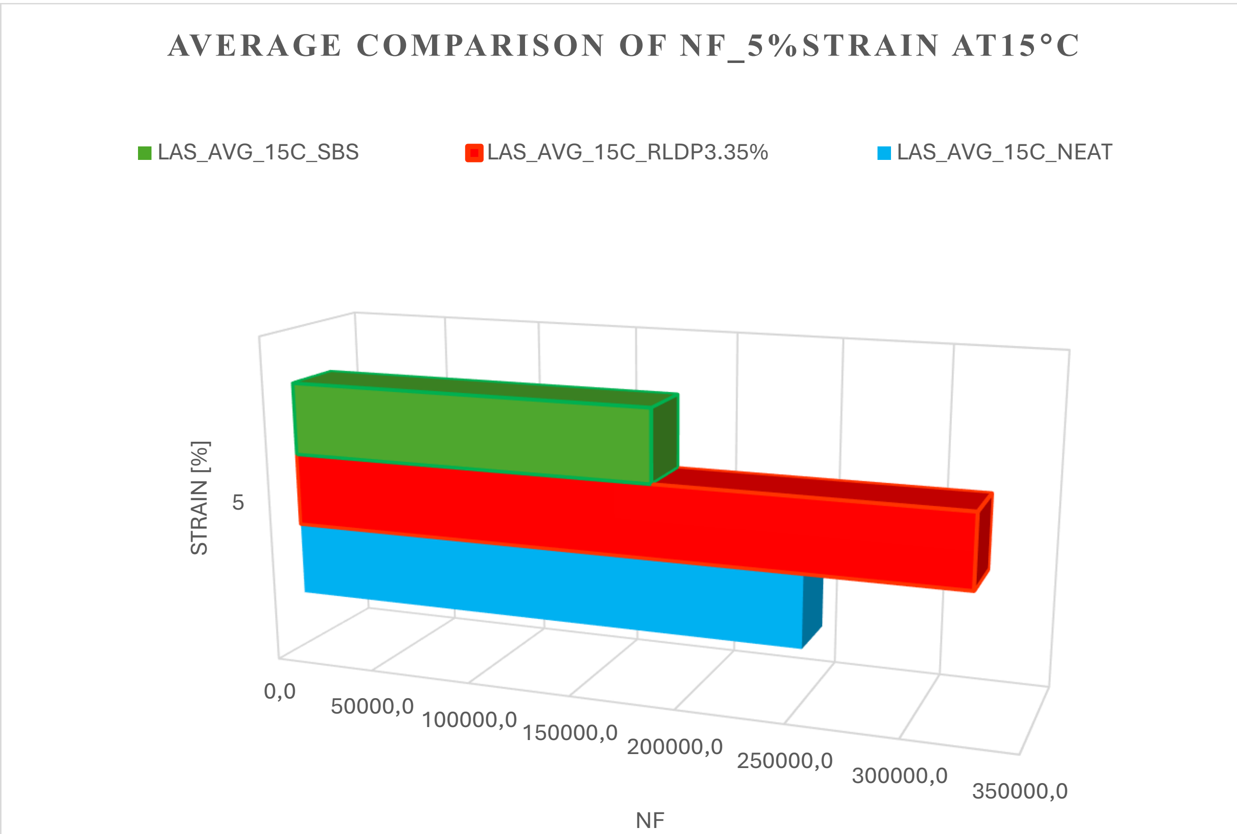


Figure 3.5.2.42average comparison of NF_5%strain through LAS protocols for SBS, RLDP3.35%, Neat5070 at 15°C

From the LAS test results, it is evident that at 15°C the 3.35% RLDP-modified binder exhibited the highest fatigue life ($N_f$), while the SBS-modified binder showed the lowest performance among the three binders. However, at 20°C a significant improvement in fatigue resistance was observed, particularly for the SBS-modified binder, which demonstrated a substantial increase of approximately 300.99% in fatigue life compared with its performance at 15°C under the LAS protocol. The 3.35% RLDP-modified binder also showed an improvement of 67% at 20°C relative to its performance at 15°C; nevertheless, its fatigue life remained approximately 33.29% lower than that of the SBS-modified binder at 20°C. Overall, the LAS results clearly indicate that increasing the temperature from 15°C to 20°C significantly enhances fatigue performance, with the SBS-modified binder consistently exhibiting the highest fatigue resistance, followed by the 3.35% RLDP-modified binder.

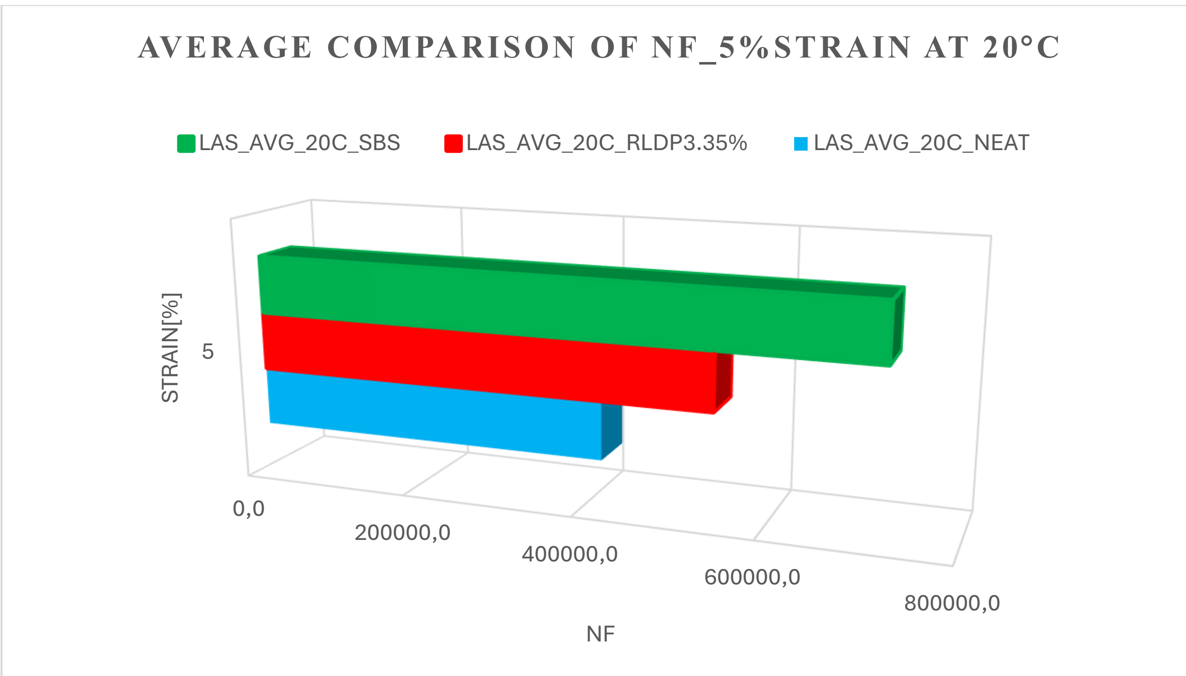


Figure 3.5.2.43-average comparison of NF_5%strain through LAS protocols for SBS, 3.35% RLDP, Neat5070 at 20°C

# CHAPTER 4-CONCLUSION

This research investigated the rheological, fatigue, and self-healing behavior of three asphalt binders: an unmodified 50/70 penetration-grade binder, an industrially produced SBS-modified binder, and a laboratory-prepared binder modified with 3.35% recycled low-density plastic (RLDP). In addition to the rheological characterization, practical observations made during specimen preparation revealed distinct differences in the handling characteristics of the three materials. The neat binder exhibited the highest sensitivity to heat and was relatively easy to trim and prepare. In contrast, the RLDP-modified binder showed greater resistance during specimen preparation and exhibited a stiffer and more brittle behavior than the neat binder. The SBS-modified binder displayed the greatest ductility and elasticity, remaining more cohesive and flexible during heating, trimming, and handling, reflecting the influence of the polymer network on its mechanical properties.

The rheological investigation demonstrated the significant influence of the recovery period on the healing performance of asphalt binders. For nearly all specimens tested at both 15°C and 20°C, the LAS Healing (LASH) tests incorporating a 30-minute rest period produced higher fatigue life than the corresponding tests conducted without a rest period. These findings confirm that the introduction of a recovery interval promotes the restoration of mechanical properties by allowing molecular diffusion and crack closure within the binder.

Temperature was also found to play a crucial role in determining the fatigue and healing performance of the investigated binders. The comparison performed at the reference strain of 5% showed that increasing the test temperature from 15°C to 20°C substantially improved the fatigue life of both modified binders, particularly under the healing protocol. The SBS-modified binder exhibited a marked improvement in fatigue performance, while the 3.3% RLDP-modified binder demonstrated an even greater relative increase, indicating that its healing response is highly temperature dependent. Conversely, the neat 50/70 binder did not benefit to the same extent from the increase in temperature and, under certain testing conditions, exhibited a reduction in fatigue life, highlighting its limited resistance to damage accumulation compared with the modified binders.

The comparison among the three binders further demonstrated that, at the selected reference strain of 5%, both the SBS-modified and the 3.35% RLDP-modified binders consistently achieved higher fatigue life than the neat binder under the healing protocols. These results confirm that binder modification significantly enhances fatigue resistance and self-healing capability. Furthermore, the satisfactory performance of the RLDP-modified binder demonstrates the potential of recycled waste plastics as sustainable modifiers for asphalt binders, contributing to improved pavement performance while supporting environmentally responsible waste management practices.

Overall, the SBS-modified binder exhibited the best rheological and fatigue performance among the investigated materials. The shear stress–strain curves showed a more gradual post-peak stress reduction and a larger area under the curve than those of the RLDP-modified binder, indicating greater ductility, toughness, and resistance to fatigue damage. In contrast, the RLDP-modified binder exhibited a steeper post-peak stress decline, suggesting a comparatively more brittle response despite its significant improvement over the neat binder. These findings indicate that SBS modification remains the most effective approach for enhancing asphalt binder performance, while RLDP modification represents a promising and sustainable alternative capable of providing substantial improvements in fatigue resistance and self-healing compared with conventional unmodified binders.

The End.

Key Academic References

*[1] Yang, K. et al. (2023). Understanding and characterizing the fatigue cracking resistance of asphalt binder at intermediate temperature: A literature review. Construction and Building Materials, 407, 133432.*

*[2] Mohammed Nouali a,*, Anne Dony a, Alan Carter b . Evaluation of fatigue life of asphalt binders using the time sweep and linear amplitude sweep tests: A literature review*

*[3] LTOB &. ES Fabrizio Miglietta, «Investigating the effect of temperature on self-healing properties of neat and polymer-modified bituminous binders,» Road Materials and Pavement Design, pp. 1-2 , 2021.*

*[4] Annarita De Leonardis. Effects of nonlinearity and time-temperature superposition in the self-healing of bituminous binders*

*[5] M. Ashouri, «Modeling Microdamage Healing in Asphalt Pavements Using Continuum Damage Theory,» North Carolina, 2014.*

*[6] LTOBES Fabrizio Miglietta, «new approach for the evaluation of time-temperature superposition effects on the self-healing of bituminous binders,» Construction and Building Materials,2021.*

*[7] Sun, Guoqiang, Yu, Huachun, Zhang, Yajie, et al. (2019). Low-temperature self-healing character of asphalt mixtures under different fatigue damage degrees. Construction and Building Materials, 223, 870–882*

*[8] Fuel, Vol. 211, pp. 609-620, 2018.*

*[9] MC a. JA Sánchez, «Fatigue and Healing of Asphalt Mixtures: Discriminate Analysis of Fatigue Curves,» Journal of Transportation Engineering, vol. 136, pp. 105-182, 2006.*

*[10] Z. ZHANG, identification of suitable crack growth law for asphalt mixtures using the Superpave indirect tensile test (idt), university of Florida, 2000.*

*[11] AH e. D. Little, adhesion in bitumen-aggregate systems and quantification of the effects of water on the adhesive bond, Aggregates Foundation for Technology, Research and Education, Texas, 2005.*

*[12] Liang, M., et al. (2021). Review on the self-healing of asphalt materials: Mechanism, affecting factors, assessments and improvements. Construction and Building Materials, 266, 120453.*

*[13]Bahia, H. U. ,& Anderson, D. A. (1993).Glass Transition Behavior and Physical Hardening of Asphalt Binders.Journal of the Association of Asphalt Paving Technologists (AAPT), 62, 93–129.*

*[14 ]Anderson, D. A., & Marasteanu, M. O. (1999). Physical Hardening of Asphalt Binders Relative to Their Glass Transition Temperatures. Transportation Research Record, 1661, 27–34.*

*[15 ]Masson, J.-F., Collins, P., & Polomark, G. (2005). Steric Hardening and the Ordering of Asphaltenes in Bitumen. Energy & Fuels, 19(1), 120–122.*

*[16] Lu, X., & Isacsson, U. (2000).Artificial Aging of Polymer Modified Bitumens. Journal of Applied Polymer Science, 76(12), 1811–1824.*

*[17] PP Riviera, Teaching material, Construction of roads, railways and airports,*

*2019/2020.*

*[18] Hunter, R. N., Self, A., Read, J., & Hobson, E. (2015). The shell bitumen handbook (Vol. 514). London, UK:: Shell Bitumen.*

*[19] AASHTO T391-20 (2024). Estimating Fatigue Resistance of Asphalt Binders Using the Linear Amplitude Sweep***.**

*[20] AASHTO T 315 Standard Method of Test for Determining the Rheological Properties of Asphalt Binder Using a Dynamic Shear Rheometer (DSR)*

*[21] ASTM D7175, 2021*

*[22] Hintz, C., Velasquez, R., Johnson, C., & Bahia, H. U. (2011). Modification and Validation of Linear Amplitude Sweep Test for Binder Fatigue Specification. Transportation Research Record: Journal of the Transportation Research Board, 2207(1), 99–106.*

*[23] Christensen, D. W. & Anderson, D. A. (1992). Interpretation of Dynamic Mechanical Test Data for Paving Grade Asphalt Cements. Journal of the Association of Asphalt Paving Technologists,* ***61****, 67–116.*

*[24] Kim, Y. R., Little, D. N., & Lytton, R. L. (2003). Fatigue and healing characterization of asphalt mixtures. Journal of materials in Civil Engineering, 15(1), 75-83.*

*[25] Nouali, M., Dony, A., & Carter, A. (2024). Evaluation of fatigue life of asphalt binders using the time sweep and linear amplitude sweep tests: A literature review. Journal of Traffic and Transportation Engineering (English Edition).*

*[26] AASHTO TP 101-14 (or the latest available version). Standard Method of Test for Estimating Damage Tolerance of Asphalt Binders Using the Linear Amplitude Sweep.*

*[27] Wang, C., et al. (2023). Addressing the healing compensation on fatigue damage of asphalt binder using TSH and LASH tests. International Journal of Fatigue, 167, 107292.*

*[28] Baglieri, O., Aurilio, R., Miglietta, F., Tsantilis, L., & Baaj, H. (2025). Article of RILEM TC 278-CHA: evaluation of self-healing properties of asphalt binders—outcomes and challenges. Materials and Structures, 58(7), 1-16.*

*[29] Little, D. N., Bhasin, A., & Darabi, M. K. (2015). Damage healing in asphalt pavements: Theory, mechanisms, measurement, and modeling. In Advances in asphalt materials (pp. 205-242). Woodhead Publishing.*

*[30] Hofko, B. (2022). M&S highlight: Di Benedetto et al.(2004), Fatigue of bituminous mixtures. Materials and Structures, 55(2), 34.*

*[31] Santagata, E., Baglieri, O., Tsantilis, L., & Dalmazzo, D. (2013). Evaluation of self-healing properties of bituminous binders taking into account steric hardening effects. Construction and Building Materials, 41, 60-67.*

*[32] Baglieri, O., Miglietta, F., Tsantilis, L., & Santagata, E. (2024). Effects of non-linearity and thixotropy in linear amplitude sweep testing for the evaluation of self-healing of bituminous binders. Materials and Structures, 57(4), 54.*

*[33] OBLTDD Ezio Santagata, Evaluation of self-healing properties of bituminous binders taking into account steric hardening effects, Construction and Building Materials, vol. 41, pp. 60-67, 2013*

*[35] Yildirim, Y. (2007). Polymer modified asphalt binders. Construction and Building Materials, 21(1), 66–72.*

*[36] Airey, G. D. (2003). Rheological properties of styrene butadiene styrene polymer modified road bitumens. Fuel, 82(14), 1709–1719.*

*[37] Garcia-Morales, M., Partal, P., Navarro, F. J., Martínez-Boza, F., Gallegos, C., González, N., González, O., & Muñoz, M. E. (2006). Viscous properties and microstructure of recycled EVA-modified bitumen. Fuel, 85(7–8), 936–943.*

*[38] Polacco, G., Filippi, S., Merusi, F., & Stastna, J. (2015). A review of the fundamentals of polymer-modified asphalts: Asphalt/polymer interactions and principles of compatibility. Advances in Colloid and Interface Science, 224, 72–112.*

*[39] Kalantar, Z. N., Karim, M. R., & Mahrez, A. (2012). A review of using waste and virgin polymer in pavement. Construction and Building Materials, 33, 55–62.*

*[40] Canestrari, F., Virgili, A., Graziani, A., & Stimilli, A. (2015). Modeling and assessment of self-healing and thixotropy properties for modified binders. International Journal of Fatigue, 70, 351–360.*

*[41] Read, J., & Whiteoak, D. (2015). The Shell Bitumen Handbook (6th ed.). ICE Publishing.*

*[42] Qiu, J., van de Ven, M., Wu, S., Yu, J., & Molenaar, A. A. A. (2012). Characterization of Bituminous Mastics Self-Healing Behavior Using a Dynamic Shear Rheometer. Materials and Structures, 45(10), 1611–1622.*